Order Number 9130386

# Modelling and analysis of the design constraints for integrated gasification combined cycle system

Weng, Li, Ph.D.

City University of New York, 1991

U·M·I
300 N. Zeeb Rd.
Ann Arbor, MI 48106

# MODELLING AND ANALYSIS OF THE DESIGN CONSTRAINTS FOR INTEGRATED GASIFICATION COMBINED CYCLE SYSTEM

by

LI WENG

A dissertation submitted to the Graduate Faculty in Engineering in partial fulfillment of the requirements for the degree of Doctor of Philosophy, The City University of New York

1991

This manuscript has been read and accepted for the Graduate faculty in Engineering in satisfaction of the dissertation requirement for the degree of Doctor of Philosophy.

May 7 91
Data

Professor Reuel Shinnar
Chair of Examining committee

5/9/91
Data

Professor Gerard Lowen
Executive Officer

Dr. Madhav Ghate

Professor Irven Rinard

Professor Gabriel Tardos

Professor Herbert Weinstein
Supervisory committee

The City University of New York

## DEDICATION

To my father, Shaolin Weng, a chief chemical engineer and my wife, Feifei Cai, whose love, encouragement and patience contributed more than anything else to the completion of this work.

## ACKNOWLEDGMENT

The author wishes to express his profound appreciation and gratitude to Professor Reuel Shinnar, his Graduate Advisor, for his guidance, inspiration and assistance at all times during the course of this work.

Financial assistance was made available by the U.S. Department of Energy (METC). This aid is gratefully acknowledged.

Table of Content

## List of Tables

## List of Figures

# SUMMARY

This thesis deals with the system studies relating to generation of clean power from coal. The main emphasis is on the modelling of a fluid bed gasifier with in bed desulfurization and IGCC (Integrated Gasification Combined Cycle Power Plant) system. A detailed evaluation of the design potential of air-blown gasifier and novel configuration of the IGCC system has been given. We tried to achieve these goals by investigating the kinetic (both gasification and desulfurization), design, and operating constraints of the air blown gasifier and gas cleanup system as well as combined cycle power plant.

Supplies of natural gas and petroleum appear for now to be adequate. Development of coal gasification technology has, however, continued with a fresh outlook and objectives. The thrust was to eliminate those process elements which made the technology economically unattractive or to substitute them with more efficient and environmentally acceptable ones. The approach is through process simplification and matching the gasifier product outlet temperature, pressure, and heating value to the IGCC power plant requirements. This is resulted in the development of hot gas cleanup technologies which are

not only less costly than the conventional cold gas cleanup technologies, but also reduce the process efficiency losses accompanied with cooling and reheating of gases. In other development work, cheap disposable sorbents which can be added to the feed coal are now in use to capture sulfur in the gasifier, greatly reducing the load on the hot gas desulfurization equipment.

To better understand the requirements and value of further research and development, we need an understanding of the total system which includes not only the gasifier, the feed preparation and gas cleanup, but also the end use. It includes the combination of boiler, combustor and combined cycle turbine system. A simulation model is needed to understand the kinetic, process, and design constraints and to quantify their thermodynamic consequences.

A thorough understanding of design constraints is essential for the development and evaluation of better processes to convert coal to electricity. An air-blown/oxygen-blown gasifier model has been developed to show the impact of the constraints on the total power plant performance. For approaching high efficiency of the power generation, The constraints have to be bypassed by using commercial available and environmental acceptable technique. In this thesis, it can be shown that there is a narrow way to

achieve a desirable solution from assessing the performances and configurations of several available techniques using constraints analysis.

Two related problem areas have been chosen for this study, which are:

A) Assessment of gasifier requirements for generation of electricity from coal in combined cycle power plants.

a) For describing the behavior of a oxygen/air-blown fluid bed gasifier and in bed desulfurization performances, a gasifier model has been developed. Both gasification and desulfurization kinetics have been included. The limitation of the operating range for the environmental and commercially acceptable design are given. The model predicts the carbon conversion, sulfur capture, oxygen requirement as given bed temperature and bed holdup. It also predicts the product gas as well as the withdraw solids composition. Agreement between pilot plant results and model prediction is reasonable.

b) Assessment of gas cleanup system has been given according to the EPA standard and future requirements. It includes the in bed and external sulfur capture processes. The model prediction has shown that it is hard to achieve the EPA standard only using the in bed desulfurization method. The different external sulfur capture processes have been

evaluated to show the impact on total thermal efficiency of the IGCC power plant.

B) Configuration of IGCC system, which include the gasifier, boiler, combustor, cleanup and combined cycle electricity generation system.

a) The constraints of producing electricity from coal have been analyzed to find out the possible paths of transferring energy from coal to electricity. A simplified model of the gas turbine and the steam turbine system has been developed. It is combined with the gasifier island model to predict the total IGCC power plant performance.

b) Different configuration of hybrid power plants has been evaluated for the further development.

The achievements are summarized as following. The air/oxygen-blown fluid bed gasifier model has been developed. It is for a better understanding of the performances and interaction of the gasification and in bed desulfurization. It predicts well the performances of several large pilot plants such as KRW and Ugas with different coals. One example is shown in Table S1. Furthermore, the impact of the hot gas cleanup operation on the total IGCC power plant has been analyzed for achieving the higher thermal efficiency. Finally, the different configurations of the IGCC power plant have been given for a better design decisions.

COMPARISON OF UGAS PILOT PLANT AND MODELLING DATA

Coal: Pitt#8 Sorbent : Dolomite

| RUN # | Lime2-5 | | Lime3-3 | | Lime3-4 | |
|---|---|---|---|---|---|---|
| | Pilot P. | Model | Pilot P. | Model | Pilot P. | Model |
| Temperature (F) | 1845 | 1845 | 1870 | 1870 | 1860 | 1860 |
| Pressure (psig) | 150 | 150 | 303 | 303 | 303 | 303 |
| Oxygen/Carbon | 0.419 | 0.420 | 0.523 | 0.534 | 0.446 | 0.438 |
| Steam/Carbon (mole) | 1.05 | 1.05 | 2.33 | 2.33 | 1.77 | 1.77 |
| Carbon Conversion | 0.90 | 0.891 | 0.947 | 0.962 | 0.959 | 0.919 |
| Product Gas/Coal (mole) | 3.66 | 3.62 | 5.71 | 5.71 | 4.55 | 4.53 |
| YCO (mole fraction) | 0.105 | 0.105 | 0.043 | 0.046 | 0.066 | 0.067 |
| YCO2 | 0.131 | 0.126 | 0.125 | 0.115 | 0.134 | 0.122 |
| YH2 | 0.121 | 0.118 | 0.083 | 0.085 | 0.108 | 0.105 |
| YH2O | 0.233 | 0.242 | 0.366 | 0.362 | 0.329 | 0.330 |
| YCH4 | 0.025 | 0.025 | 0.015 | 0.015 | 0.022 | 0.022 |
| YN2 | 0.384 | 0.384 | 0.365 | 0.378 | 0.339 | 0.352 |
| Eq. H2S in Gas (ppm) | | 617 | | 1057 | | 809 |
| H2S in Gas (ppm) | 1066 | 711 | 1907 | 1160 | 2161 | 966 |
| Ca/S (mol) | 2.59 | 2.59 | 1.72 | 1.72 | 2.25 | 2.26 |
| HHV of Gas (wt) Btu/scf | 105 | 109 | 61.0 | 65.7 | 84.8 | 91.4 |

Table S1

# Chapter I INTRODUCTION

Research and development continue on Integrated Gasification Combined Cycle (IGCC) power plants using air-blown gasifiers. The use of mathematical simulation models of such plants is an important aid understanding the influence of design variables, feed coal types, and processing conditions on the total plant performance. Furthermore, such models are useful tools for scale-up, design, and optimization.

There has been considerable attention paid recently to the technology assessment of Integrated Gasification Combined Cycle (IGCC) systems (Dawkins 1985). Total plant thermal efficiency is a very important consideration in the conversion of coal to electricity. Any clues to the improvement of thermal efficiency are valuable.

However, the constraints that limit thermal efficiency are not really thermodynamic but are mainly due to kinetic, process, and materials limitation as well as environmental considerations, all of which interact in a complex way. Thermodynamic analysis can be used as a tool to understand the effects of these constraints on various process configurations and to find ways of improving their designs. No such a system assessment including all the considerations mentioned above is

to be found in the literature.

One of the achievements of this thesis is an kinetic model of an air-blown/oxygen-blown gasifier with in bed desulfurization has been developed. It predicts well the performances of several large pilot plants such as KRW and UGas. The chief aim of this thesis is to use the constraints analysis to assess the performances and configurations of IGCC and hybrid power systems with fluidized bed gasifier.

A conceptual scheme of a combined cycle power plant with a fluidized bed air-blown gasifier is shown in Figure 1.1. The coal is fed into the gasifier with desulfurization sorbent through the bottom jet. Air and steam are fed in as oxidation and gasification agents. Devolatilization, combustion and gasification occur in the gasifier to produce the low BTU fuel gas. After going through a Zinc-Ferrite hot gas cleanup system, the fuel gas is fed into a combustion chamber of a gas turbine and combusted with air for the expansion turbine to generate electricity. The exhaust gas is sent into a heat recovery steam generator to produce steam for a reheat steam turbine system for recovery of the low grade energy. The unconverted carbon in the gasifier withdrawal is fed in a boiler to oxidize the sorbent (CaS to $CaSO_4$) and generate the process steam. The total plant efficiency of this system is about 40 % based on HHV of the input coal.

Air-blown fluidized bed gasifiers are at present being commercialized for use in an Integrated Gasification Combined Cycle (IGCC) power plant (Haldipur 1989, Dawkins 1985). They showed considerable promise of providing an attractive means to convert coal to electricity at high efficiency in an environmentally acceptable way. The main part of the simulation studies in this paper is based on a fluidized air-blown gasifier with in bed desulfurization.

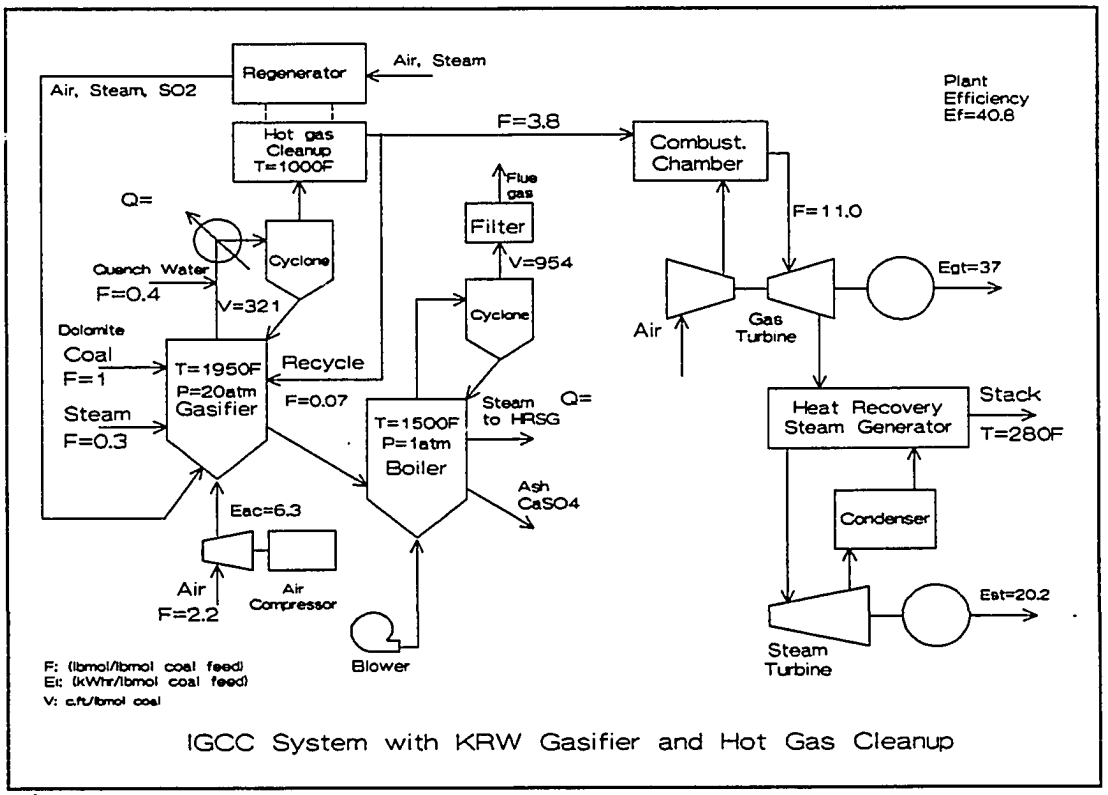


IGCC System with KRW Gasifier and Hot Gas Cleanup

Figure1.1

Another recent development research is the hybrid power plant (Shinnar 1989). These consist of a pressurized fluidized bed combustor with a turbine expander and a fluidized bed coal gasifier. The product gas of the gasifier is used to superheat the combustor flue gas before expanding them in the turbine. A typical example is shown in Figure 1.2.

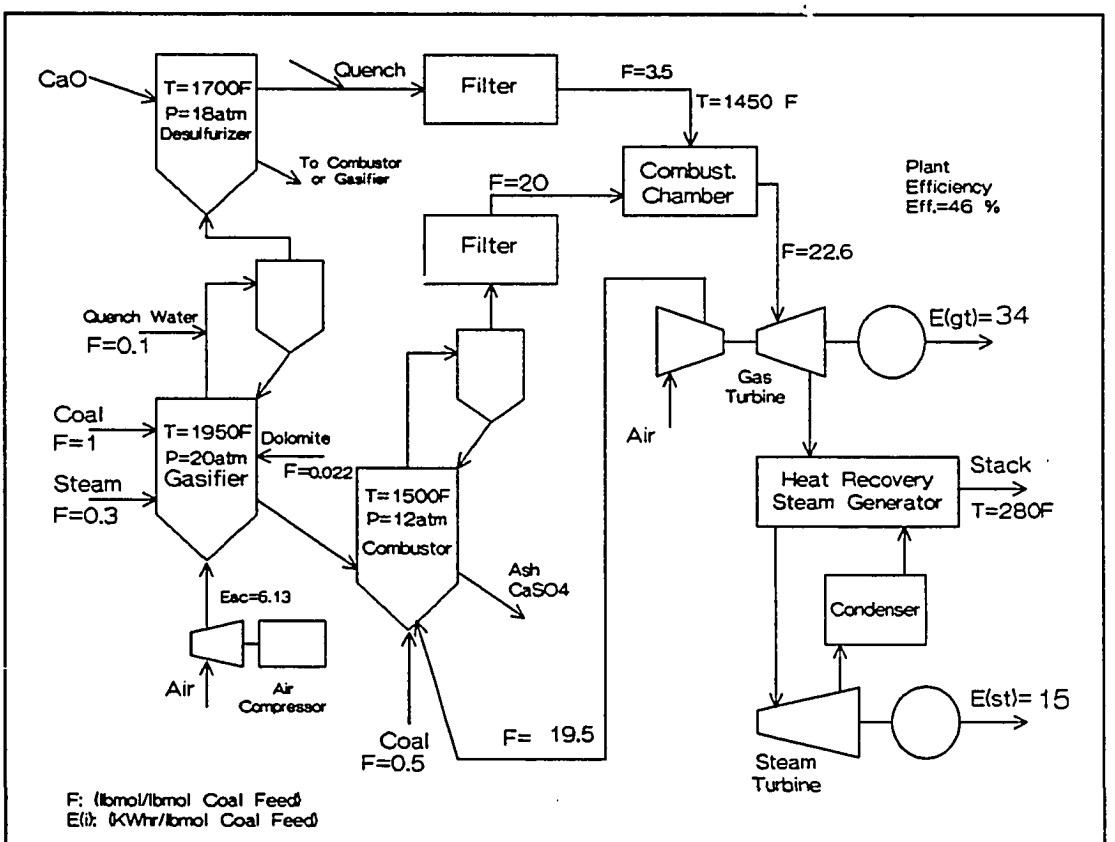


IGCC System with Air-Blown Gasifier and High Pressure Combustor

Figure1.2

The IGCC and the hybrid power plant have some common features (for example: gasifier, combustor, gas cleanup system

and combined cycle power generation system), which can be seen from Figure 1.1 and 1.2. The principal objective of this paper is how to use the thermodynamic tools to combine these features for our special purpose, which is the higher total plant thermal efficiency. A simulation model of a gasifier has been developed for predicting the gasification and in bed desulfurization performances in this study. Furthermore, the impact of gasifier thermodynamic and kinetic performance on the total power plant design and operation has been investigated.

Essentially, most gasification processes can be grouped into three generic types of reactors, based upon the gas-solid contacting method:

- o Moving bed - countercurrent reactor
- o Fluidized bed - mixed solid phase
- o Entrained bed - concurrent flow

Chapter II is concentrated on the simulation of an air-blown fluidized bed gasifier. The advantages of using an air-blown fluidized bed gasifier for the IGCC system have been shown in reference (Shinnar 1989). A good review of the various gasifiers and their operating conditions is given by reference (Simbeck 1983). The details of gasifier modelling are described in Chapter II. The basic constraints of gasifier operation can be seen from the operating map, which

is generated using the model and is shown in Chapter III.

Another constraint is the operating temperature of the gas cleanup system for emission control. The external sulfur capture process has to be used in IGCC system. It is difficult to achieve the EPA standards by using the in bed desulfurization. The current gas cleanup system available for the IGCC system involves cold gas cleanup such as Selexol gas-liquid absorption process. or hot gas cleanup such as Zinc-ferrite gas-solid adsorption process which was developed by METC DOE. The impact of cleanup method on the total power plant efficiency is studied in Chapter IV.

In Chapter IV, the evaluation of the hot gas cleanup systems have been given for getting the clean power from the IGCC power plant. The impact of cleanup temperature on the total plant efficiency has been discussed. The heating value of fuel gas leaving the gasifier and cleanup system is another constraint. This has to be higher than 100 BTU/scf for current combustion chamber control technology. The operating range of the gasifier and cleanup system are limited by this constraint.

The thermodynamic characteristic of the IGCC system will be discussed in Chapter V and VI. The basic configuration of the IGCC system and the hybrid power plant will be given for

further analysis.

One of the hard constraints in gas turbine design is the temperature of the combustion chamber, which is due to the materials limitation for gas turbine blades. Recent technology allows this temperature to be as high as 2200 °F. The thermal analysis will start from this limitation in Chapter VI.

The principle of thermodynamic constraints analysis has been discussed by R. Shinnar(1982). But much more work is required to provide the practicing engineer with a sound theoretical basis and methodology to deal with the IGCC power plant design systematically. One of the main goal of this study is to supply this framework.

# CHAPTER II GASIFIER SIMULATION

A steady state model of fluid bed coal gasifier has been developed based on the previous work (Shinnar 1988). A simplified two parameter gasification kinetics is used to predict char conversion. A shrinking core model for desulfurization kinetics is used to predict sulfur capture behavior. The solids residence time distribution is now calculated using a CSTR (Continue Stirred Tank Reactor) model.

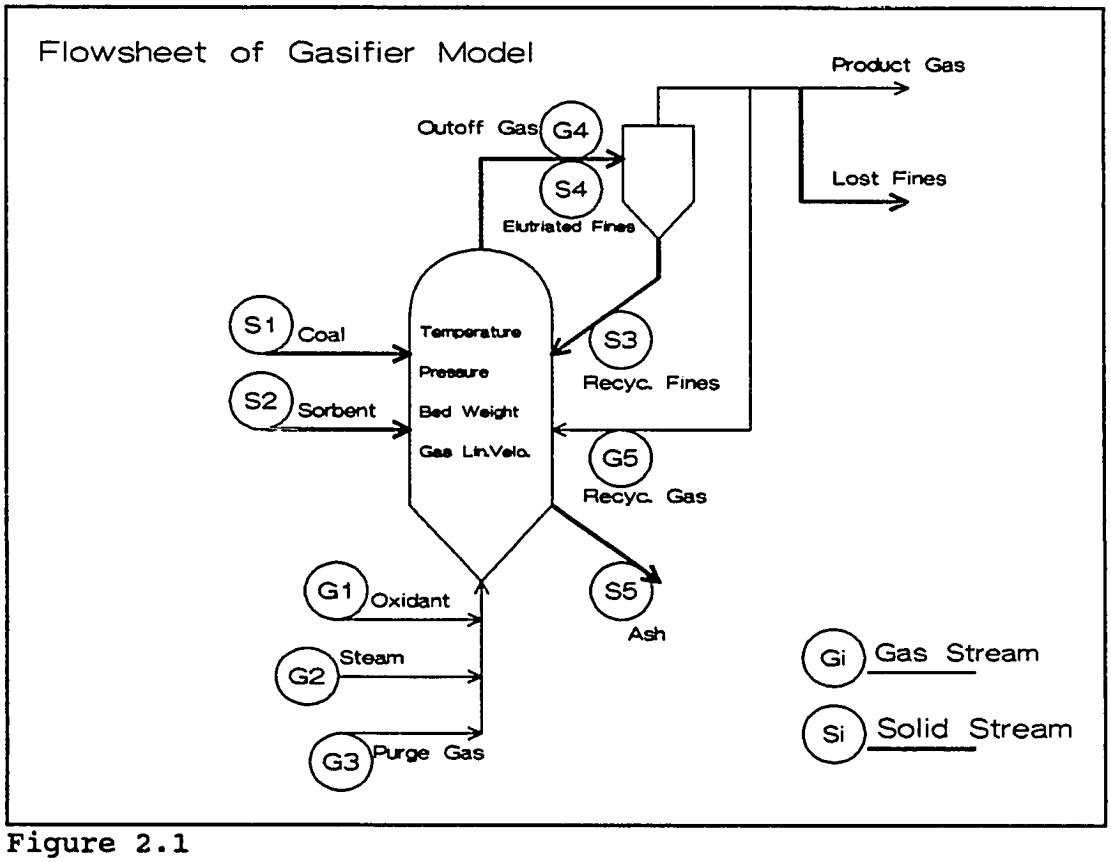


Figure 2.1

The mass and energy balance are solved simultaneously with gasification and desulfurization kinetics to predict the gasifier performance with in bed sulfur capture. The model predictions are tested against actual pilot plant data.

## 2.1 Basic Assumptions

A simulation model of an air/oxygen-blown fluid bed gasifier with in-bed desulfurization has been developed for predicting the steady state operational behavior. The flowsheet of the gasifier is shown in Figure 2-1.

The model accounts for gasification kinetics and sulfur capture kinetics. These two kinetics expressions are integrated with CSTR residence time distribution flow pattern for both gas and solid phases. The basic assumptions are described as following.

### 2.1.1 Hydrodynamics

The solid phase (coal, desulfurization sorbent) and the gas phase (oxidant, steam, recycle gas) can be injected into the fluid bed from different positions. It is assumed that the gases and solids in the bed are fully mixed. There is no consideration of the momentum balance for both gas and solid phases.

There is no consideration of coal particle size in gasification calculation. It is because that the reaction rate of coal gasification in the fluid bed is much slower than the gas diffusion in the solid particle. But, It can be seen later that the particle size of the sorbent has the strong effect on the sulfur capture.

### 2.1.2 Thermodynamics

The gas phase is assumed to follow the ideal gas law. This is justified because of the industry range of the operating temperature (1500 °F to 2000 °F) and pressure (1 atm to 40 atm).

The heat capacities of the gases and the solids are expressed as the functions of the operating temperature. The heat balance calculations are based on the total enthalpy of the input and output streams as shown in Figure 2.1.

The water shift reaction

$$CO + H_2O = CO_2 + H_2 \qquad (2.1)$$

is assumed to be at thermodynamic equilibrium at the gasifier operating conditions for all the CO, $CO_2$, $H_2$ and $H_2O$ generated by the combustion, devolatilization and gasification. This is justified because the water shift reaction is about 1000 times

faster than the gasification at the gasifier operating temperature.

### 2.1.3 Coal Devolatilization

When the coal is injected into the bed, it is assumed that devolatilization occurs instantaneously compared to gasification(Wen 1983). The program calculates the devolatilization carbon conversion with consistence of concentration of the volatile in the coal. It is assumed that the volatiles are evaluated into the gas phase and cracked to CO, $CO_2$, $H_2$, $H_2O$ and $CH_4$.

### 2.1.4 Char Combustion

Combustion kinetics are assumed to be instantaneous. Char and volatiles combustion with oxygen occur much faster than the gasification reaction at the operating conditions of the gasifier(Wen 1977, Amundson 1979). The oxygen disappears in seconds after being fed into the gasifier flame zone. Refer to the calculation in the Appendix D. However, the complete char gasification requires hours. Compared to this, the calculation of combustion kinetics can be neglected in the gasifier simulation.

Combustion products are $H_2O$, CO, and $CO_2$. Char combusts

with oxygen to yield CO and $CO_2$ at a molar ratio of unity based on the carbon oxygen reaction:

$$C + 1/\phi\ O_2 = 2(1 - 1/\phi)\ CO + (2/\phi - 1)\ CO_2 \quad (2.2)$$

with $\phi$=1.333 (Shinnar 1988, Wen 1983).

### 2.1.5 Char Gasification

Gasification occurs uniformly through the bed based on the CSTR assumption both for gases and solids. Species present in the gasification zone are: CO, $CO_2$, $H_2$, $H_2O$, $N_2$, $CH_4$, $H_2S$, $NH_3$, char, ash and sorbent (Higher-order hydrocarbons are unstable at normal gasifier operating temperatures and crack to CO, $CO_2$, $H_2$, and $CH_4$).

### 2.1.6 Sulfur Capture

The amount of sulfur released to the gas phase as $H_2S$ is proportional to the converted carbon in the coal . The released sulfur reacts with CaO to form CaS. The CaS is removed without oxidation. The CaO is formed from calcination of dolomite or limestone.

The algorithm for computing the sulfur capture rate depending upon whether or not the $CO_2$ partial pressure is above or below that required at equilibrium has been incorporated into the program. According to the dissociation

reaction of

$$CaCO_3 \rightleftharpoons CaO + CO_2 \qquad (2.3)$$

if the partial pressure of $CO_2$ is lower than the equilibrium for the reaction above, assume that the reaction occurs completely, and that there is no $CaCO_3$ existing in the solid withdrawal. The sulfur capture driving force is calculated according the reaction of

$$CaO + H_2S = CaS + H_2O \qquad (2.4)$$

If the partial pressure of $CO_2$ is higher than the equilibrium of Eq.(2.3), CaO disappears in solid withdrawal. The sulfur capture equilibrium calculation depends on the reaction of

$$CaCO_3 + H_2S = CaS + CO_2 + H_2O \qquad (2.5)$$

In this case, the driving force for the kinetics is calculated according the equilibrium of Eq.(2.4).

Based on these assumptions, A gasifier simulation model is developed with mass and energy balance which can be found in Appendix C. A simplified two parameter char gasification kinetic expression and a shrinking core desulfurization kinetic expression have been used and are described in Section 2.3 and 2.4.

## 2.2. Model Description

The input and output streams shown in Figure 2.1 are described as follows.

Coal can be fed to the middle or bottom of the gasifier (Stream S1). The moisture and volatiles in the coal are released to the gas phase immediately. The carbon conversion of devolatilization is calculated as the stoichiometric amount based on the ultimate and approximate analysis of the coal and the pyrolysis experiment data. The devolatilized char and released volatile combust with oxygen in the combustion zone. The remained char reacts with the gases in the bed. The carbon conversion due to gasification is calculated by the gasification kinetic expression shown in Appendix A.

Oxidant enters the bottom of the gasifier (Stream G1) and reacts with the char or gases (include released volatiles). The composition of the oxidant can be specified by the user to correspond to air, Oxygen enriched air or pure oxygen. Oxidation of char to CO and $CO_2$ takes place instantaneously, and reaction-limited char gasification then takes place uniformly throughout the bed. (Actually, the oxygen penetrates into the dense phase and disappears within few inches which is shown in Appendix D).

Steam is fed into bottom of the bed as a gasification agent and the combustion zone coolant (Stream G2). The water gas shift reaction is assumed to be in equilibrium. All gases behave ideally. The gas entrance jets are assumed to have a negligible effect on the reactor performance.

Dolomite or limestone can be fed into the gasifier as a desulfurization sorbent at different ratio of $CaCO_3$ to $MgCO_3$ (Stream S2). The $MgCO_3$ dissociation occurs completely due to the thermodynamic equilibrium. The calcination reaction of the $CaCO_3$ depends on the $CO_2$ equilibrium partial pressure of the calcination reaction(Eq.2.3). The output solid stream (S4, S5) contains $CaCO_3$, CaO, MgO, CaS, ash and unconverted char depending upon the calcination equilibria, gasification and desulfurization kinetics. The sulfur capture calculation is given by Appendix B.

Of the many gaseous species involved in coal gasification, six--CO, $CO_2$, $H_2$, $H_2O$, $CH_4$, and $N_2$-- typically account for more than 99% by volume of the in-bed and pyrolysis gases. These are the only species included in the gasification calculation. The impact of recycle gases and solids also can be handled by the model.

The following discussion will concentrate on the details of coal devolatilization, char combustion and the kinetics of

gasification and desulfurization.

## 2.3 Two Parameter Char Gasification Kinetics

Since the char gasification reaction is much slower than combustion and devolatilization, the volume of the gasifier is dependent on the gasification rate of char (Amundson 1978, Chen 1982, Katta 1981, Matsui 1987, Rhinhart 1987). A proper understanding of char gasification is essential for gasifier modelling. Effect of temperature, pressure, and gaseous compositions on the rate of char gasification have been extensively studied by various investigators (Dutta 1977, Arri 1978, Katta 1981, Kumpinsky 1983, Muhien 1985, van Heek 1985, Matsui 1987, Raghunathan 1989, Goyal 1989). Raghunathan, R and I. Matsui have shown that in fact all the models exhibite the same gasification kinetic behavior below a carbon conversion of 70%. Carbon reactivity decreases above 70 % conversion, and different descriptions of the high conversion behaviors have been given by the investigators. A brief summary will be presented as following.

The expression of gasification kinetics can written as

$$\frac{dx}{dt} = KR_o f(x) \qquad (2.6)$$

where x is the carbon conversion of the gasification and

defined by

$$x = \frac{gasified\ carbon}{input\ carbon} \qquad (2.7)$$

The gasification kinetics can be divided up by two parts. One is initial reactivity, $KR_o$, where K is a catalyst factor to account for different coal structures and mineral content, $R_o$ is the function of temperature, pressure and external gas composition. The another part is the function of carbon conversion, f(x), which express the reactivity change with carbon conversion. Different expressions for these two parts have been used by different investigators. The assumptions will be given for different kinds of gasification kinetics.

### 2.3.1 Chemical Reactions and Expressions of Rate Terms

The following are the important reactions in the gasification of carbon(Amundson 1979):

$$C + H_2O = CO + H_2 \qquad (2.8)$$

$$C + CO_2 = 2\ CO_2 \qquad (2.9)$$

$$CO + H_2O = CO_2 + H_2 \qquad (2.10)$$

On the basis of information available in the literature, the rate of reaction of char with steam and carbon dioxide appears to depend on the following factors:

A) The type of the coal from which char is prepared, and the heating rate of the preparation;

B) The change in reactivity with the char pore structure during gasification;

C) The temperature and pressure in the reactor;

D) The gaseous composition surrounding the char particles;

E) The mineral content of the char.

Based on these factors, several gasification reaction rate expressions have been presented in the literatures.

One expression is based on the grain model for gas-solid non-catalytic reaction and is of the form

$$\frac{dx}{dt} = R_o(1 - x)^m \qquad (2.11)$$

The parameter m is the grain shape factor. It can also be viewed as the order of the reaction with respect to the solid (Ishida 1971). Equation (2.11) for m=1 or 2/3 has been widely used to fit char gasification data. For m=1, Equation (2.11) becomes a volume reaction model and the integration is:

$$x = 1 - \exp(-R_o t) \qquad (2.12)$$

For m=2/3, a shrinking core model with surface reaction controlled is obtained, and the integration yields:

$$x = 1 - (1 - \frac{1}{3}R_o t)^3 \qquad (2.13)$$

or

$$\frac{t}{\tau} = 1 - (1 - x)^{\frac{1}{3}} \qquad (2.14)$$

where $\tau$ is the complete reaction time of a char particle.

The random pore model based on pore evolution was given by Bhatia and Perlmutter (1980); and by Gavalas (1980). this model has the form

$$\frac{dx}{dt} = R_o(1 - x)\,[1 - \phi \ln(1 - x)]^{\frac{1}{2}} \qquad (2.15)$$

An empirical expression developed by Jonson (1974) has been widely used for gasification simulation. It has the form

$$\frac{dx}{dt} = f_L k_T (1 - x)^{(2/3)} \exp(-\alpha x^2) \qquad (2.16)$$

where $f_L$ is a relative reactivity factor characteristic of each coal, $k_T$ is the reactivity of the char at 0% carbon conversion, and $\alpha$ is the reactivity decay factor which is a function of partial pressures of hydrogen and steam, but is essentially constant at 0.98 at gasification operating conditions.

Jonson's gasification kinetic expression is actually a two parameter model which describes well the initial and final behavior of the single particle gasification process. However, it can not be integrated analytically. In the gasifier simulation, the residence time distribution has to be considered and integrated with respect to the gasification kinetics (See Appendix A). For modelling simplicity, a two parameter single particle kinetic expression has been used in this study.

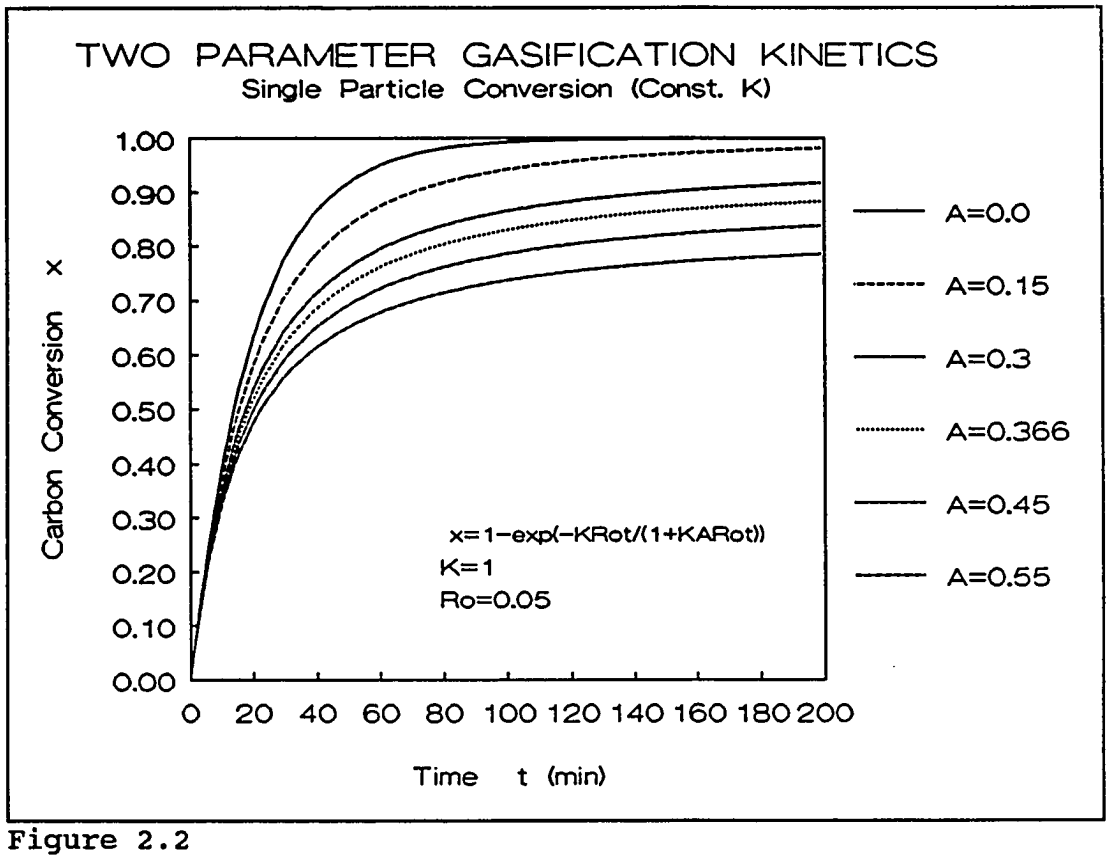


Figure 2.2

For modification of the one parameter volume model, single particle non catalytic reaction can be described as

$$x = 1 - \exp\left(-kR_o \frac{t}{1 + AkR_o t}\right) \qquad (2.17)$$

x is the carbon conversion defined by the ratio of reacted carbon to the initial carbon in the char. where K is a relative reactivity factor for each coal, $R_o$ is the initial reactivity at 0% carbon conversion and A is a conversion decay factor to describe the reactivity decaying with increasing the carbon conversion. Obviously, with A=0, this model becomes

the volume model. However, it can be reproduce any model discussed above by changing A from 0 to 0.35.

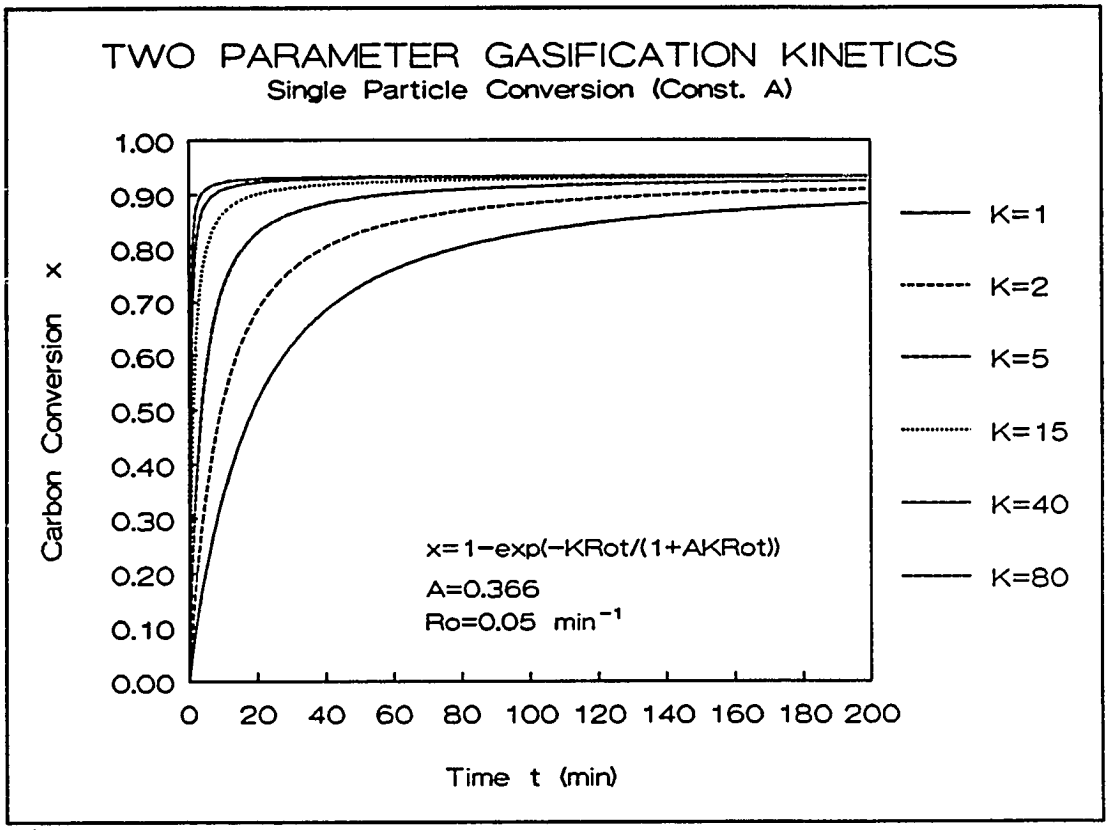


Figure 2.3

In Figures 2.2 and 2.3, the plots of different values of the parameters K and A are given at fixed $R_o$ which can be calculated using the expression of Muhlen (1985).

It is convenient to get the parameters K and A directly from the TGA data. the integration with different residence time distribution functions for calculate the average conversion in the reactor are shown in Appendix A. A Continuous Stirred Tank Reactor residence time distribution

model is used for the solids in this fluid bed gasifier simulation .

## 2.4 Shrinking Core Model Sulfur Capture Kinetics

For predicting sulfur capture using dolomite or limestone in a gasifier, a shrinking core model with ash layer controlling was built into the gasifier simulation program. The sulfur capture and coal conversion can be solved simultaneously with interaction of gas and solid compositions.

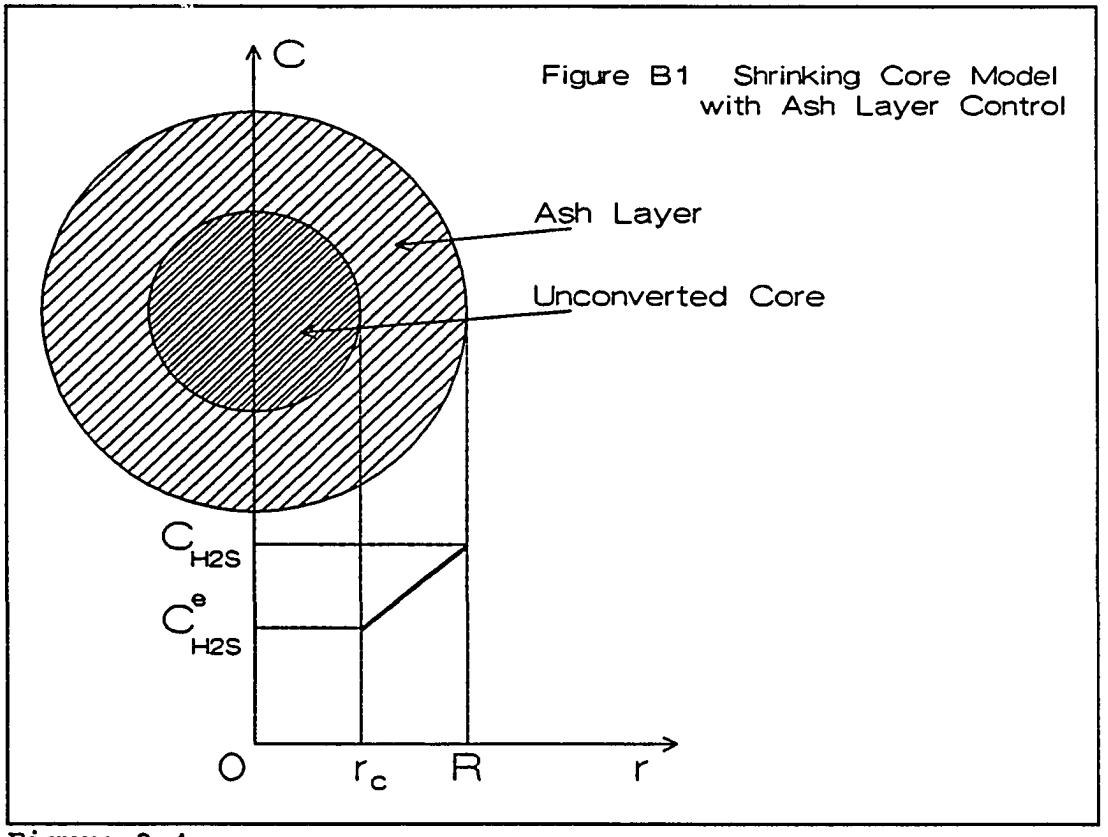


Figure 2.4

The shrinking core model is a one parameter model which describes the non-catalytic gas solid reaction as shown in Figure 2.4. The reaction front advances from the outer surface into the solid leaving behind a layer of completely converted and inert solid called the ash or product layer. At the same time the core of unconverted solids shrinks and finally disappears.

Consider the reaction of CaO and $H_2S$,

$$CaO + H_2S \rightleftharpoons CaS + H_2O \qquad (2.18)$$

According to Figure 2.4, assuming the concentration of the reaction gas $C_{H2S}$ equals to equilibrium concentration $C_{H2S}^e$ at $r = r_c$, the total reaction rate equals to the diffusion rate through the ash layer. The reaction rate of gas and solid can be written as:

$$-\frac{dn_{H2S}}{dt} = 4\pi r^2 D_{H2S} \frac{dC_{H2S}}{dr} \qquad (2.19)$$

where $D_{H2S}$ is the diffusion coefficient of $H_2S$ through the ash layer. Integrating Eq.(2.19) from $r=r_c$, $C_{H2S}=C_{H2S}^e$, to $r=R$, $C_{H2S}=C_{H2S}$, which is bulk gas phase concentration.

$$-\frac{dn_{H2S}}{dt}\left(\frac{1}{r_c} - \frac{1}{R}\right) = 4\pi D_{H2S}(C_{H2S} - C_{H2S}^e) \qquad (2.20)$$

From Eq.(2.18), we have the mass conservation:

$$-dn_{CaO} = -dn_{H2S} = -\rho_p \, dV_p = -4\pi\rho_p \, r_c^2 dr_c \qquad (2.21)$$

where $\rho_p$ is the density of the solid particle, substituting Eq.(2.21) to Eq.(2.20) and integrating it, the result is

$$t = \tau(1-3(\frac{r_c}{R})^2 + 2(\frac{r_c}{R})^3) \qquad (2.22)$$

where $\tau$ is the time for complete conversion of the solid particle, and can be calculated by

$$\tau = \frac{\rho_p R^2}{6D_{H2S}(C_{H2S} - C^e_{H2S})} \qquad (2.23)$$

The relation between the particle conversion and radius of shrinking core is

$$1 - x = (\frac{r_c}{R})^3 \qquad (2.24)$$

Finally, the shrinking core model can be written as a dimenssionless expression which is only the function of single particle conversion.

$$\frac{t}{\tau} = 1 - 3(1 - x)^{(2/3)} + 2(1 - x) \qquad (2.25)$$

Eq.(2.25) describes the reaction history of a single particle. For estimating the average conversion of total particles in the reactor Xav, we have to integrate Eq.(2.25) with residence time distribution density function, first CSTR flow model:

$$Xav = \int_0^{\infty} x \frac{1}{Tav} \exp\left(-\frac{t}{Tav}\right) dt \qquad (2.26)$$

where Tav is the total particles average residence time through the reactor. Substituting Eq.(2.25) into Eq.(2.26), yield:

$$Xav = \exp\left(-\frac{\tau}{Tav}\right) + \left[\int_0^1 2\left(\frac{\tau}{Tav}\right) x\left((1-x)^{(1/3)} - 1\right) \exp\left(-\frac{\tau}{Tav}\right)\left(1 - 3(1-x)^{(2/3)} + 2(1-x)\right) dx\right] \qquad (2.27)$$

Obviously, Xav is the function of ($\tau$/Tav) only, and $\tau$ is the total conversion time of single particle which is the function of temperature, pressure, and gas composition. $\tau$ can be calculated by

$$\tau = \frac{0.000706\,(15.0 d_p + 710 d_p^2)\sqrt{T}}{(y_{H2S} - y_{H2S}^e)} \qquad (2.28)$$

Tav is the average residence time of all the particles flow through the reactor which is the ratio of total bed weight to solid withdraw rate.

The sulfur capture performance strongly depends on the sorbent particle size and the sorbent to sulfur ratio Ca/S as well as the average residence time of solids through the bed Tav. Another effect is operating temperature and steam

concentration on the equilibrium of CaO and $H^2S$ reaction. These effects can be seen from Figure 2.5 to Figure 2.7.

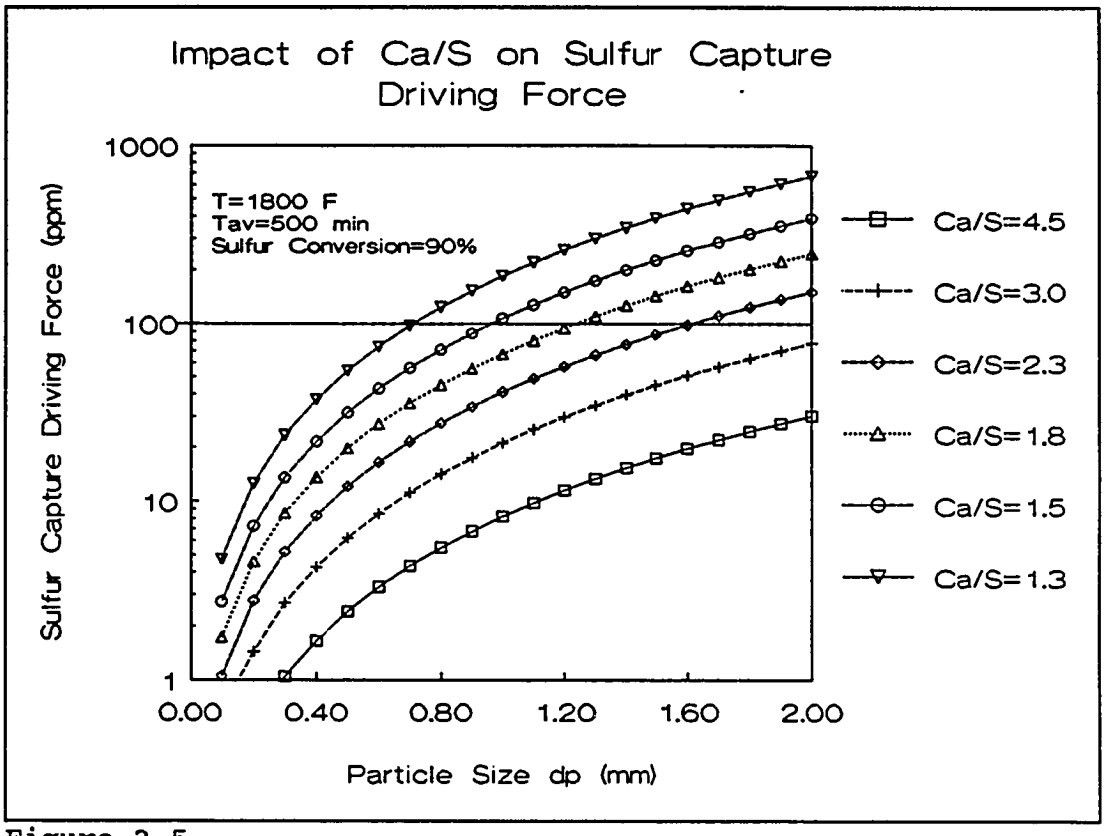


Figure 2.5

Figure 2.5 shows the impact of calcium to sulfur ratio and the sorbent particle size on the driving force in Eq.(2.28). This is the difference of the output $H_2S$ and the equilibrium concentration. It is required for 90% sulfur capture at temperature of 1800 °F. From Eq.(2.28), It is clear that the temperature has less effect on sulfur capture kinetics. The average residence time based on the solid withdrawal is 500 min. It can be seen from this plot that the

acceptable sorbent particle size and Ca/S ratio are located below the driving force of 100 ppm, if the high sulfur coal is fed (the sulfur concentration is 3000 to 4000 ppm without sulfur capture) and the equilibrium concentration is about 200 ppm.

The effect of the average residence time can be seen from Figure 2.6. For a shorter residence time of the solids based on the withdrawal rate, a smaller particle size is required for achieving 90% sulfur capture. A detailed

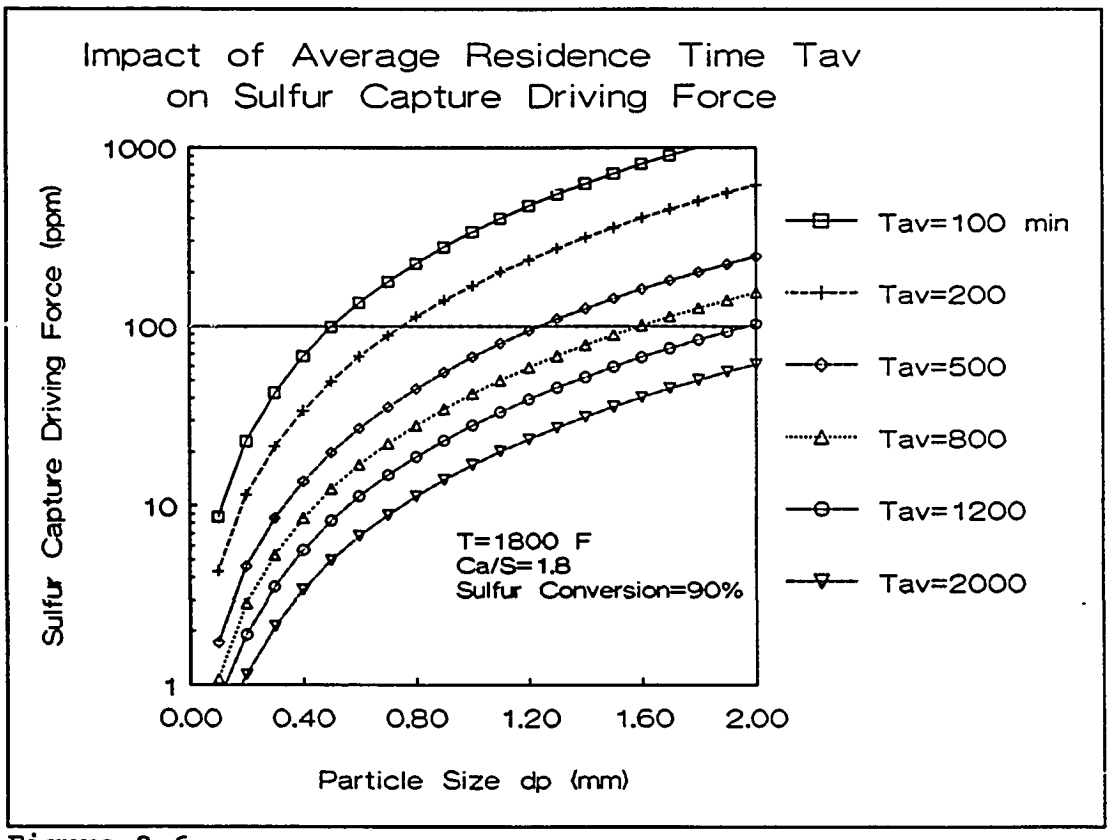


Figure 2.6

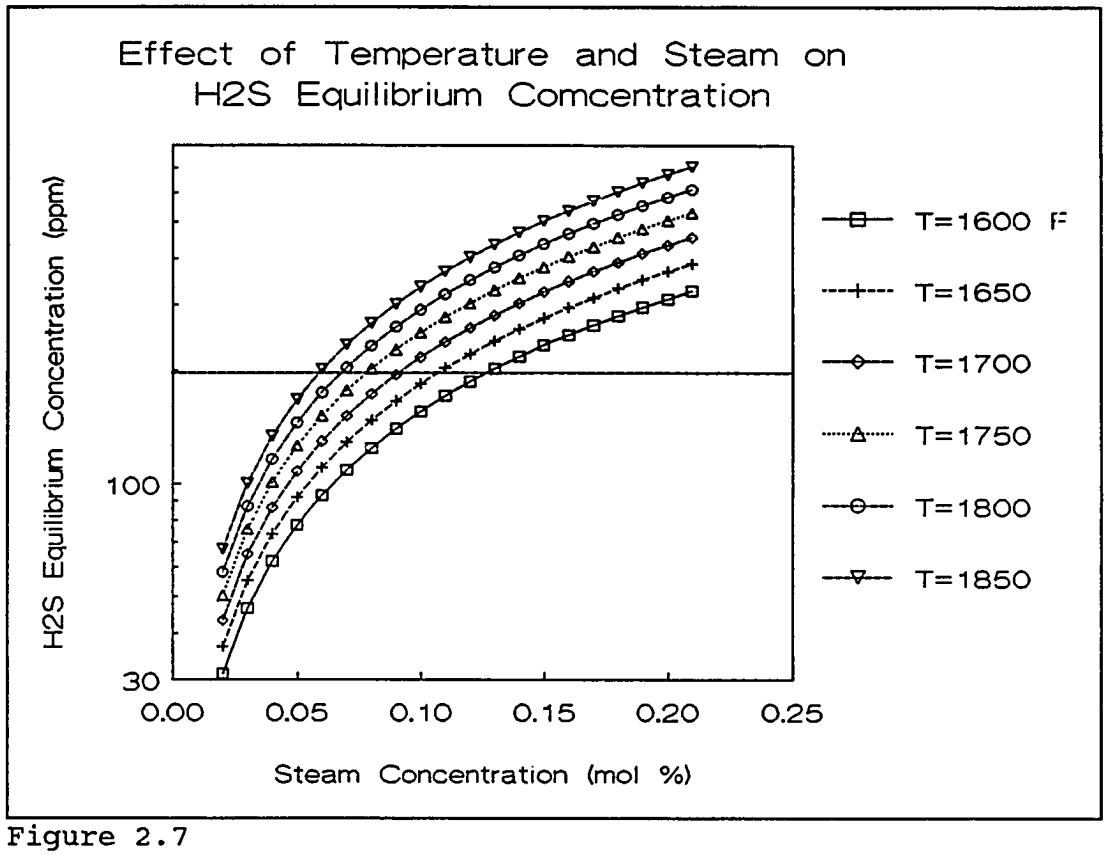


Figure 2.7

discussion of the residence time effect will be given in next Chapter.

In the simulation model, all the effects shown in Figure 2.5 and Figure 2.6 are based on the equilibrium concentration of $H_2S$ in the operating conditions of the gasifier, which will be discussed in next Chapter. The effects of temperature and steam concentration are shown in Figure 2.7. It shows the constraints of the operating conditions due to the sulfur capture. If the higher limit of the equilibrium $H_2S$ is 200

ppm, the steam concentration must to keep below 14% in the product gas. The lower gasifier operating temperature, the better sulfur capture performance can be achieved.

In this chapter, the fluid bed gasifier simulation model was given to predict gasification and desulfurization performances. Next Chapter will concentrate on the operating maps which are generated by this model and constraints analysis of the gasifier for the IGCC power plant design and operation.

# Chapter III GASIFIER MODEL VALIDATION AND CONSTRAINTS ANALYSIS

The initially generated solution of the gasifier model were tested extensively by manually checking mass and energy balances. This model was modified as a friendly using version and tested by IGT and GRI at Chicago. The testing with their gasifier mass and energy balance model showed that it is 100% agreement in the mass balance and 0.5% in the energy balance different between the IGT model and our model. It is due to the different source of the thermal data were used. The comparison of the pilot plant data and the model prediction are given as following.

## 3.1 Comparison to Pilot Plant Data

Six runpoints from KRW and IGT pressurized fluid bed gasifiers were simulated. The results are shown in Table 3.1 and Table 3.2. In the model prediction, the coal used is Pittsburgh #8 and it is as same as the coal used in the pilot plant. The calculation temperature and steam feed are specified as same as the pilot plant data. The prediction of the model are carbon conversion, product gas flow rate and the composition as well as the sulfur capture performance.

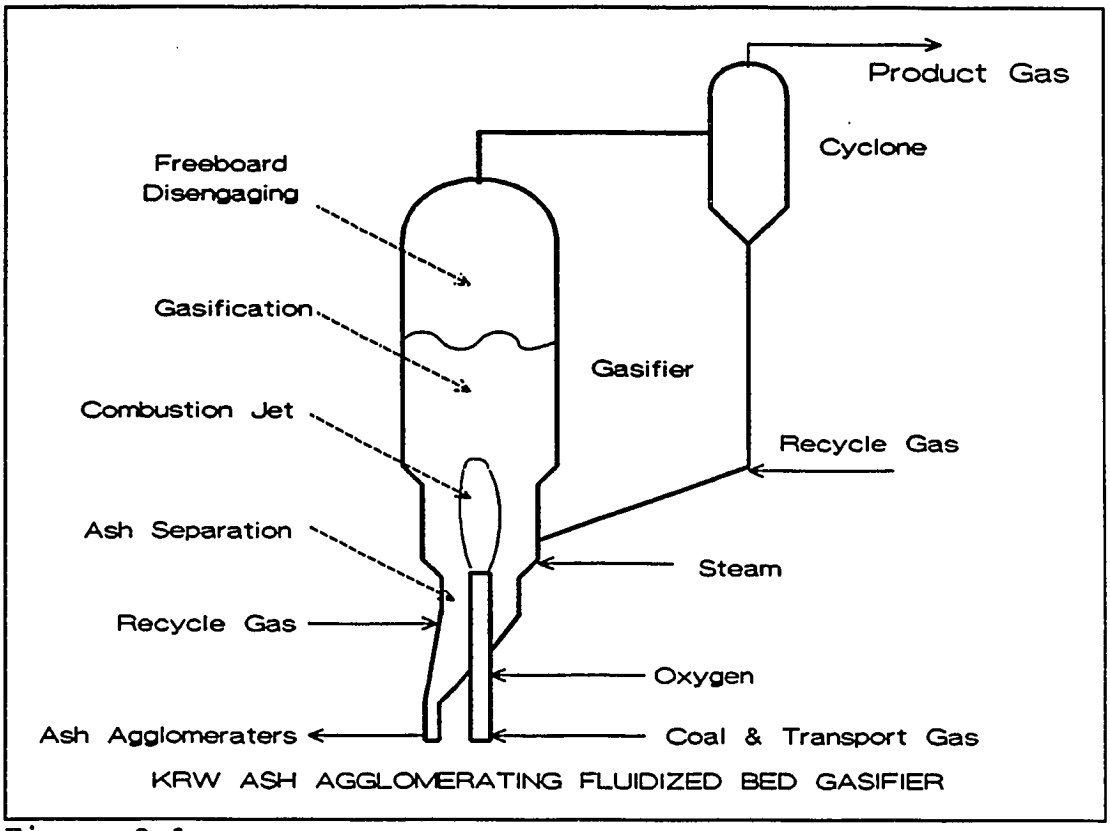


Figure 3.1

### 3.1.1 Comparison of KRW Pilot Plant Data and Model Prediction

The KRW fluid bed gasifier pilot unit was shown in Figure 3.1. The diameter of the fluid bed is 2 ft. and the operating bed is about 20 to 30 ft high. The coal and the sorbent are fed into the bed through the bottom jet. The transportation gas is the recycle product gas. Steam was fed into the flame zone for the temperature control and as the gasification agent.

COMPARISON OF KRW PILOT PLANT AND MODELLING DATA

Coal: Pitt#8 Sorbent : Dolomite, Limestone (SS3D)

| RUN # | TP-36-4-4B | | TP-37-3-2B1 | | TP-36-5-SS3D | |
|---|---|---|---|---|---|---|
| | Pilot P. | Model | Pilot P. | Model | Pilot P. | Model |
| Temperature (F) | 1971 | 1971 | 1832 | 1832 | 1850 | 1850 |
| Pressure (psig) | 215 | 215 | 215 | 215 | 215 | 215 |
| Oxygen/Carbon (mole) | 0.436 | 0.464 | 0.64 | 0.511 | 0.424 | 0.433 |
| Steam/Carbon (mole) | 0.215 | 0.215 | 0.552 | 0.552 | 0.250 | 0.250 |
| Carbon Conversion | 0.91 | 0.90 | 0.92 | 0.89 | 0.85 | 0.86 |
| Product Gas/Coal (mole) | 3.55 | 3.74 | 4.93 | 4.62 | 3.38 | 3.46 |
| YCO (mole fraction) | 0.174 | 0.175 | 0.122 | 0.099 | 0.193 | 0.165 |
| YCO2 | 0.06 | 0.071 | 0.07 | 0.089 | 0.066 | 0.081 |
| YH2 | 0.115 | 0.073 | 0.073 | 0.068 | 0.129 | 0.076 |
| YH2O | 0.048 | 0.061 | 0.075 | 0.104 | 0.04 | 0.064 |
| YCH4 | 0.005 | 0.007 | 0.003 | 0.003 | 0.028 | 0.025 |
| YN2 | 0.598 | 0.601 | 0.655 | 0.622 | 0.559 | 0.587 |
| Eq. H2S in Gas (ppm) | | 275 | | 331 | | 217 |
| H2S in Gas (ppm) | 367 | 305 | 462 | 336 | 1119 | 481 |
| Ca/S (mol) | 2.0 | 2.0 | 3.6 | 3.6 | 1.3 | 1.3 |
| HHV of the Gas (Btu/scf) | 99.0 | 99.3 | 67.1 | 65.3 | 113 | 108 |

Table 3.1

From Table 3.1, the model prediction matches the pilot plant in a reasonable range for the gasification results. The sulfur capture prediction for the $H_2S$ concentration are lower than the pilot plant data. It is due to the model calculation without considering the gas bypass effect. However, the trends of the operating condition can be seen from Table 3.1. With the higher Ca/S ratio and the lower steam concentration, the better sulfur capture results can be achieved.

### 3.1.2 Comparison of Ugas Pilot Plant Data and Model Prediction

The high pressure Ugas fluid bed gasifier at IGT, Chicago, is a 8 in. diameter and has the similar structure as KRW gasifier shown in Figure 3.1. The operating bed height is about 3 to 5 ft. The coal is fed into different position of the bed above the flame zone. A large amount of the steam is fed in to keep the fluidization operation. A large amount of

COMPARISON OF UGAS PILOT PLANT AND MODELLING DATA

Coal: Pitt#8 Sorbent : Dolomite

| RUN # | Lime2-5 | | Lime3-3 | | Lime3-4 | |
|---|---|---|---|---|---|---|
| | Pilot P. | Model | Pilot P. | Model | Pilot P. | Model |
| Temperature (F) | 1845 | 1845 | 1870 | 1870 | 1860 | 1860 |
| Pressure (psig) | 150 | 150 | 303 | 303 | 303 | 303 |
| Oxygen/Carbon | 0.419 | 0.420 | 0.523 | 0.534 | 0.446 | 0.438 |
| Steam/Carbon (mole) | 1.05 | 1.05 | 2.33 | 2.33 | 1.77 | 1.77 |
| Carbon Conversion | 0.90 | 0.891 | 0.947 | 0.962 | 0.959 | 0.919 |
| Product Gas/Coal (mole) | 3.66 | 3.62 | 5.71 | 5.71 | 4.55 | 4.53 |
| YCO (mole fraction) | 0.105 | 0.105 | 0.043 | 0.046 | 0.066 | 0.067 |
| YCO2 | 0.131 | 0.126 | 0.125 | 0.115 | 0.134 | 0.122 |
| YH2 | 0.121 | 0.118 | 0.083 | 0.085 | 0.108 | 0.105 |
| YH2O | 0.233 | 0.242 | 0.366 | 0.362 | 0.329 | 0.330 |
| YCH4 | 0.025 | 0.025 | 0.015 | 0.015 | 0.022 | 0.022 |
| YN2 | 0.384 | 0.384 | 0.365 | 0.378 | 0.339 | 0.352 |
| Eq. H2S in Gas (ppm) | | 617 | | 1057 | | 809 |
| H2S in Gas (ppm) | 1066 | 711 | 1907 | 1160 | 2161 | 966 |
| Ca/S (mol) | 2.59 | 2.59 | 1.72 | 1.72 | 2.25 | 2.26 |
| HHV of Gas (wt) Btu/scf | 105 | 109 | 61.0 | 65.7 | 84.8 | 91.4 |

Table 3.2

the solid withdrawal has been found in the cyclone due to the high superficial velocity of the gas through the bed (4 to 5

ft/sec at about 300 psi.). The higher carbon conversion achieved in these runs (see Table 3.2) compare to KRW pilot plant data is due to the higher steam input (about 10 times as KRW runs). The more energy in the coal is used for keeping the heat balance of the gasifier.

In Table 3.2, the prediction shows the drawback to feeding more steam. The more steam is fed in, the less sulfur capture can be achieved. The higher heating value of the product gas is reduced by increasing steam feed.

Impact of Water Content in Coal on Carbonizer Performance

Coal:Pitt#8 Bed Height=15 ft. P=14 atm dp=1 mm *dp=0.2 mm ∘dp=2 mm

| Water Content wt% | 6.0 | 30 | 45 |
|---|---|---|---|
| Temperature (F) | 1650 | 1650 | 1650 |
| Oxygen/Carbon | 0.186 | 0.301 | 0.414 |
| Carbon Conversion | 0.459 | 0.656 | 0.809 |
| Gas HHV (BTU/scf) | 178 | 132 | 103 |
| Cold Gas Efficency % | 37.2 | 45.7 | 49.9 |
| Prod. Gas mol/mol Coal | 1.45 | 2.41 | 3.35 |
| Eq. H2S in Gas (ppm) | 86 | 287 | 487 |
| H2S in Gas (ppm) | ∘566 242 *98 | ∘753 442 *299 | ∘851 606 *497 |
| Sulfur Capture % | ∘88.5 95.1 *98.0 | ∘82.2 89.6 *92.9 | ∘77.4 83.9 *86.8 |
| Air/Prod. Gas (mole) | 0.611 | 0.595 | 0.589 |

Table 3.3

This model not only can be used to show the existing pilot plant operation, also can be used to prepare a pilot plant testing matrix. Table 3.3 shows a example to predict the impact of water content in the coal on a carbonizer performance for Forster Wheeler, which is actually a low conversion gasifier.

From this table, It is not suggested that to use more water for making the slurry. Using the smaller sorbent size is for the better sulfur capture performance.

## 3.2 Operating Maps of the Air-blown Gasifier

This model can be used to investigate the operating range of the gasifier for a coal power plant. The simulation results are presented as operating maps. Each map is a compilation of numerous simulation run-points plotted such that the control variables (oxygen and steam) are parametrically imposed on the performances (such as conversion, coal throughput, product gas heating value) and temperature coordinates.

The operating maps have been plotted using the gasifier model for an input coal of Pittsburgh #8. The dolomite (60 wt% $CaCO_3$, 40 wt% $MgCO_3$) is fed as 1.5 times as stoichiometric

requirement for sulfur capture. The operating maps are shown in Figure 3.2 - 3.5 as the gasifier performances versus the operating temperature at constant oxygen to carbon and steam to carbon ratio.

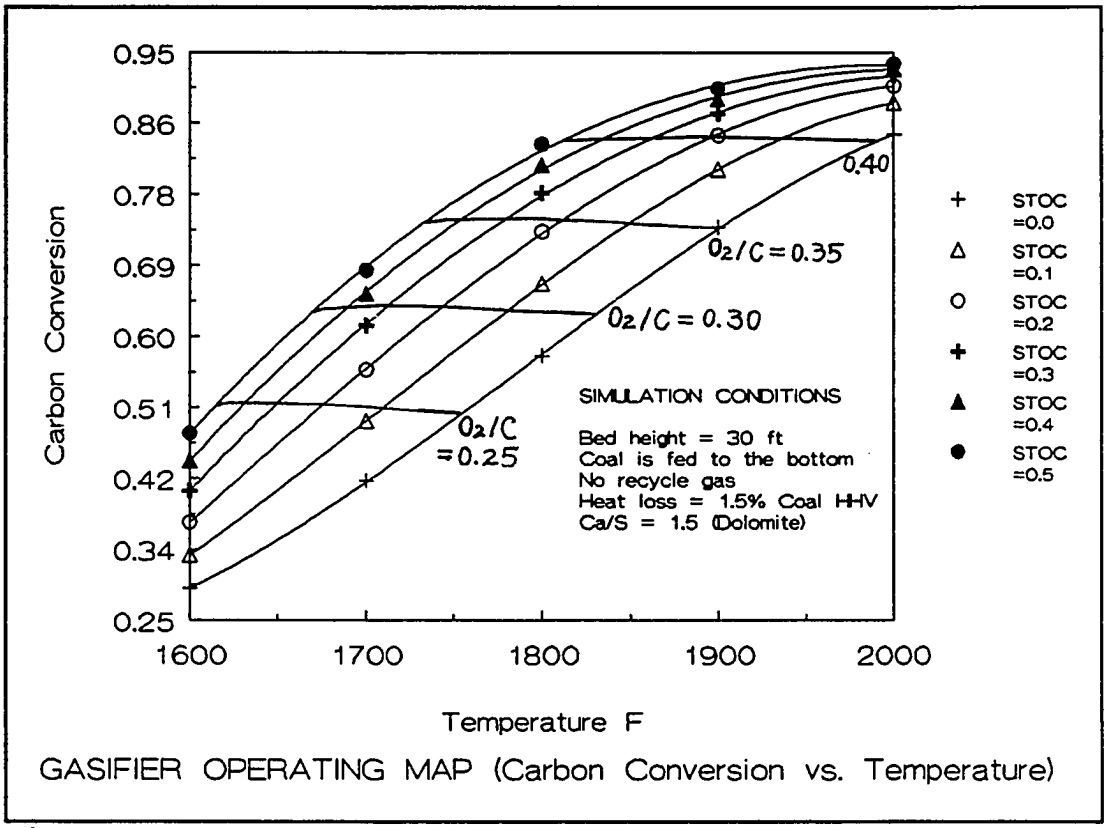


Figure 3.2

The explanation of how an operating map is obtained will be given as following. The operator really has three free variables, namely, the three feed rates for coal, air and steam. But these are not completely free for keeping the fluid bed operation. It is assumed that control of the steady state is based on a constant total bed height, which is controlled by changing the solids withdrawal. Furthermore,

the gas velocity must be maintained in a rather narrow range. A low gas velocity will promote clinkering and defluidization; a high gas velocity will lead to excessive elutriation. In this simulation gas velocity is fixed at 2 feet/second which is in the range of the KRW pilot plant operation. The only impact of changing gas velocity in this model is to change the residence time of the solids for fixing coal feed rate.

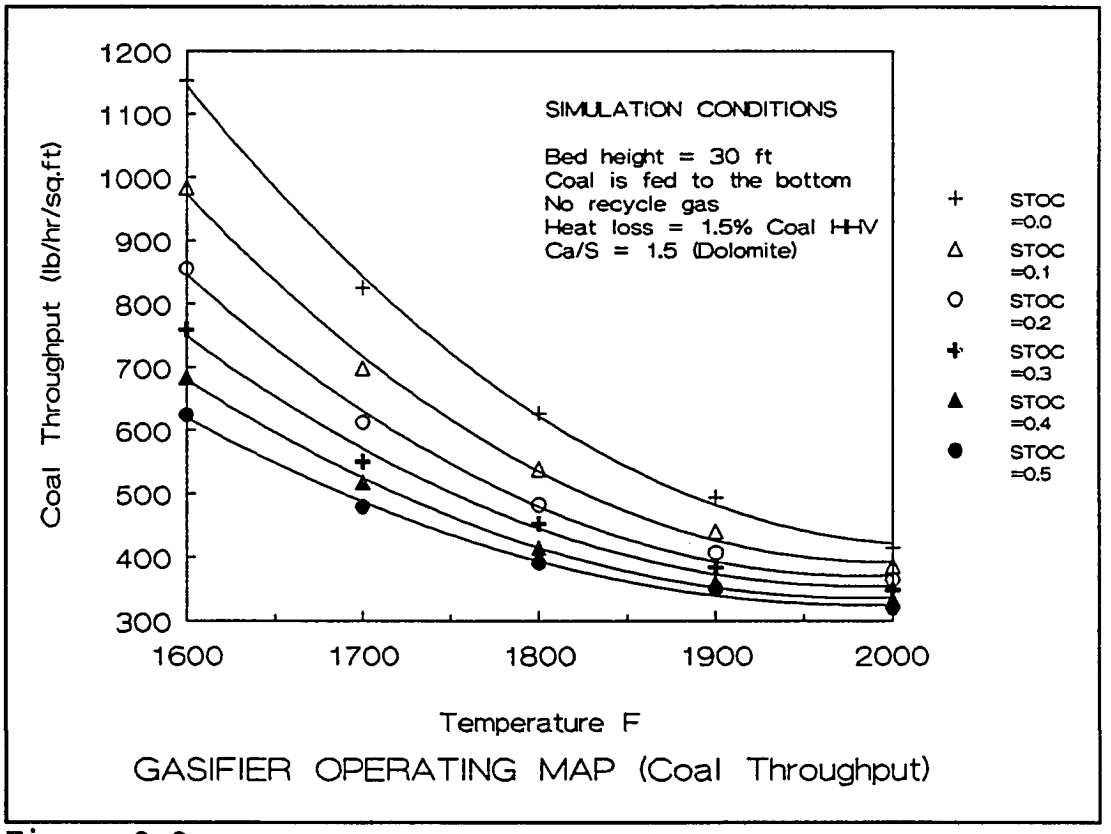


Figure 3.3

Having fixed the pressure, temperature and the total linear velocity of the product gas, only one free variable is left and it is chosen as steam-to-air ratio (or steam-to-

carbon ratio). The oxygen requirement is then a model output, so is carbon conversion and the BTU content of the gas, which depends on the gas composition. If fixing the oxygen feed rate, it needs the iteration to calculate the bed temperature. In reality, the operator adjusts steam-to-air ratio and coal feed rate to keep the temperature below a certain value, but for computational purposes it makes no difference how we arrive at a certain operating condition.

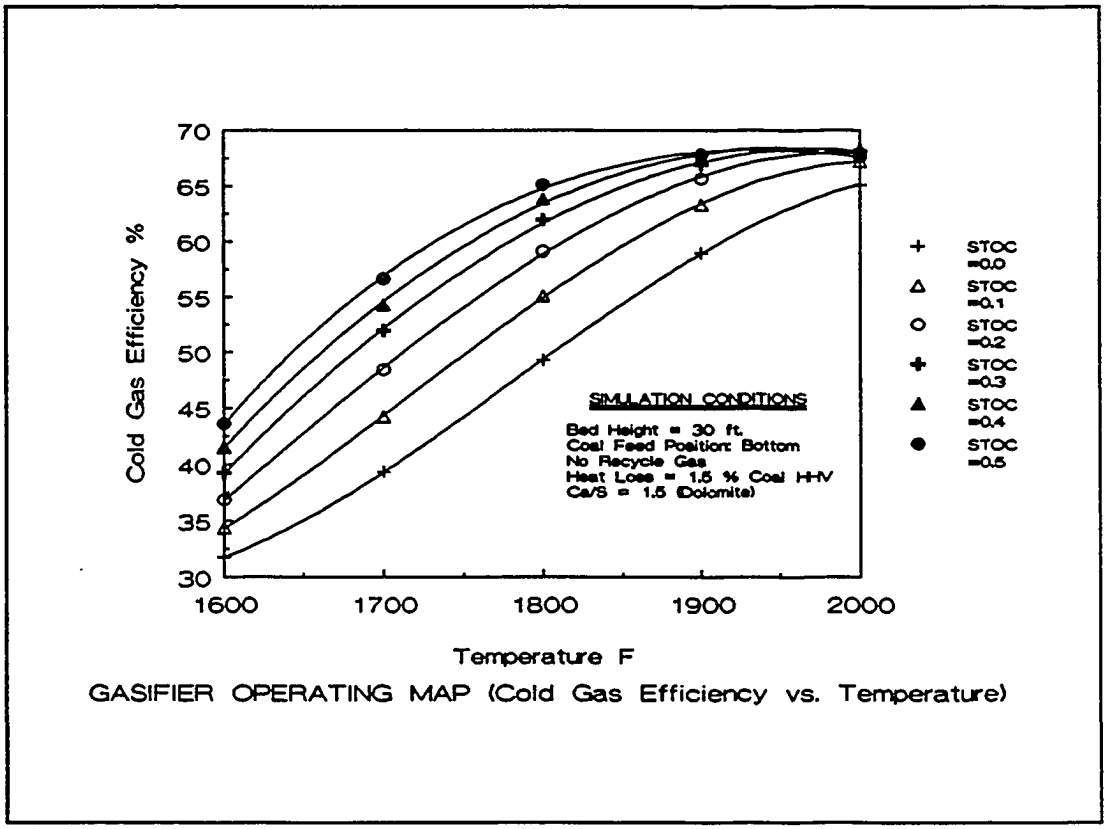


Figure 3.4

In Figures 3.2-3.5 the operating maps for a fluidized bed gasifier, similar to the KRW, are given. We only eliminated

the recycle gas, as it puts a penalty on the performance which will be discussed later.

The key figure used here is Figure 3.2, where the carbon conversion versus the bed temperature with the operating conditions in terms of steam-to-carbon and oxygen-to-carbon ratio. Every points in this figure corresponds to the steam and oxygen feed conditions for a fixed amount of coal feed (Pittsburgh #8) and fixed bed height.

Carbon conversion is a main design and operation parameter. It is strongly changed by varying the temperature and the oxygen to carbon feed ratio. There is a very small effect of steam changes on the carbon conversion, but the bed temperature goes down with increasing the steam feed. It is clear that to control the bed temperature by changing the steam feed rate in a certain range without other disturbance.

Looking at Figure 3.2, it is noted that at constant bed height and gas velocity the main variable that affects gasifier temperature is oxygen-to-carbon ratio. Increase of steam use will increase the oxygen-to-carbon ratio required to achieve a given temperature, which allows a higher carbon conversion at a given temperature. But the range of steam-to-coal ratios which we can chose is severely limited due to the following constraints:

A) Steam adversely affects sulfur capture by the sorbent, as the reaction of calcium oxide with $H_2S$ is thermodynamically limited which was shown in last Chapter.

B) The steam present in the product gas reduces the BTU content of the gas which will be seen in Figure 3.5.

These are the reasons to limit the curves to a steam-to-carbon ratio of 0.5.

Carbon conversion is an important constraint to the overall design. We note that carbon conversions above 90 percent are hard to obtain in this design. It requires either very high temperature or high steam-to-carbon ratios which both are the drawback to sulfur capture and product gas heating value.

As the gas velocity is kept as constant, coal throughput changes and is shown in Figure 3.3. It gives a clear picture of the solids residence time based on the coal feed. The more solids residence time can be achieved, the less coal can be fed into the bed or the larger bed holdup is required. At a given temperature, the coal throughput decreases with increasing steam-to-carbon ratio.

Figure 3.4 gives the cold gas efficiency, which increases with increasing carbon conversion. It will decrease for very

high steam-to-carbon ratios, but the ratios are not practically here for the reasons stated above.

Figure 3.5 gives the HHV of the wet product gas. It decreases both with temperature and increasing ratio of steam-to-oxygen. This Figure gives the range of changing steam for the temperature control, which is 0 to 0.5 steam to carbon ratio.

Figures 3.2-3.5 give a complete picture of the design constraints of the gasifier. The impacts of these constraints on the IGCC plant will be discussed in the later Chapters.

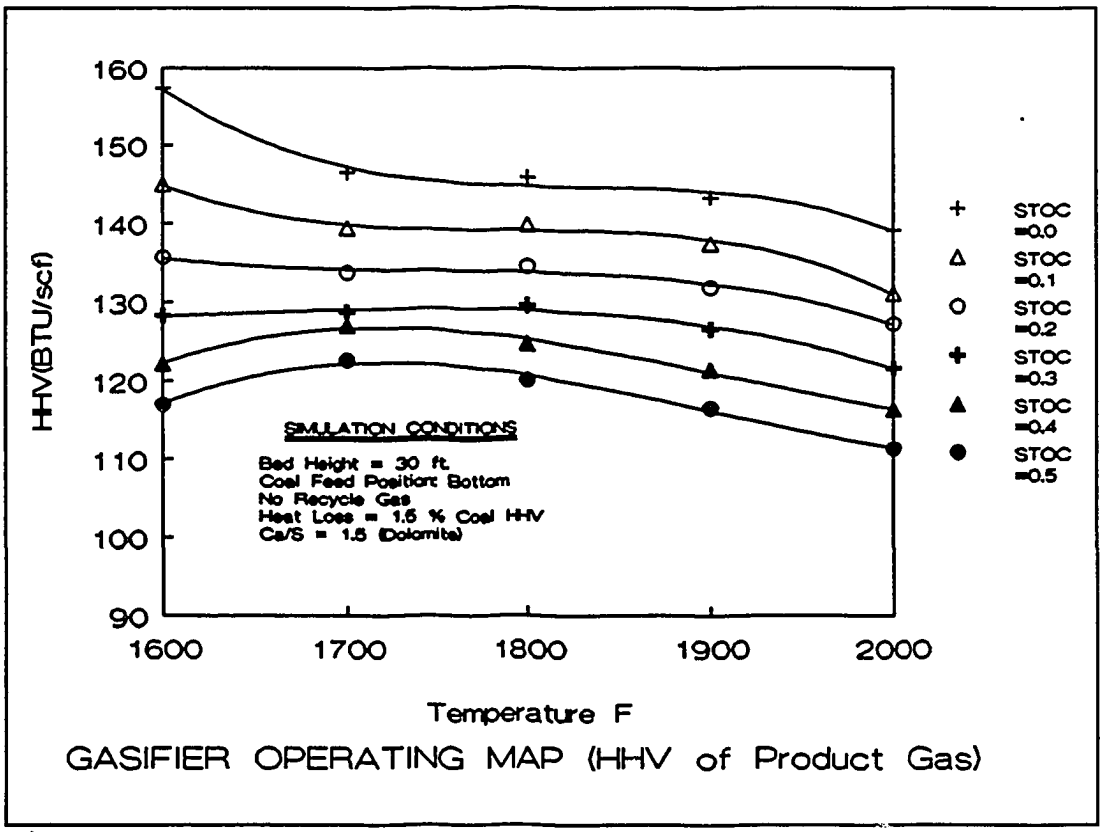


Figure 3.5

One constraint not included in the map is the fact that, above 1800°F, the product gas will be hard to go directly to the cyclone. It is due to that high temperature solid fines in the gas will stick on the cyclone wall. It is suggested to add some water quenching down the temperature of the product gas, but it would further reduce the BTU content of the gas. Alternatively one could use a waste heat boiler before the cyclone but this would complicate the design.

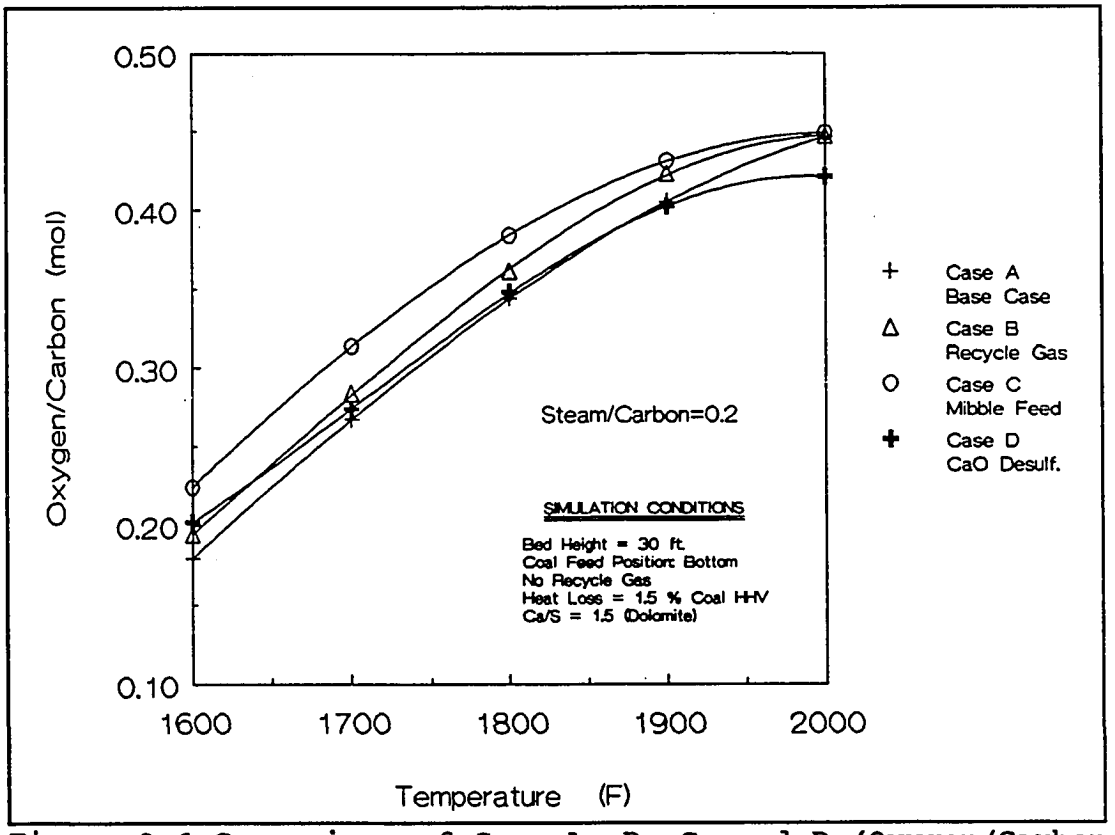


Figure 3.6 Comparison of Case A, B, C, and D (Oxygen/Carbon vs. Temperature)

In Figures 3.6-3.10, we look at the effect of design modifications. Three additional cases have been given which

illustrate the prime variables at the disposal of the designer.

Case A) Case A is the base case for plotting Figure 3.2 to Figure 3.5. Assume 20 percent oxygen combusts with char and 80 percent combusts with volatile released from coal. It simulates the situation of bottom coal feed and no recycle gas used.

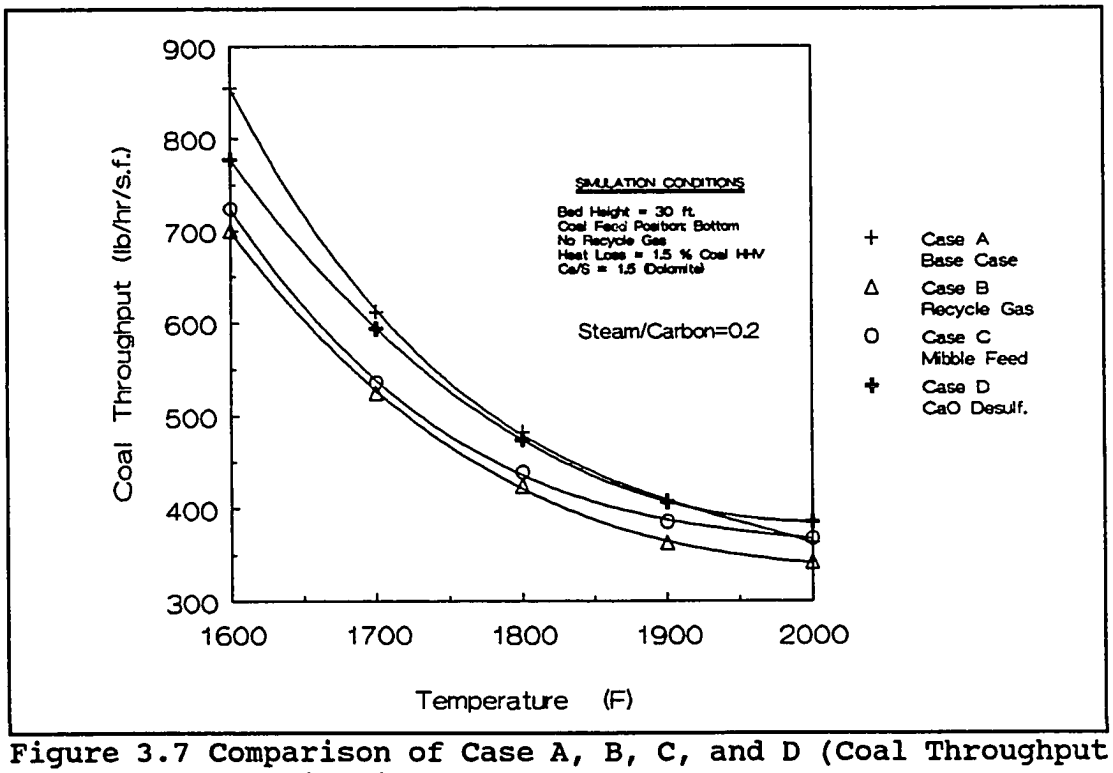


Figure 3.7 Comparison of Case A, B, C, and D (Coal Throughput vs. Temperature)

Case B) This case is representative of the proposed KRW design. Here the recycle gas was included at a rate of 0.5 lb recycle gas per lb coal. The oxygen combusts with the

recycle gas and the volatile, therefore, almost no oxygen combusts with char in the bottom of the bed.

Case C) In this case the coal is fed together with the 10 percent of the air into the middle of the bed, about 6 feet above the air vent. Without dolomite or some other additive this is not feasible with the caking coal. But if dolomite is used, then introducing the coal into the combustion zone introduces a strong penalty without a clear benefit.

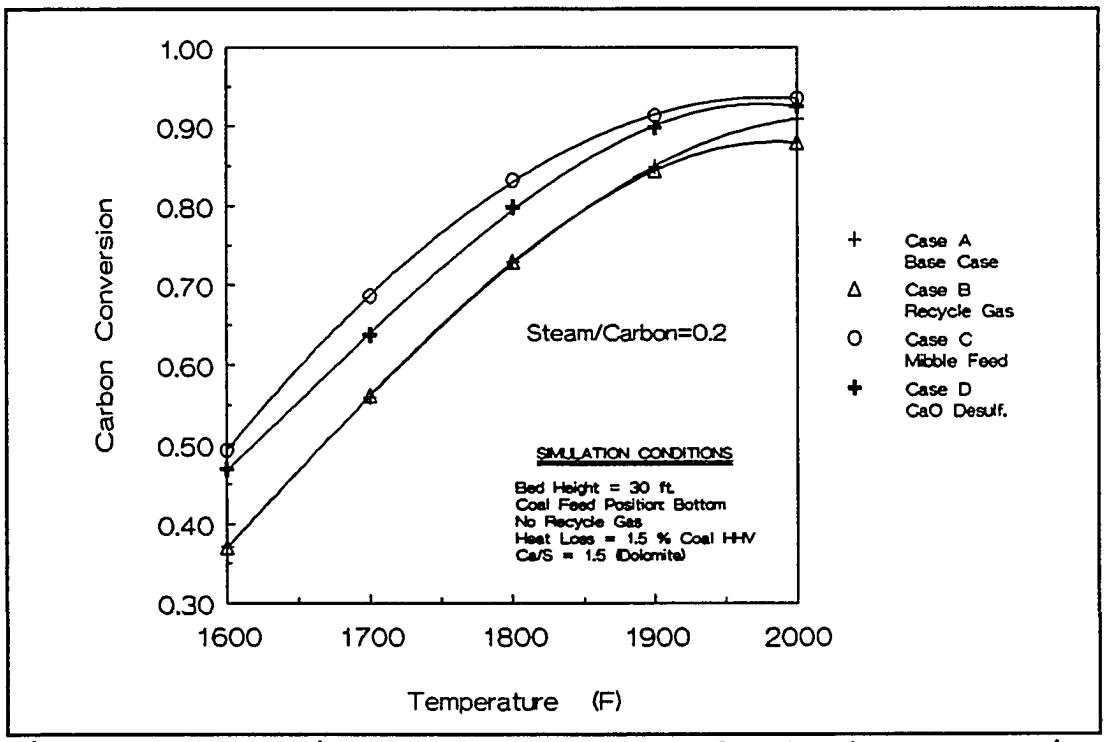


Figure 3.8 Comparison of Case A, B, C and D (Carbon Conversion vs. Temperature)

The penalty is due to the fact that volatiles have a higher reaction rate than the char. We want to preserve all the gaseous volatile and crack the tars formed. The tars and char formed by tar cracking are more reactive for gasification than the char left at high conversion. The reactivity of the char decreases with conversion. It is important that the oxygen reacts with char and not with volatile or recycle gas. In our computation, the amount of oxygen reacting with char is a critical parameter. We assume it would be 20 percent for Case A, 0 percent for Case B, and 80 percent for Case C because of the coal feed position and the transportation gas.

Case D) Here we assume that the dolomite, before entering the gasification zone, is heat exchanged with the product gas. This could be done in a separate reactor (see Chapter IV) or by feeding it from the top. In the first case, we will achieve not only preheat of the dolomite, but also the dissociation of the calcium carbonate. If we feed the dolomite from the top, only part of dissociation reaction will occur. Case D represents the first case.

If the gasifier temperature would be high enough there would be no difference between Case A and Case C, which can be seen from Figure 3.6 to Figure 3.9. In that case, the reaction would approach thermodynamic equilibrium. Obviously,

There is no effect of coal feeding position for Case A and C. Case B and D would still be different as the feeding positions. Case B represents a heat loss due to the cooling of the recycle gas. Case D is equivalent to supplying the calcined dolomite and at a higher temperature.

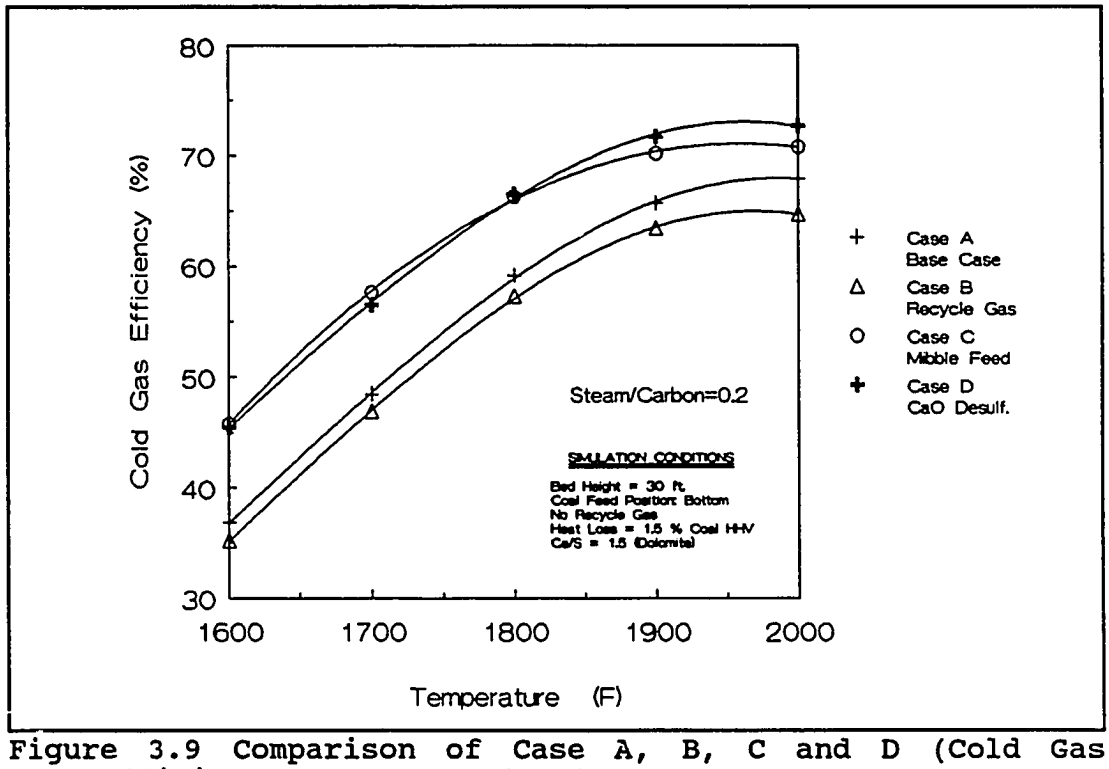


Figure 3.9 Comparison of Case A, B, C and D (Cold Gas Efficiency vs. Temperature)

Now the bed height required to approach equilibrium depends on coal reactivity and temperature. For the coal used here the required temperature is well above 2000°F for reasonable bed heights. The lower the temperature, the stronger the impact of the design.

We give instead in Figures 3.2-3.5 the constant steam-to-carbon ratio lines at 0.2 for each of the Figures 3.6-3.10. If we compare Case B with the base case we note that the main impact is a lowering slightly of the BTU value of the gas (see Figure 3.10).

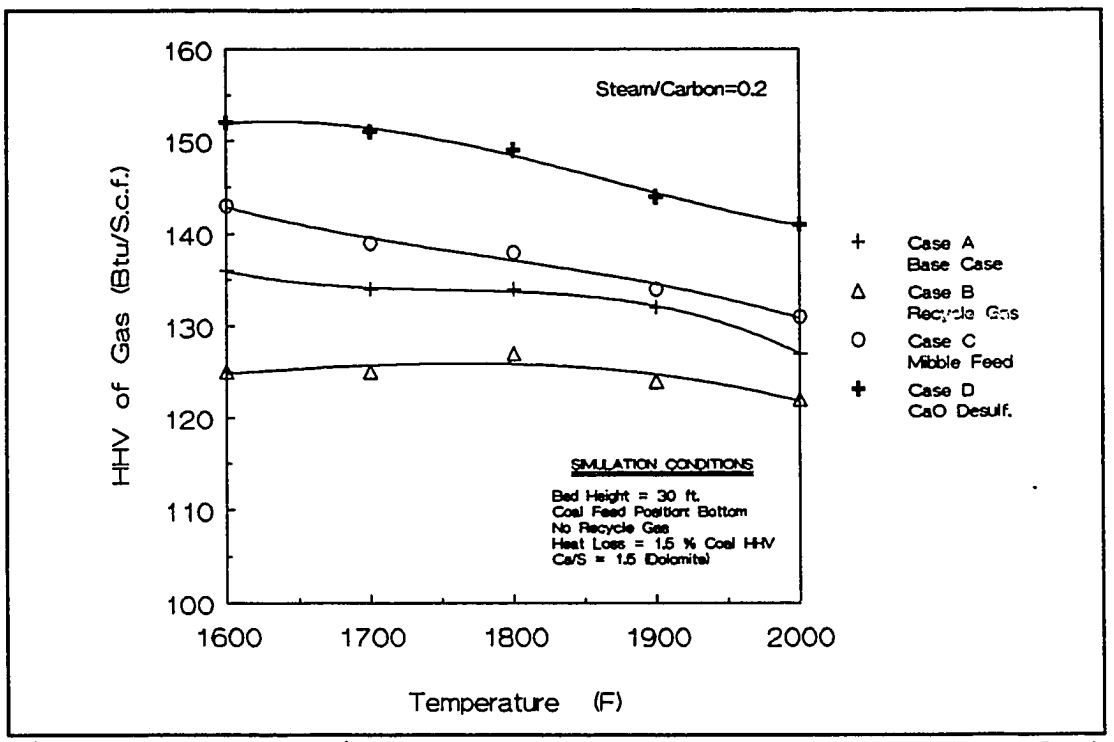


Figure 3.10 Comparison of Case A, B, C and D (HHV of Product Gas vs. Temperature)

To illustrate the effects of the required quench on product gas HHV, three cases are given in Figure 3.11. Four cases are given in Table 3.3. It gives design cases at 1950 F for Cases B and C. The third case is a design case for Case D. In such cases the curves give the higher heating value (HHV) of the wet gas as a function of quenched temperature.

The steam content of the gas can be found in this figure. The HHV of the gas would be too low to be sent to the gas turbine if it is quenched lower than 1000 °F.

On the other hand, the impact of the coal feed position is also important. The oxygen-to-carbon ratio at constant temperature and constant steam-to-oxygen ratio increases. This is due to the fact that the reaction of oxygen with char, forming a mixture of CO and $CO_2$, gives less heat per mole oxygen than the reaction of oxygen with volatile. As 80 percent of the oxygen reacts with char, this increases conversion and it is possible at 1900°F to approach 95

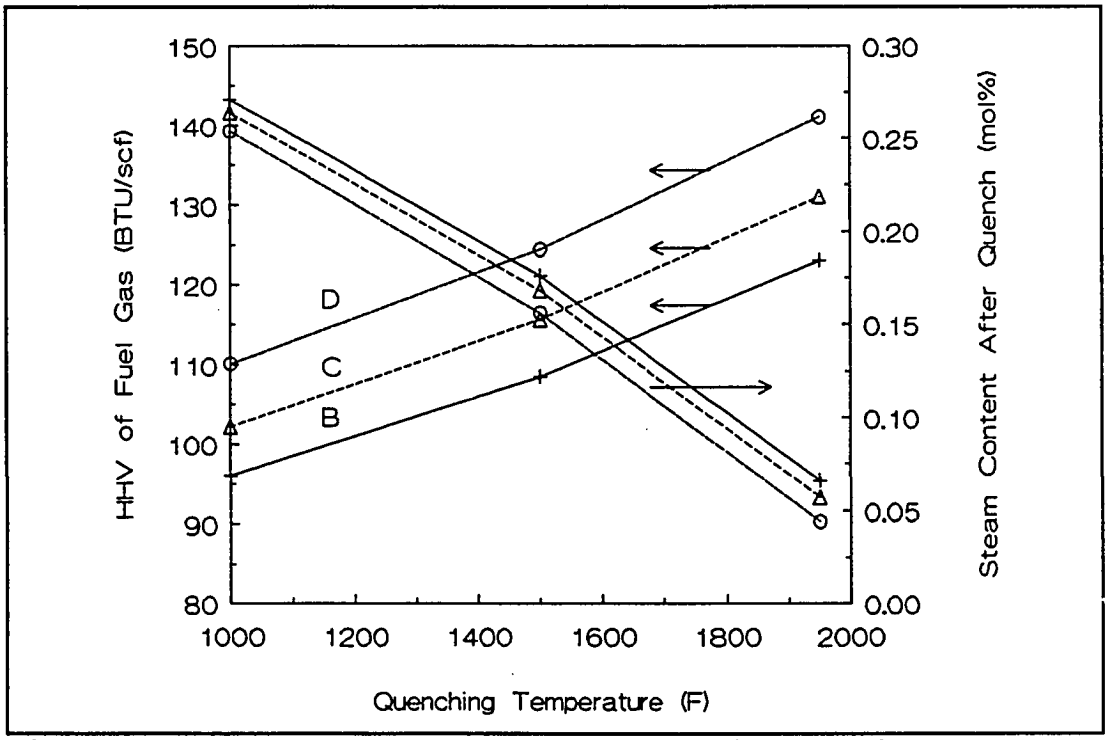


Figure 3.11 Effect of Product Gas Quenching (Design Case B, C and D)

percent conversion. At 1950°F this is feasible at low steam-to-carbon ratios, giving the designer much more freedom. Surprisingly, the BTU content of the gas stays constant in spite of the higher conversion. Therefore, the coal gas efficiency increases significantly, which should increase the overall efficiency of the system.

AIR BLOWN GASIFIER PERFORMANCES (CASE STUDY)

Coal:Pitt#8,(Ca/S=1.5) Case A,B:Bottom feed coal, Case C,D:Middle feed coal

| | | Case A | Case B | Case C | Case D |
|---|---|---|---|---|---|
| Temperature | (F) | 1950 | 1950 | 1950 | 1950 |
| Pressure | (psi) | 250 | 250 | 250 | 250 |
| O2/Coal | (mol/mol Coal) | 0.428 | 0.443 | 0.449 | 0.427 |
| Steam/Coal | (mol/mol Coal) | 0.20 | 0.20 | 0.20 | 0.20 |
| Recycle Gas | (lb/lb mafCoal) | 0.0 | 0.39 | 0.0 | 0.0 |
| Carbon Conversion | (%) | 88.4 | 87.8 | 93.5 | 92.5 |
| Coal throughput | (lb/hr/sq.ft.) | 383 | 349 | 368 | 386 |
| Cold gas efficiency | (%) | 67.3 | 64.9 | 70.8 | 72.7 |
| Product Gas | (mol/mol Coal) | 3.14 | 3.19 | 3.27 | 3.12 |
| YCO | (mol. fraction) | 0.233 | 0.222 | 0.239 | 0.251 |
| YCO2 | | 0.056 | 0.059 | 0.053 | 0.039 |
| YH2 | | 0.129 | 0.122 | 0.127 | 0.144 |
| YH2O | | 0.062 | 0.066 | 0.057 | 0.044 |
| YCH4 | | 0.006 | 0.006 | 0.006 | 0.006 |
| YN2 | | 0.514 | 0.523 | 0.517 | 0.509 |
| HHV of gas | (Btu/scf) | 129 | 123 | 131 | 141 |

Table 3.4

Case D is slightly different. On the gasifier, the impact is small. Conversion at constant temperature is slightly lower, compensated by slightly increasing gasifier temperature. The main advantage of D is that final gas temperature is lower. The gas before the turbine has to be cool to allow use of control value; a lower outlet temperature at constant conversion is a great advantage in the overall

design.

In Table 3.4, we give the overall thermal efficiency of the cases in Table 3.3. To estimate this thermal efficiency, we used a flowsheet given in Figure 3.12. In all cases, dolomite is added to the gasifier in a stoichiometric ratio of Ca/S of 1.5. The gas in all cases is quenched to 1500°F and then cooled in a boiler to 1000°F. A hypothetical hot-gas cleanup process is used. The unconverted char/dolomite mixture is fed to an atmospheric fluid bed boiler where the uncovered carbon is combusted and the sulfide is oxidized to CaSO4.

Product gas is quench to 1500 F. and Cooled to 1000 F by a Boiler

| Process | Case A Gasifier | Case B Gasifier | Case C Gasifier | Case D Gasifier |
|---|---|---|---|---|
| Gasifier Temp. (F) | 1950 | 1950 | 1950 | 1950 |
| Cleanup Temp. (F) | 1000 | 1000 | 1000 | 1000 |
| Gas Turbine Temp. (F) | 2200 | 2200 | 2200 | 2200 |
| HHV of Fuel Gas (Btu/scf) | 114 | 116 | 115 | 124 |
| Power Output (KWhr/MMBtu) | | | | |
| Gas Turbine | 90.3 | 89.0 | 94.9 | 94.8 |
| Steam Turbine | 53.0 | 52.9 | 51.2 | 52.7 |
| Plant Heat Rate (Btu/KWhr) | 7974 | 8126 | 7882 | 7739 |
| Efficiency (%) | 42.8 | 42.0 | 43.3 | 44.1 |

Table 3.5 IGCC Performances with Case A, B, C and D Gasifier

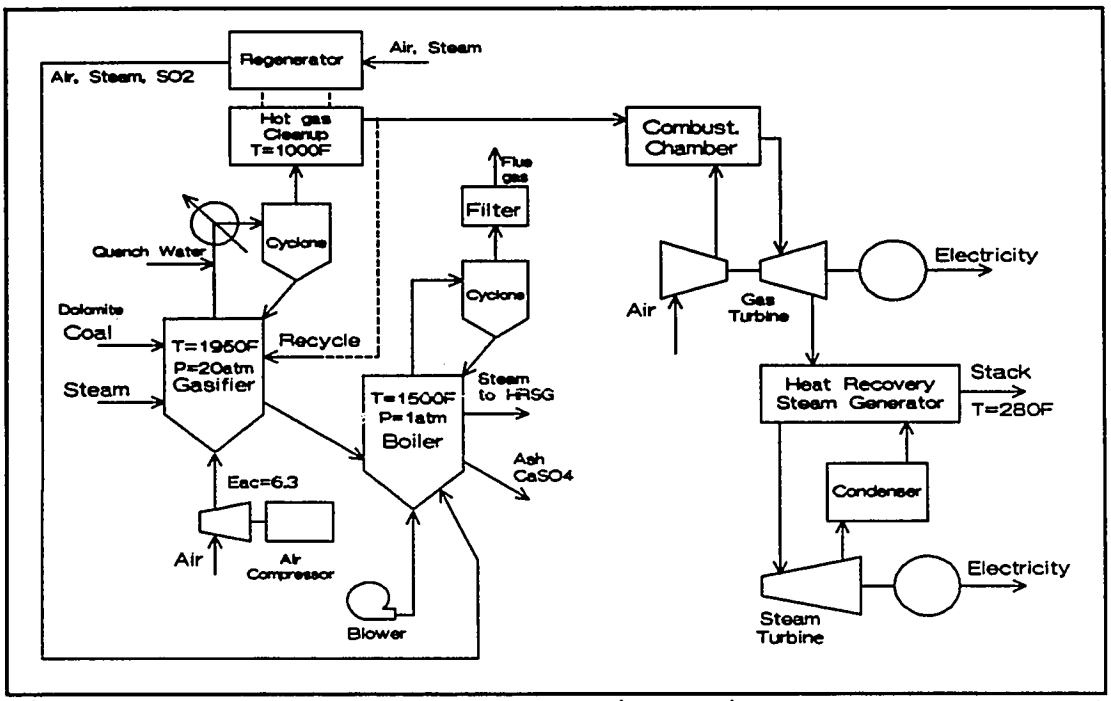


Figure 3.12 IGCC System for the Discussion of Case A,B,C and D

We note that there is a significant advantage to the modified gasifier design (Case C) compared to the original KRW case (Case B) which has bottom coal feed and uses recycle gas. The advantage is due to two reasons:

A) The higher conversion in the gasifier. As the unconverted carbon is converted in a steam cycle with lower efficiency, maximum conversion in the gasifier has an advantage.

The disadvantage of lower conversion can be reduced by using a pressurized fluidized bed combustor instead of an

atmospheric boiler and feeding the hot flue gas to the gas turbine combustor. This will be discussed in Chapter IV.

B) The higher BTU content of the gas in Case C reduces the amount of gas that has to be cooled to the temperature of the hot-gas cleanup. As both quenched or cooled by a waste heat boiler introduce a penalty in thermal efficiency, it is desirable to minimize them.

COMPARISON OF THE KRW AND THE MODIFIED DESIGN CASES

Coal: Pitt#8,(Ca/S=1.5)KRW Gasifier: Bottom feed, Modified Gasifier:Middle feed

| | | KRW Gasifier | KRW Gasifier | Modified Gasifier | Modified Gasifier |
|---|---|---|---|---|---|
| Temperature | (F) | 1800 | 1950 | 1850 | 1950 |
| Pressure | (psi) | 250 | 250 | 250 | 250 |
| O2/Coal | (mol/mol Coal) | 0.384 | 0.457 | 0.429 | 0.4624 |
| Steam/Coal | (mol/mol Coal) | 0.34 | 0.34 | 0.34 | 0.34 |
| Recycle Gas | (lb/lb mafCoal) | 0.38 | 0.37 | 0.0 | 0.0 |
| Carbon Conversion | (%) | 78.2 | 90.0 | 91.1 | 94.9 |
| Coal throughput | (lb/hr/sq.ft.) | 397 | 332 | 379 | 346 |
| Cold gas efficiency | (%) | 60.7 | 65.9 | 70.3 | 70.8 |
| Product Gas | (mol/mol Coal) | 3.01 | 3.41 | 3.31 | 3.48 |
| YCO | (mol. fraction) | 0.191 | 0.199 | 0.214 | 0.213 |
| YCO2 | | 0.077 | 0.071 | 0.067 | 0.066 |
| YH2 | | 0.149 | 0.127 | 0.145 | 0.131 |
| YH2O | | 0.095 | 0.090 | 0.079 | 0.081 |
| YCH4 | | 0.006 | 0.005 | 0.006 | 0.006 |
| YN2 | | 0.481 | 0.506 | 0.488 | 0.501 |
| HHV of gas | (Btu/scf) | 122 | 117 | 128 | 123 |

Table 3.6

The gasifier model was compared with the pilot plant results (Table 3.1) and was found to predict well the actual

results. But the pilot plant runs use far more recycle than actual operations merit. In Table 3.6, we give gasifier performance of a few design cases, some of them based on the KRW design and some based on the design represented by Case C. These cases are not meant to represent the optimum but rather to illustrate the options available to the designer.

Product gas is quench to 1500 F, and Cooled to 1000 F by a Boiler

| Process | KRW Gasifier | KRW Gasifier | Modified Gasifier | Modified Gasifier |
|---|---|---|---|---|
| Gasifier Temp. (F) | 1800 | 1950 | 1850 | 1950 |
| Cleanup Temp. (F) | 1000 | 1000 | 1000 | 1000 |
| Gas Turbine Temp. (F) | 2200 | 2200 | 2200 | 2200 |
| HHV of Fuel Gas (Btu/scf) | 108 | 103 | 113 | 109 |
| Power Output (KWhr/MMBtu) | | | | |
| Gas Turbine | 82.8 | 91.1 | 92.3 | 96.8 |
| Steam Turbine | 56.2 | 51.4 | 51.7 | 50.8 |
| Plant Heat Rate (Btu/KWhr) | 8184 | 8106 | 7956 | 7810 |
| Efficiency (%) | 41.7 | 42.1 | 42.9 | 43.7 |

Table 3.7 Comparison of Different Design Cases

In Table 3.7, we give the overall thermal efficiency of the cases given in Table 3.6. To estimate this thermal efficiency we used a flowchart given in Figure 3.11. In all cases, dolomite is added to the gasifier in a stoichiometric ratio of Ca/S of 1.5. The gas in all cases is quenched to 1500°F and then cooled in a boiler to 1000°F. A hypothetical

hot-gas cleanup process is used. It is assumed also that a reheat steam turbine is used in the steam cycle. If the smaller unit is used, the total efficiency decreases and the penalty of a lower conversion gasifier increases.

## 3.3 Integration of the Calcium Sulfate Oxidizer into the IGCC

In the IGCC power plant using an air-blown gasifier, the gasifier solid withdrawal has to be fed to a fluid bed combustor to convert the calcium sulfide to sulfate. The process is shown in Figure 3.13, As the char contains significant amounts of unconverted carbon, this char must also be combusted to allow complete conversion of sulfide to sulfate. At 90% char conversion this would lead to quite a large size vessel (twice the diameter of the gasifier). A circulating fluid bed combustor is here not suitable, as we need a long residence time of the calcium carbonate in the combustor.

The preferred design would be a pressurized fluid bed combustor, which could then be integrated with the IGCC plant. This could be done by feeding the combustor gases after filtration directly to the turbine. This would again require modifying the turbine as the air-to-the-fuel ratio changes. Furthermore, if such a system is developed it would reduce the

need to achieve a high conversion in the gasifier. It would obtain a higher BTU content in the gas. This will be discussed in Chapter IV.

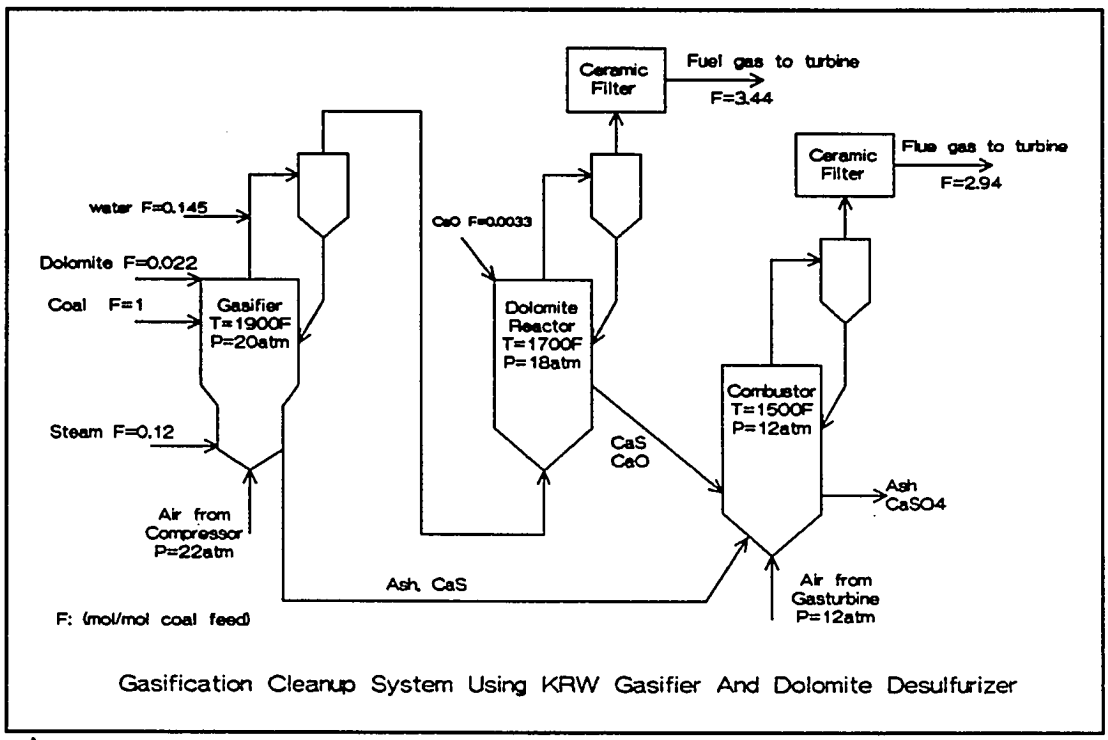


Gasification Cleanup System Using KRW Gasifier And Dolomite Desulfurizer

Figure 3.13

# CHAPTER IV HOT GAS CLEANUP

IGCC systems are promising alternatives for clean power from coal. One system that has attracted attention and is still in the pilot plant stage is a system which is based on an airblown fluidized bed gasifier and hot gas cleanup (Dawkins 1985).

The system proposed is based on a gasifier developed by KRW with Ca-based additive. The hot-gas cleanup system is

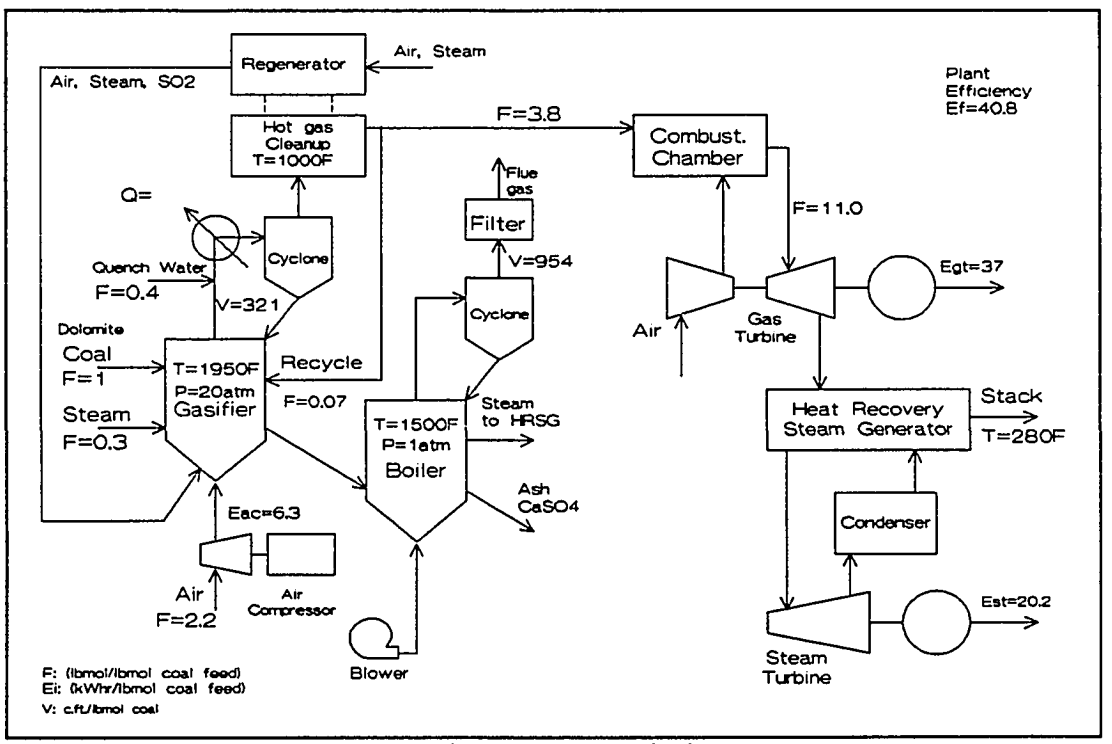


Figure 4.1 IGCC System with KRW Gasifier and Hot Gas Cleanup

developed by the U.S. Department of Energy's Morgantown Energy Technology Center and based on a zinc ferrite adsorbent. This system was tested in the KRW pilot plant. The evaluation is divided into two parts. One deals with the operability and readiness for scaleup of the hot-gas cleanup system. The second deals with an evaluation of the concept itself, from the general view of the goals of obtaining clean power from coal based system.

## 4.1. Evaluation of the Status of Hot-Gas Cleanup Based on Zinc Ferrite

The process uses a packed bed of solid zinc ferrite particles to adsorb the $H_2S$ in the gas. The main reaction occurs in the bed is:

$$ZnOFe_2O_3 + H_2 + 3\ H_2S = ZnS + 2\ FeS + 4H_2O \qquad 4.1$$

The bed is regenerated by passing a mixture of air and steam through the bed. The reaction is:

$$ZnS + 2\ FeS + 5O_2 = ZnO{\cdot}Fe_2O_3 + 3SO_2 \qquad 4.2$$

This releases the sulfur as $SO_2$. The steam is the coolant for this highly exothermic reaction. The intention is to recycle the regeneration gas to the gasifier without condensing the steam. The $SO_2$ is captured in the gasifier by the dolomite and thus, the sulfur is removed from the gasifier as calcium

sulfide or maybe a mixture of calcium sulfide and sulfate.

A better alternative is to feed the regeneration gas straight to the combustor (See Figure 4.2). This makes it easier to keep the operating conditions in the gasifier at an optimal level. If a pressurized combustor is used, this does not result in any penalty, and the sulfur is easier to be captured in the oxidation atmosphere.

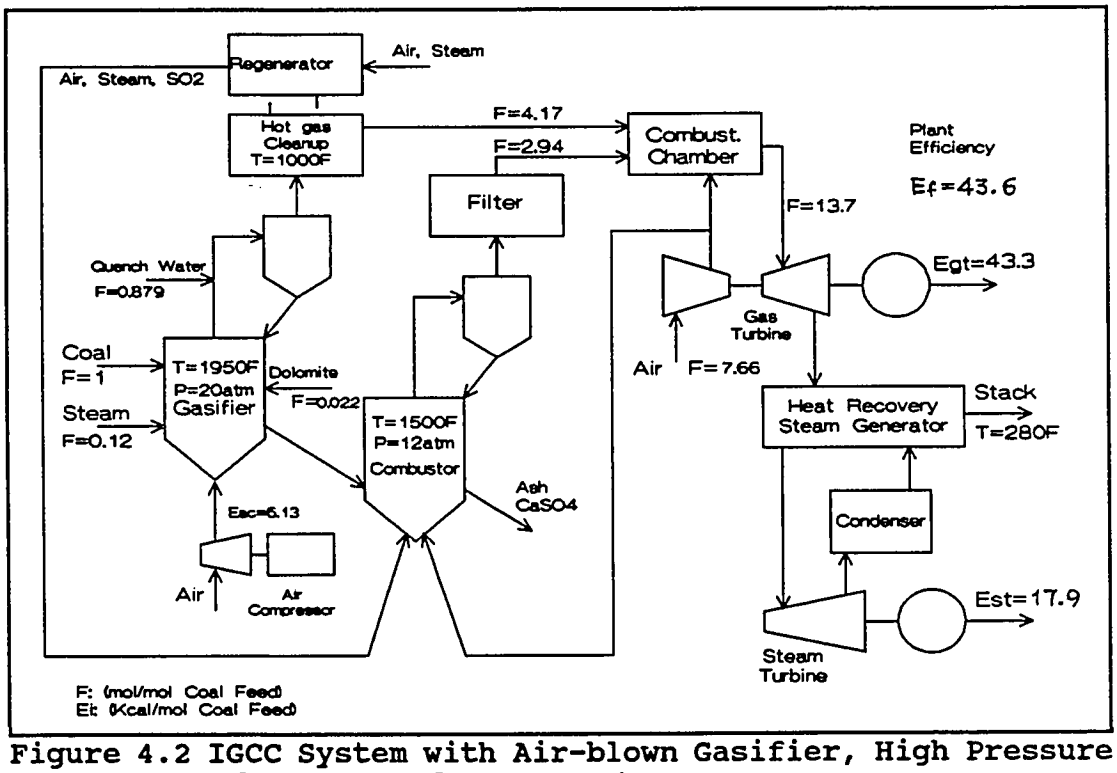


Figure 4.2 IGCC System with Air-blown Gasifier, High Pressure Combustor and Hot Gas Cleanup System

The KRW's test program has been investigated and our comments are summarized below.

The results show a strong nonuniformity of $SO_2$ removal across the cross-section of the bed. It was attributed to a maldistribution of flow. In the normal packed beds, it is less problem due to the comparable maldistribution. The main problem is locally selective deactivation of catalyst due to nonuniform cooling, more pronounced either in the middle or at the wall. This is normally caused by the fact that real packed beds are not completely adiabatic and are cooled near the wall. One should check if this nonuniformity does not indicate a temperature sensitivity of the process. Such data are lacking at present.

In one run, the zinc ferrite disintegrated. In that run, no quench was used and the steam content of the gas was low. This seems to prove that the disintegration noted before was mainly due to carbon formation via the reverse Boudouart reaction.

$$CO_2 = CO + C_{(soot)} \qquad 4.3$$

As said in the previous paragraph, the observed nonuniformity of the gas composition already indicates a strong temperature sensitivity.

There is an option to change the equilibrium of the Boudouart reaction by increasing the steam content of the gas. This can be done by quenching the gasifier product gas with water. This approach is used in commercial steam reforming of

natural gas. However, the amount of steam required is too large. This can be seen from Figure 4.3. Where the steam requirement to depress carbon formation is plotted as a function of temperature. The same conclusion can also be reached by looking at Figure 4.4, which is optional from the reference by Haldipur (1989). Figure 4.3 assumes a typical gas composition for the KRW gasifier which is given in the legends.

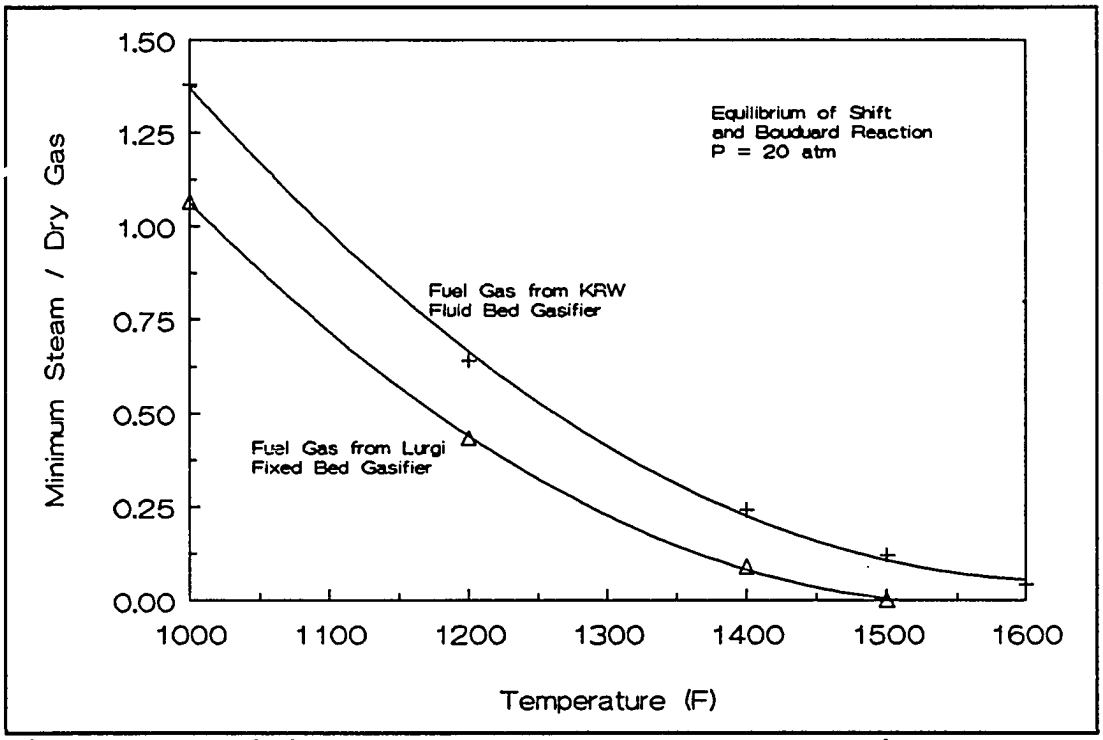


Figure 4.3 Minimum Steam Content for Protection of Soot Formation

We note that to reliably depress carbon formation would require a steam content of 50 percent which is too high. It would reduce the BTU content of the gas to below 80 BTU/SCF.

There are several alternatives to overcome this problem.

1) Changing the sorbent. Zinc titanate is reported to not promote carbon formation.

2) Increasing the temperature to reduce the steam content of the gas required to suppress carbon formation. Zinc ferrite operates at higher temperature, though no long range data are available for higher temperatures. Increasing temperature increases the volatility of zinc oxide, however.

3) Modifying the process such that it can operate in the presence of carbon formation. In the Fischer-Tropsch process this was done by using a slurry reactor. The catalyst disintegrates due to carbon formation but stays in the liquid.

Furthermore, the process has to be operated with more frequent regeneration to burn off the carbon. GE proposed a moving bed process which utilizes this approach .

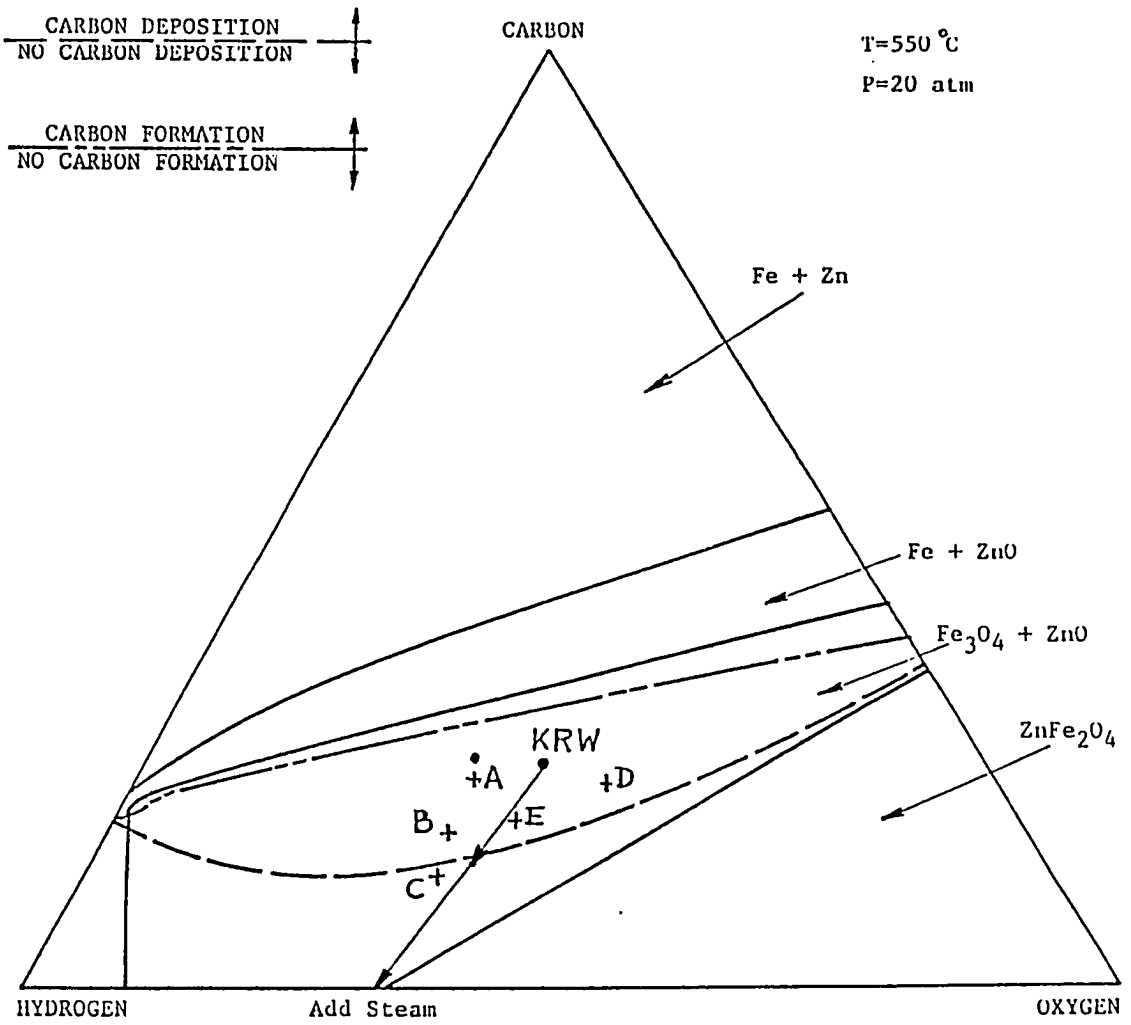


**Figure 4.4 PHASE EQUILIBRIA AT 550 °C AND 20 ATM**

**Labeled gas composition: A-GE-PDU low steam; B-GE-PDU medium steam; C-GE-PDU high steam; D-KRW-PDU oxygen blown; E-KRW-PDU air-blown.**

We would suggest a fluid bed design which is significantly cheaper and allows operation with smaller particles. We have no kinetic data on carbon formation over zinc ferrite to be able to analyze quantitatively. Such quantitative data are desirable before any pilot plant work is started.

But there is another problem with all zinc compounds in the presence of hydrogen or CO. Zinc vaporizes at relatively low temperatures. The zinc formed could deposit on the turbine blades. The volatility of zinc has been a problem in using zinc compounds in catalytic reactors, even at 800°F.

To look at the problem more quantitatively, we give a thermodynamic equilibrium phase data plot in Figure 4.4 for a temperature of 550°C or (1020°F). The design point with various amounts of steam has been given. We note again that steam addition is beneficial, to suppress zinc formation.

Regrettably, the thermodynamic data in Figure 4.4 refer to zinc ferrite. They do not include the zinc sulfide formed or zinc titanate. These would not affect the equilibrium condition for carbon formation but would affect the partial equilibrium pressure of gaseous zinc.

However, thermodynamic computations are only useful if

one can operate well within a safe range. That does not mean one cannot operate a design under these conditions. It just means one needs more detailed kinetic data which are lacking. One thing is clear from the thermodynamics. High steam levels are useful both in reducing carbon formation and reducing the devolatilization of zinc.

| System | Zn-Fe Cleanup | CaO Cleanup |
|---|---|---|
| Gasifier Temperature (F) | 1950 | 1950 |
| Gasifier Pressure (atm) | 20 | 20 |
| Carbon Conversion (%) | 94.1 | 93.3 |
| Cold Gas Efficiency (%) | 67.1 | 69.4 |
| Gasifier Gas HHV(Btu/scf) | 120 | 130 |
| Fuel Gas Temperature (F) | 1000 | 1450 |
| Fuel Gas HHV (Btu/scf) | 58* | 117 |
| Steam in Fuel Gas (mol %) | 55.5** | 15.2 |
| IGCC Efficiency (%) | 37.2 | 45.5 |

* Assume low BTU gas can be used. ** For protection of soot formation

Table 4.1 Comparison of Gasifier Performances Using Zn-Fe and CaO Hot Gas Cleanup System

If a high partial pressure of steam solves these problems, it introduces another one, namely, the BTU content of the gas will be low, probably below 100 BTU/SCF. Without quench, we estimate the heating value to be between 120-130 BTU/SCF (see Table 4.1).

Now, turbine combustors can combust a gas of 100 BTU/SCF or even less and some commercial gas turbines are ready to accept low BTU gas with 100 BTU/SCF. The problem is in the control system and therefore, a lower heating value gas will require a different turbine than the standard combined cycle turbine designed for natural gas.

One way to overcome this would be to use enriched air for the gasifier, say 30-40 percent oxygen. It can be obtained using a pressure swing adsorber to enrich the air. This would result in a gas with the proper BTU content. The gasifier would easily handle this but an exact evaluation of the cost impact of this version is outside the scope of this study.

One of the real problems in all solid adsorbents, in which there is a chemical reaction, is the life of the solid adsorbent. What normally limits it are solid side products and recrystallization phenomena that cause pore plugging. The present version of zinc ferrite has been tested for 45 cycles in a small pilot plant. This is equivalent to 3 months on stream or 6 months total time. This is the minimum. The main concern here is that in the small microreactor conditions are more constant and isothermal. We noted before that the actual results in the pilot plant raise some concern that will only be resolved in a continuous long term test.

## 4.2 An Alternative Hot Gas Cleanup Process

It became clear during our analysis that the zinc ferrite process is not presently ready for implementation in large scale trial. Future work with either zinc titanate or the GE moving bed process could remedy the shortcomings, but we still lack sufficient kinetic data to judge their chance of success.

On the other hand, there are attempts to develop systems based on an airblown gasifier to a full scale demonstration. Several such proposals were submitted under the CCT program.

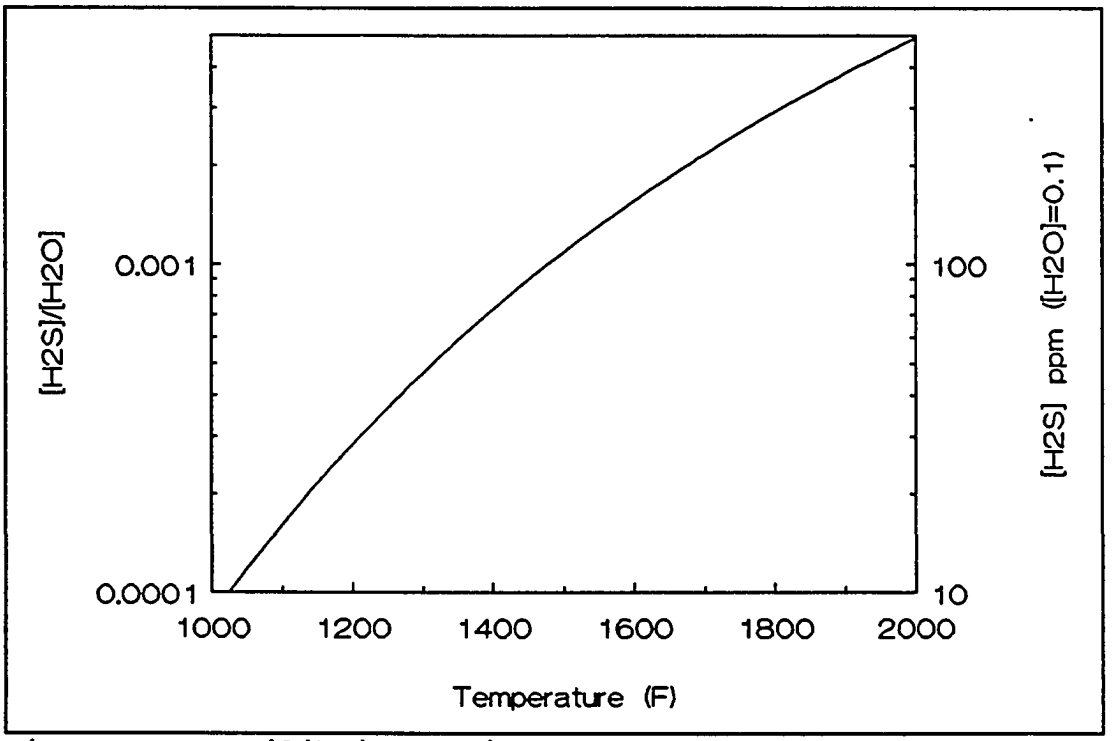


Figure 4.5 Equilibrium Ratio of $H_2S$ to $H_2O$ vs. Temperature

It would be very hard to meet the specification for

sulfur reduction solely by relying on sulfur capture by the dolomite in the gasifier. At 2000°F the equilibrium is not favorable as can be seen from Figure 4.5., where we plot the equilibrium ratio of $PH_2S/PH_2O$ over CaO as a function of temperature. Figure 4.5 translates this into ppm $H_2S$ for a steam content of 10%.

For a coal of 3 percent sulfur we would need to achieve a level of 400ppm for 90% sulfur capture. As it is hard to approach equilibrium in a fluid bed due to bypass and imperfect contacting (see Table 3.1 and 3.2), relying on it would be very risky.

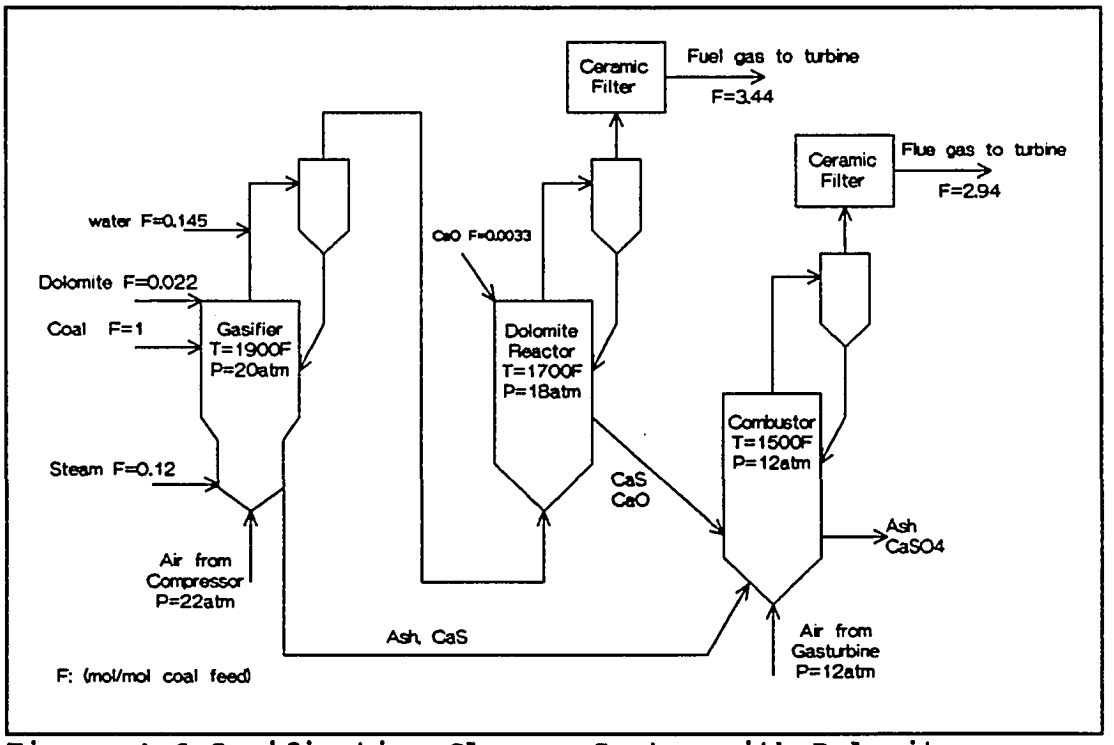


Figure 4.6 Gasification Cleanup System with Dolomite Desulfurizer

It is need to look for other ways to achieve hot-gas cleanup. The reasons why we can't achieve the sulfur removal required by the specifications in the gasifier is due to bypass and the high temperature. A separate sulfur removal reactor filled with dolomite can be used. This is described in Figure 4.6. It is a circulating fluid bed fed with fresh dolomite and operating at 1650-1700°F. The dolomite gets calcined simultaneously. As a second stage is provided, bypass is strongly reduced.

Furthermore, the equilibrium level is lower, the dolomite is fresh, and the reaction rate of sulfur capture is five times higher than at the average conditions in the gasifier. This is due to the fact that the reaction rate of sulfur capture in dolomite is diffusion controlled, resulting in a shrinking core of calcium oxide (see Appendix B). The high sulfur content of the dolomite increases the distance that the $H_2S$ has to diffuse and therefore the average reaction rate is lower.

By modelling, we therefore predict a sulfur capture of 95 percent for the gas system in Figure 4.6 versus 85 percent for the gasifier itself. Such a system could be designed now, relying on available design information for fluid beds.

This arrangement has another advantage. The dolomite

gets preheated and calcined. It improves the gasifier performance (see the case D in Chapter III). But most important, there is less need to cool down the product gas. We have removed one constraint on thermal efficiency introduced by the hot-gas cleanup. Our main constraint on temperature is now due to the control valve and the metal volatile. Valves are available for operation at 1450°F. The vapor pressure of the metal volatiles are very low below this temperature.

It can be pointed out that the hot-gas cleanup process proposed here is easier to implement. It does not have the development difficulties of the zinc ferrite or titanate. However, Zinc ferrite has practically no equilibrium constraints and allows reduction of $H_2S$ to levels below 20 ppm. This cannot be achieved in the system in Figure 4.6. But it could allow a demonstration plant to be built now.

## 4.3 Impact of the Hot Gas Cleanup on the Total System

As discussed in Section 4.1, hot-gas cleanup is essential for an IGCC system based on an airblown fluid bed gasifier. The main reason of using hot gas cleanup is that the penalty to cool the gas to room temperature is bigger than in an oxygen-blown entrained bed gasifier. It is due to that the

product gas of air-blown gasifier is about double of the oxygen-blown gasifier.

However, the envisioned hot-gas cleanup system has one large penalty, namely, that it rejects sulfur as dilute $SO_2$. It also cannot economically capture the full amount of $H_2S$ from a sulfur-rich coal. The presently envisioned system therefore relies on removing the major part of the sulfur as calcium sulfide in the gasifier. This has been achieved by adding dolomite. This permits recycling the regeneration gas to either the gasifier or the combustor. The dolomite has a very positive impact on the gasification itself (Haldipur 1989), but causes several severe problems for the total system. These include:

A) The CaS has to be converted in a separate fluidized bed combustor, which increases total investment and makes the system more complex. The combustor is almost as big and expensive as the gasifier.

B) It creates a large solid waste problem. While the waste is easier to store than the sludge from a scrubber, it still presents problems. Calcium sulfate can be leached into the ground water.

This problem does not yet appear in EPA regulations.

There is a large probability that, if large amounts of waste are generated, such laws will ultimately appear. And the amounts of waste generated are huge, about 40 weight percent of coal input. The following will put this into perspective. There is tremendous concern now about the solid municipal waste in the U.S. There is no palace to put it. Now, if all present coal-fired power plants would use this method, the waste (ash + dolomite) generated would be equal to the total solid municipal waste of the U.S. (about 1 ton per person per year). If coal use increases, this could be locally a severe constraint. It is therefore essential to find a use for this waste.

Ash from an oxygen-blown, entrained bed gasifier is only 25 percent of this amount and is easier to dispose of, as it can be used as a filler in road construction and similar uses. There is also experience from conventional power plants.

If such an alternative cannot be found, one could also think about developing a process such as Kellogg developed in the 1970's which converts the calcium sulfide to calcium oxide and sulfur. This is an expensive process and has never been fully demonstrated.

This also strongly reduces the advantage of IGCC over a fluidized bed coal fire boiler, which has the same problem of

solid waste. The only advantage left would be a potential for lower particulate emission, which relies on a high grade, efficient ceramic filter, which as yet has not been fully developed. Actually, such a ceramic filter could also be used in a pressurized fluid bed boiler, but the throughput would be three times larger. This is hardly a decisive advantage.

Without such a filter both a fluidized bed boiler and a fluid bed IGCC would have similar or larger particulate emissions than a conventional coal-fired boiler. And particulate emissions are the most damaging emissions in terms of health.

Here, wet $H_2S$ removal has decisive advantage. If the wet gas cleanup is properly designed all particulate, including submicron particles, are removed.

## 4.4. Development needs for Hot-Gas Cleanup

There is a great incentive to develop a hot-gas cleanup process that produces elemental sulfur. The present processes used for oxygen blown gasifiers have this property but they require cooling to room temperature. This has the advantage that one can use a liquid quench which totally removes all particulate, resulting in a system that competes with natural

gas in terms of emissions.

Present effort on hot-gas cleanup has focused on 1000°F, which eliminates all liquid processes. No good process that produces elemental sulfur has been found. In Reference (Shinnar 1987), it is discussed that the hot-gas cleanup needs for oxygen-blown IGCC. It was found that a cleanup process operating between 350°F and 400°F would be a very promising compromise. We could use water solution cleanup to clean the gas as long as the process operates above the dewpoint of the gas. This would remove all particulate.

There are two cost penalties associated with cooling the gas. One is due to the cooling and reheating itself. The other is due to the condensation of steam. In an oxygen-blown IGCC one can reduce the first penalty by cooling the stream with a water quench. If the steam is not condensed but fed to the turbine, it expands in the turbine. In this case the penalty on total efficiency is relatively small. In an airblown IGCC one cannot do that without reducing the heat content of the gas below 100 BTU/SCF, so one would have to use a mixture of boiler cooling and water quench.

As our main goal is to prevent the condensation of steam, we could use a water solution of a salt for removing the $H_2S$, provided the temperature is equal to the boiling point of

the solution at the partial pressure of the steam. At a partial pressure of 150 psi, this temperature is 360°F. A temperature of 400°F would raise the partial pressure to 250 psi.

That means we have to look at processes in which $H_2S$ is either adsorbed by a salt at this temperature, directly reacted in the liquid with $SO_2$ to form sulfur. Reacting the sulfide formed with $SO_2$ has the advantage that we don't rely on solubility but on a stoichiometric reaction, which is easier to do at higher temperatures.

Such a process would be very valuable for both fluid bed and entrained bed IGCC. Another advantage would be that the quench itself would completely remove all solids without a large penalty. The example is given in Chapter VI. The IGCC total plant efficiency is 37% versus 30% which using room temperature cleanup.

# CHAPTER V INTEGRATION OF MILD GASIFICATION INTO A POWER PLANT WITH AN AIR-BLOWN FLUIDIZED GASIFIER

Mild gasification, a low temperature carbonization in absence of oxygen, is one of the oldest coal technologies. It provided one of the first resources for organic chemicals in the chemical industry. The interest in it has been renewed with the energy crisis and the search for more efficient utilization of coal. Any liquefaction or upgrading of coal into hydrocarbons involves either insertion of hydrogen or rejection of carbon. However, in a stand alone plant, it has three disadvantages.

(1) The gases evolved have to be utilized.
(2) Heating and cooling the coal and char are expensive and the cost of this operation has to be minimized.
(3) The rejected char is harder to utilize in power plants than coal.

It has been previously suggested that one way to overcome these difficulties is to integrate mild gasification technology into a power plant. An IGCC plant based on a fluidized-bed gasifier has that potential. A description of

the process is given in Figures 5.1 and 5.2.

Figure 5.1 shows the gasification part, which basically consists of two fluid beds with hot char circulating between them. The fresh coal is fed into the pyrolyzer and mixed with recirculating hot char. Dolomite is either fed together with the coal or fed into the gasifier section. The pyrolyzer is fluidized with hot steam. The pyrolysis products are quenched and all liquid hydrocarbons are condensed. The mixture of the cold gas and gasifier offgas is then sent to a conventional hot-gas cleanup or to the dolomite bed discussed in Chapter 4.

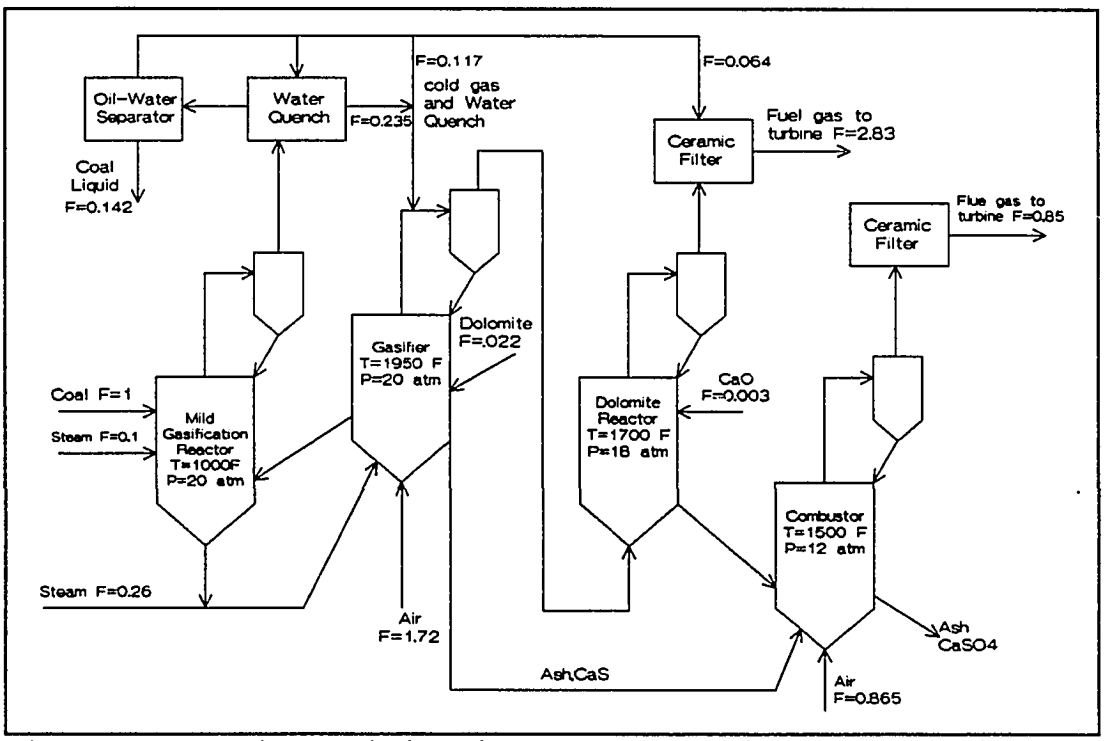


Figure 5.1 Mildgasification and Dolomite Desulfurization System

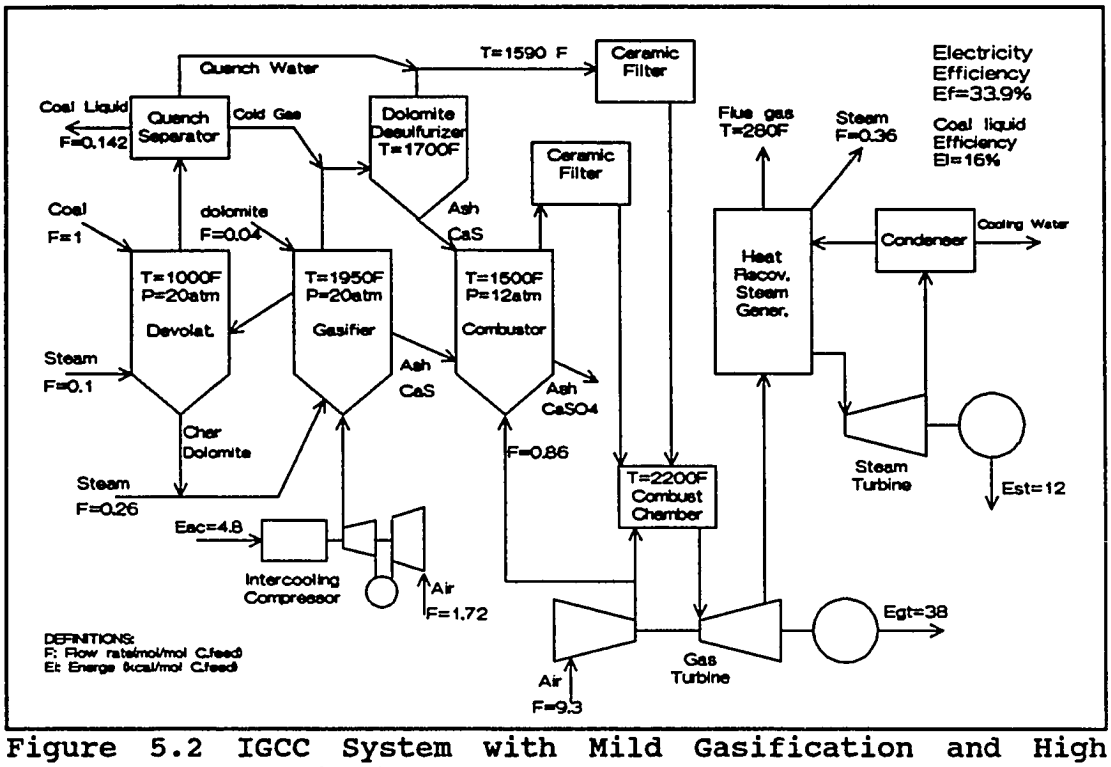


Figure 5.2 IGCC System with Mild Gasification and High Pressure Combustor

Alternately, it could be sent to a hot-gas cleanup system based on zinc ferrite. The gas is then mixed with hot gas from the gasifier and sent either to hot- gas cleanup or to the turbine. The char formed in the pyrolyzer, together with the recirculating char/ash/dolomite mixture, is sent to the gasifier using hot steam as a transport gas and gasified.

The gases coming out of the dolomite reactor have to be quenched to 1400 F - 1500 F for removal of evaporated alkali metal, which will deposit on the particles floating in the gas streams. These particulate will be removed through the

cyclone and sent to the combustor directly, as shown in Figure 5.1.

The fuel gas will go through a ceramic filter and feed to the combustion chamber of a gas turbine. Instead of feeding in the excess air to cool down the combustion temperature to proper operating conditions, the high pressure-high temperature combustor flue gas will be used as adjusting air for the gas turbine. In this way the energy of unconverted char in the gasifier can be recovered in the combustor and give about a 2 percent total plant efficiency increase.

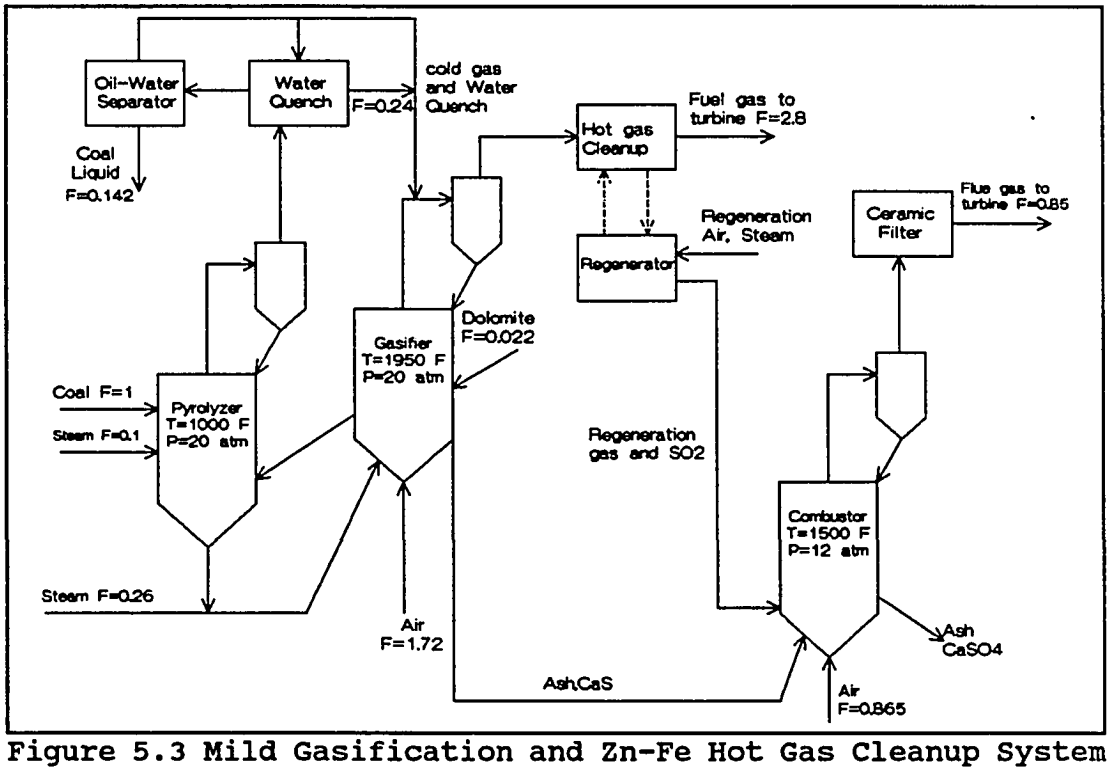


Figure 5.3 Mild Gasification and Zn-Fe Hot Gas Cleanup System

Another option is to use zinc ferrite hot-gas cleanup, which was developed by DOE (see Figure 5.3). The gas mixture coming out of mild and regular gasifiers is sent to a zinc ferrite adsorber for desulfurization. Before that, the gas stream has to be cooled down 1000 F to approach zinc ferrite operating conditions. The clean, hot gas will be sent to the combustion chamber with the flue gas from the high pressure combustor. The regenerating gas from the hot-gas cleanup system is sent back to the gasifier to adsorb the SO2. We will give the detailed calculations of the impact of regeneration gas for different sulfur inputs and different gasifier in-bed desulfurization efficiencies.

The comparison of mild gasification and the KRW system is given in Table 3.1. The use of mild gasification overcomes all of the difficulties mentioned before. The BTU content of the gasifier gas would be significantly lower than from the regular gasifier. Adding to it the gases evolved in the mild gasification reactor compensates for this loss. The BTU content of the mixture gas is similar to that obtained with a gasifier operating with fresh coal. Thus, we not only utilize the gases, but also compensate for the difference between fresh coal and char for the gasifier.

Furthermore, as the hot char is fed to the gasifier, we have no thermal penalty in heating it. The only thermal

penalty is in the quench of the products and condensation of the steam feed for devolatilization. These penalties are far less than in a stand-alone plant. In a stand-alone plant the heat would have to be supplied either indirectly, which is expensive, or by combustion of char, which would result in a much larger thermal penalty in the quench section.

| | | Pyrolyzer | Gasifier | MG | KRW |
|---|---|---|---|---|---|
| Coal Type | | Pitt.#8 | – | | Pitt.#8 |
| Sorbent (lb/lbmol Coal Feed) | | – | 2.58 | 2.58 | 2.58 |
| Temperature ( F) | | 1000 | 1950 | | 1900 |
| Pressure (psi.) | | 20 | 20 | 20 | 20 |
| Oxygen/Coal (mol./mol Coal F.) | | – | 0.375 | 0.375 | 0.456 |
| Steam/Coal (mol./mol. Coal F.) | | 0.1 | 0.26 | 0.36 | 0.120 |
| | | | | | |
| Total Carbon Conversion (%) | | | | 98.4 | 92.0 |
| Coal Liquid (mol./mol. Coal F.) | | 0.142 | – | 0.142 | – |
| Gas Yield (mol./mol. Coal F.) | | 0.416 | 2.41 | 2.65 | 3.29 |
| Gas Composition | YCO | 0.058 | 0.214 | 0.204 | 0.233 |
| | YCO2 | 0.092 | 0.076 | 0.084 | 0.051 |
| | YH2 | 0.127 | 0.086 | 0.099 | 0.133 |
| | YH2O | 0.435 | 0.062 | 0.056 | 0.054 |
| | YCH4 | 0.251 | – | 0.039 | 0.003 |
| | YNH3 | 0.033 | – | 0.001 | – |
| | YH2S | 0.003 | – | 0.001 | – |
| | YN2 | 0.002 | 0.562 | 0.513 | 0.523 |
| Gas HHV (Btu/s.c.f.) | | 313 | 96.5 | 137.2 | 128 |
| Cold Gas Efficiency (%) inc.tars | | 38.7 | 40.6 | 79.3 | 66.9 |

Table 5.1 Comparison of Operating Performances of Mild Gasification System (MG) and KRW System

In Table 3.2, we compare the two systems, an IGCC plant with mild gasification and one without. Both use the same gasifier and turbine and having the same power output. A one gigawatt power plant would produce about 7300 barrels of liquid products at a thermal efficiency of 75 percent. We

defined this thermal efficiency by dividing the heating value of the liquid products by the heating value of the incremental coal needed to produce constant power.

| Gasification Process | MG | | KRW | |
|---|---|---|---|---|
| Cleanup Process | Hot gas Cleanup | CaO Desulfur. | Hot gas Cleanup | CaO Desurfur. |
| Liquid Yield (FOE barrels/day) | 6780 | 6460 | – | – |
| Power Generation (MW) | | | | |
| Gas Turbine | 957 | 913 | 905 | 889 |
| Steam Turbine. | 257 | 289 | 296 | 297 |
| Power Consumption in Plant | 213 | 203 | 202 | 187 |
| Net Plant Power | 1000 | 1000 | 1000 | 1000 |
| Power Efficiency % (Net Plant Power/HHV of Coal) | 32.3 | 33.9 | 39.5 | 42.7 |
| Coal Liquid Efficiency % (HHV of Liqud/HHV of Coal) | 16.1 | 16.1 | | |
| Total Thermal Efficiency % | 48.4 | 50.0 | 39.5 | 42.7 |

Table 5.2 Comparison of IGCC Performance Using Mild Gasification and KRW System

We are aware of no system that could produce liquid products from coal at similar thermal efficiency and cost. The system, however, needs to be proven in a larger pilot plant.

# CHAPTER VI HYBRID POWER PLANT

When we look at present options and trends for second generation, coal-fed power plants, we note two distinct alternatives. One is IGCC power plants based on oxygen-blown entrained bed gasifiers, such as the Cool Water plant based on the Texaco gasifier, and a similar power plant based on the

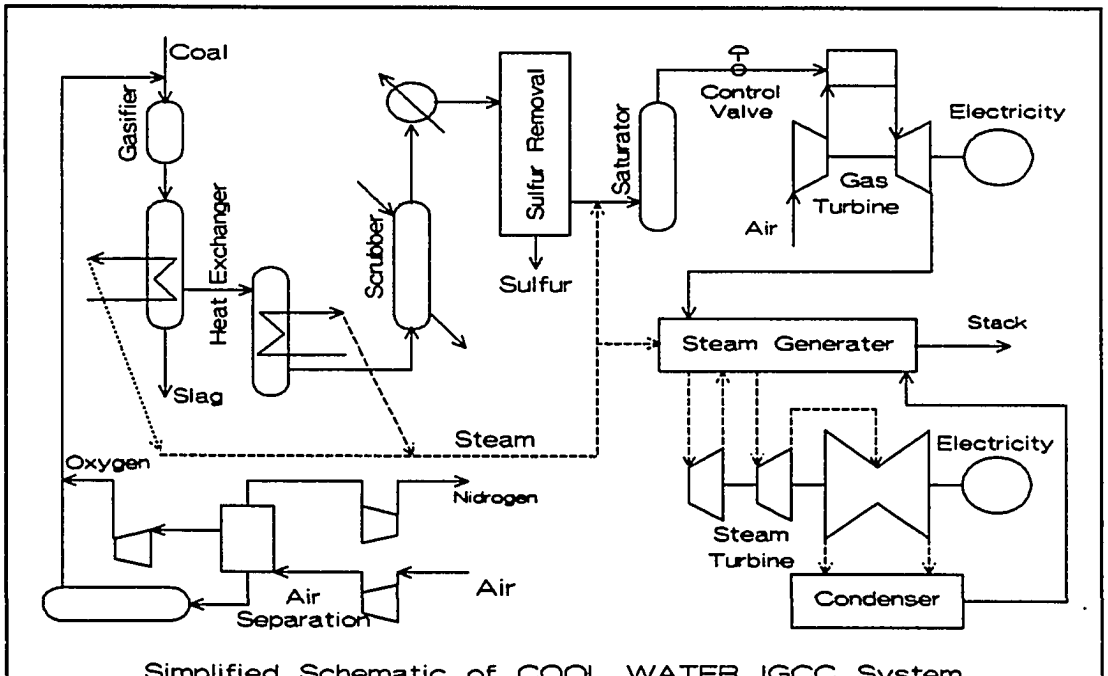


Figure 6.1

Shell gasifier. Dow has developed a similar gasifier for subbituminous coals which has operated in a large cogeneration

plant. The advantage of this route is the potential to generate power from coal which is as clean as power generated from natural gas. Their main disadvantage is the need to generate oxygen and use it in a power plant environment. The conceptual flowsheets of Cool Water and Dow IGCC power plant are shown in Figure 6.1 and Figure 6.2.

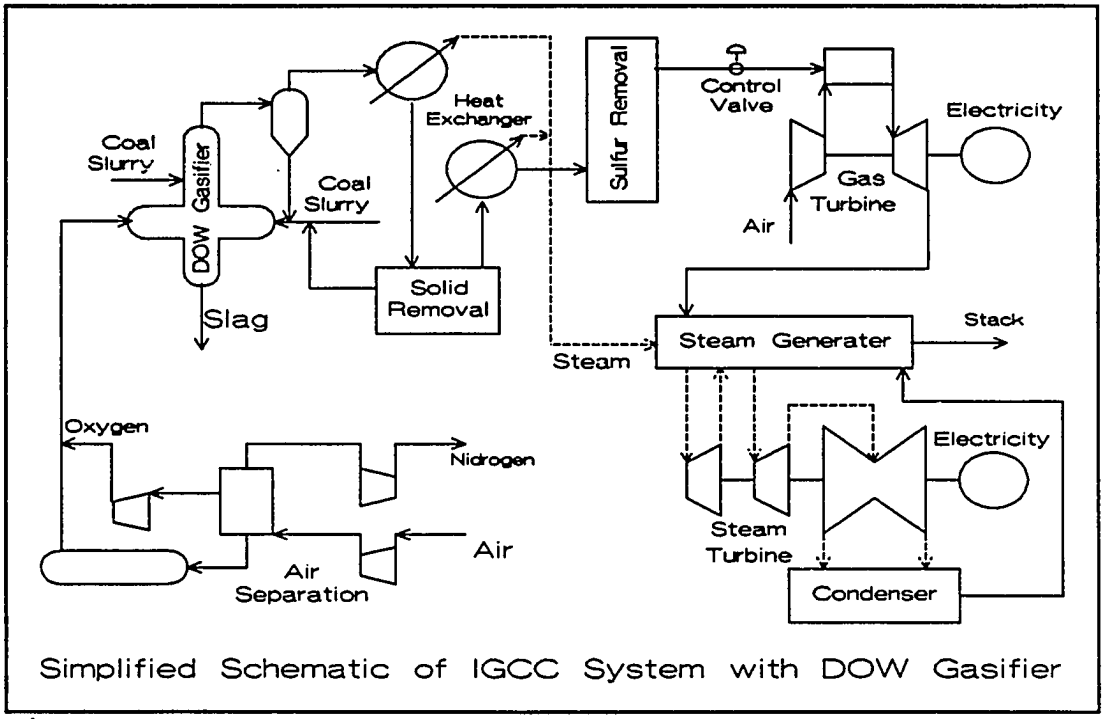


Figure 6.2

The other alternative is characterized by the pressurized fluidized bed combustor with an expander turbine, implemented by AEP. In this case, the sulfur is removed as calcium sulfate in the bed. The particulate generated are removed by a hot filter, for which various designs have been proposed.

Pressurized fluidized bed boilers have two advantages over conventional coal fired powered plants equipped with scrubbers.

A) The nitrogen oxide emissions are strongly reduced due to the lower combustion temperature. They can be further reduced by using a two-stage air injector which helps to reduce oxides from organic nitrogen. This is the main driving force towards fluidized bed combustors. Conventional power plants require catalytic converters to reduce the nitrogen oxide.

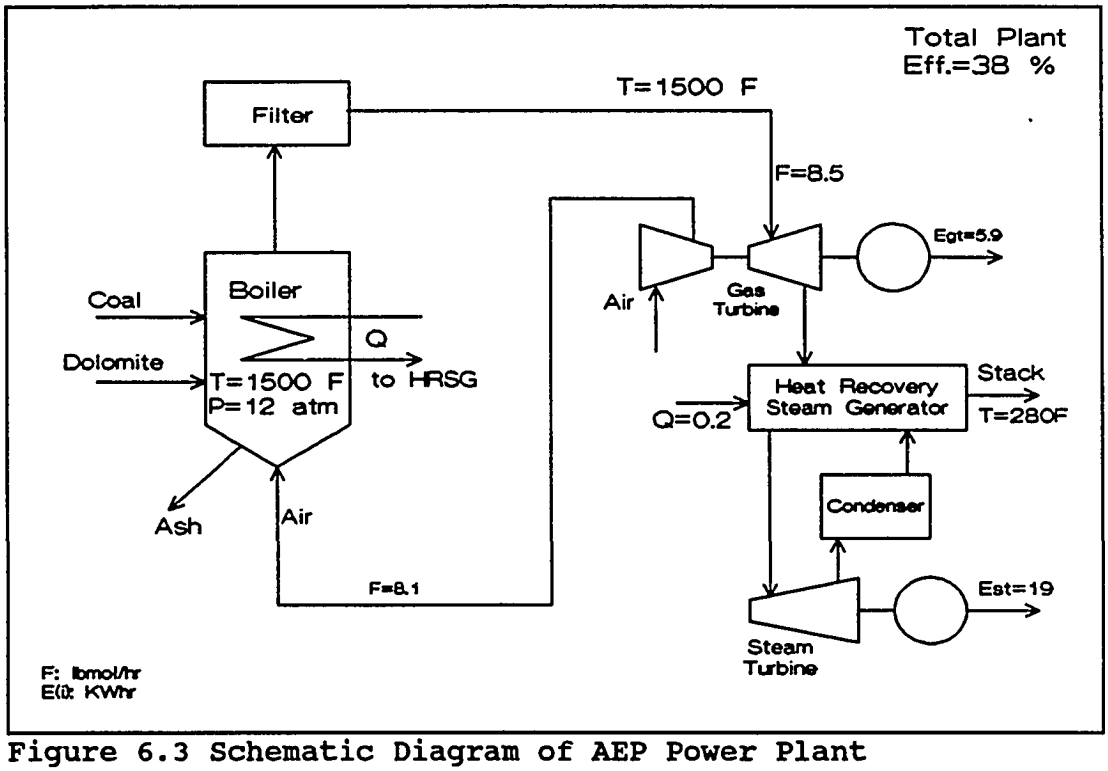


Figure 6.3 Schematic Diagram of AEP Power Plant

B) Dolomite/ash/calcium sulfate mixture is obtained in a

dry form which is easier and cheaper to dispose, though it is still a large waste disposal problem. The disadvantage of present atmospheric fluidized bed boilers is that their volume is large. The desire to reduce their diameter has led to the development of the pressurized fluidized bed boiler.

AEP together with Asea-Brown-Bovari has built a prototype which will soon be tested. To recover the energy needed to compress the air the flue gases are expanded in a turbine similar to the practice in FCC regenerators (Figure 6.3). If the temperature of the flue gas is high enough, the energy from the expander is significantly larger than that needed for compression and it becomes a major source of the net energy generated.

The main limitation on the temperature is, at present, volatile alkaline compounds. It is formed in the combustor and could deposit on the turbine blades. The maximum permissible temperature is still under evaluation but is probably around 1400-1500°F. Temperatures of 1600°F have been mentioned.

The maximum temperature permissible will be a function of the ash composition and therefore, strongly coal dependent. Operating at high temperatures could be quite risky. The safer way is to operate at 1400-1450°F and superheat the flue

gas before it enters the turbine (Figure 6.4).

Alternatively one could operate the combustor at slightly higher temperatures (up to 1600 °F) and cool the gases before entering the cyclone, by bypassing air. The simplest

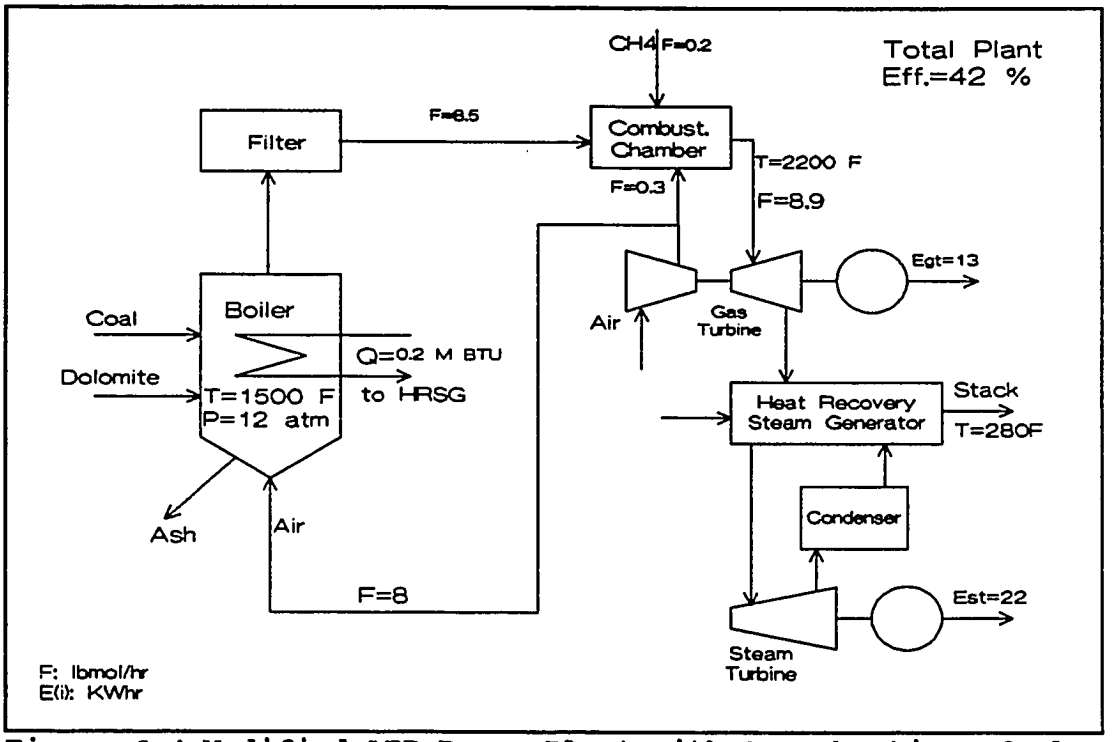


Figure 6.4 Modified AEP Power Plant with Superheating of Flue Gas by Methane

way to do so, is to use natural gas for the superheat. This increases the overall thermal efficiency. The incremental efficiency of utilizing methane is 52 percent. This will probably be the next step development of this technology, and needs no further development once the viability of the boiler itself is established.

In this case, one would substitute a gas turbine for the expander turbine. The main problem with this system is in the removal of solids. Fluid bed combustors generate more fines than conventional boilers. Efficient removal of particulate emissions is essential. The volume of gas is much smaller before expansion. It is therefore, preferable to filter the hot gas before the expander.

This is also needed to protect the turbine. Various hot gas filters have been developed and await large scale long-range testing (Haldipur 1989). There is a good hope that such filters will meet the current specification for solid emissions. However, there are claims that these specifications will be tightened in the near future.

Some of the particulate are, from a health point of view, the worst pollution caused by coal-burning power plants, as they settle very slowly and are inhaled. They also contain trace elements and are a major cause of smog formation. If coal is to be used in densely populated urban areas, efficient and reliable removal of such submicron particulate will be required.

The Cool Water system, due to its liquid quench, has still a significant advantage. The quench and liquid gas cleanup scheme are properly designed. However, the limits on

the performance of hot filters are not known. This is a critical part of the overall development program.

The system built by AEP uses a pressurized fluid bed combustor. This development started before atmospheric circulating fluid bed combustors became commercial. In atmospheric fluidized bed boilers, circulating fluid bed combustors have become clear winners due to their smaller size and better performance and flexibility.

Furthermore, there were originally large differences between the various models of circulating fluidized bed combustors, the different designs have converged and are now quite similar. Therefore, it is expected that if AEP is successful, there will be a similar development of circulating pressurized fluidized bed combustors and, in the end, the development will be towards pressurized circulating fluid beds. In our overall discussion, there is no difference between the two types of fluid bed combustors.

Now let us relook at the system in Figure 6.4. Once the superheater is introduced, an additional degree of freedom has been gained. Without it, the excess air for the boiler has to be kept at a reasonable limit. Reducing the excess air increases the fraction of the heat going into the steam generator. The plants use efficient reheat steam turbines.

To use such a turbine, the minimum size of the total plant has to be quite large (above 250 MW). In this section, it is assumed that all cases use higher efficiency steam turbine (38 percent of energy in the recovered steam is converted to electricity) than those given in Chapter V. If we use a source for superheat, there is no need to generate any steam in the fluid bed combustor (Figure 6.5). The combustor is as an air preheater for the gas turbine, but one would probably not go that far due to the freedom of the control.

We present this case just to illustrate the choices the designer of the system has. Figure 6.5 is really a combined

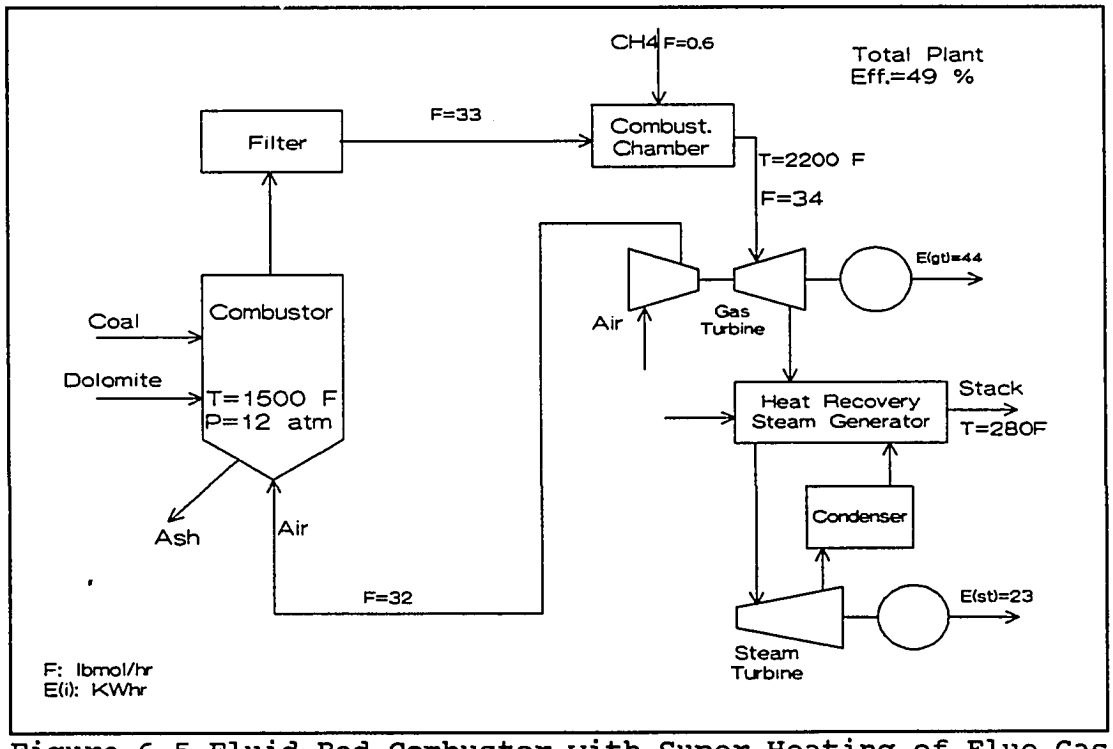


Figure 6.5 Fluid Bed Combustor with Super Heating of Flue Gas by Methane

cycle power plant using a mixture of coal and natural gas. The scheme in Figure 6.5 has a significant advantage in thermal efficiency over the system in Figure 6.4. Steam generation in a boiler has, however, one advantage. It allows higher turndown ratio. It also requires less methane at pilot plant. However, the system without steam generation has a slightly higher thermal efficiency.

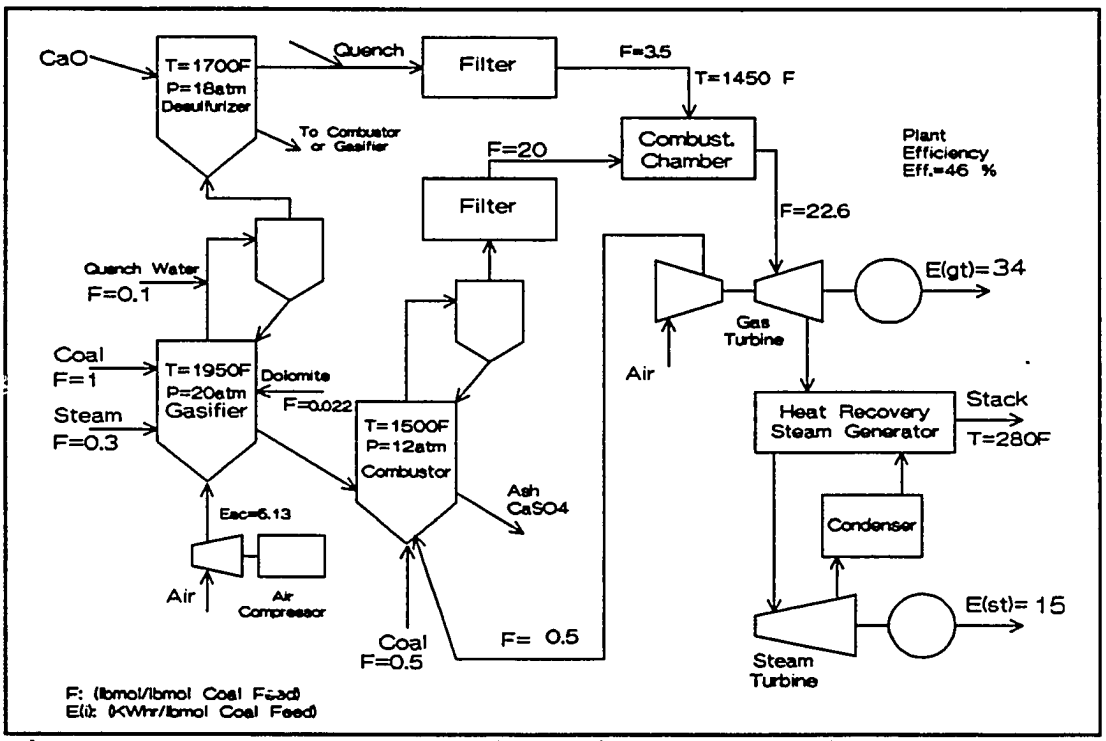


Figure 6.6 IGCC System with Air-Blown Gasifier and High Pressure Combustor

The systems in Figures 6.4 and 6.5, or any similar design, the amount of heat contributed by natural gas is about 30-45 percent. However, this does not mean that this ratio reflects the fuel use of the plant. The control of the power

output can be achieved by adjusting the gas input to the combustor in front of the turbine. As most power plants operate less than 40 percent of the time at peak load. The actual use of gas could be as low as 10-15 percent of total power output. It makes the system overall quite attractive.

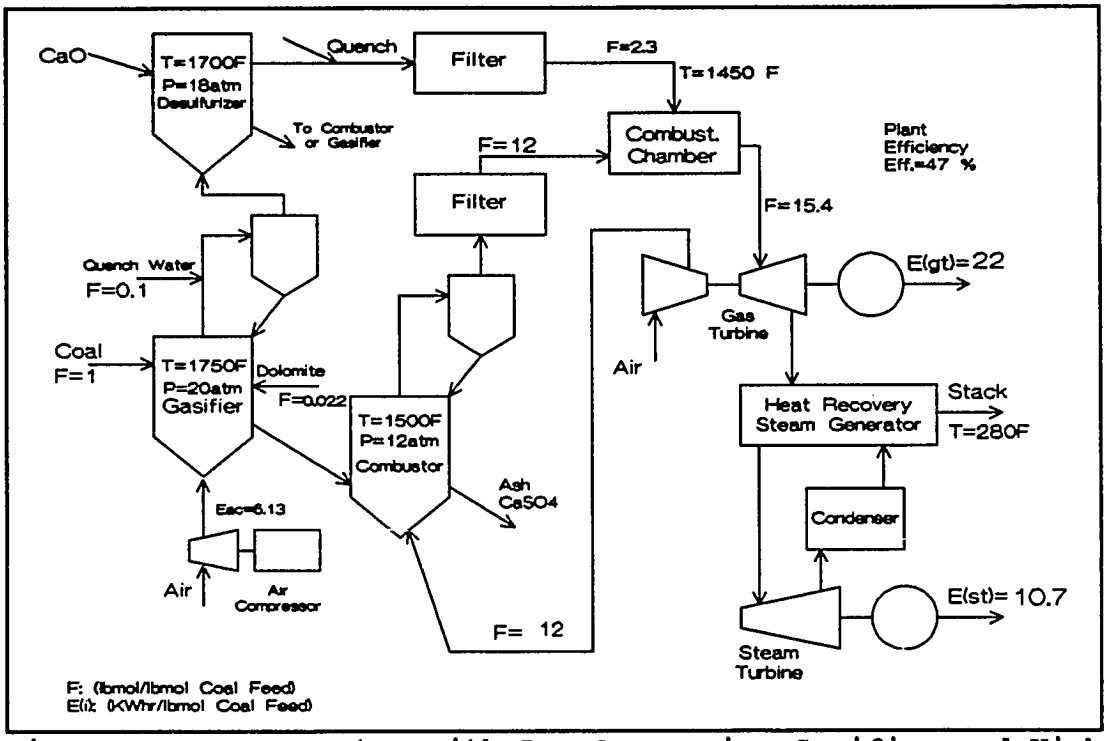


Figure 6.7 IGCC System with Low Conversion Gasifier and High Pressure Combustor

The next logical step is to replace the natural gas which in Figure 6.5 a coal gasifier. There are several options. A standard fluid bed gasifier can be used to supply the heating. The unconverted char from the gasifier is fed to the combustor together with fresh coal (Figure 6.6). If the amount of heat needed is less than 45% of the total, we can

also use a low conversion gasifier, sometimes called a carbonizer (Figure 6.7), in which carbon conversion may range from 40 to 60 percent.

There is a significant advantage for operating the gasifier at lower temperatures and conversions. If dolomite is used to capture sulfur, the optimal thermodynamic temperature for sulfur capture ranges from 1650-1750°F. Furthermore, lower temperatures minimize problems of clinkering.

There is one significant difference between the gasifier proposed here and the KRW design. The coal is injected into the middle of the bed which gives a superior performance as compared to bottom injection used at KRW.

The system in Figure 6.6 is also similar to what was discussed in Chapter III. Consider first a KRW gasifier, in which the dolomite ash mixture is fed into an atmospheric fluid bed combustor. Its main purpose is to oxidize the calcium sulfide to sulfate. To do so, all the unconverted carbon has to be burned off first. The combustor has to be oversized to make sure that it is able to do so even at slightly lower carbon conversion. Such a combustor is quite large, much larger than the gasifier (see Figure 6.8).

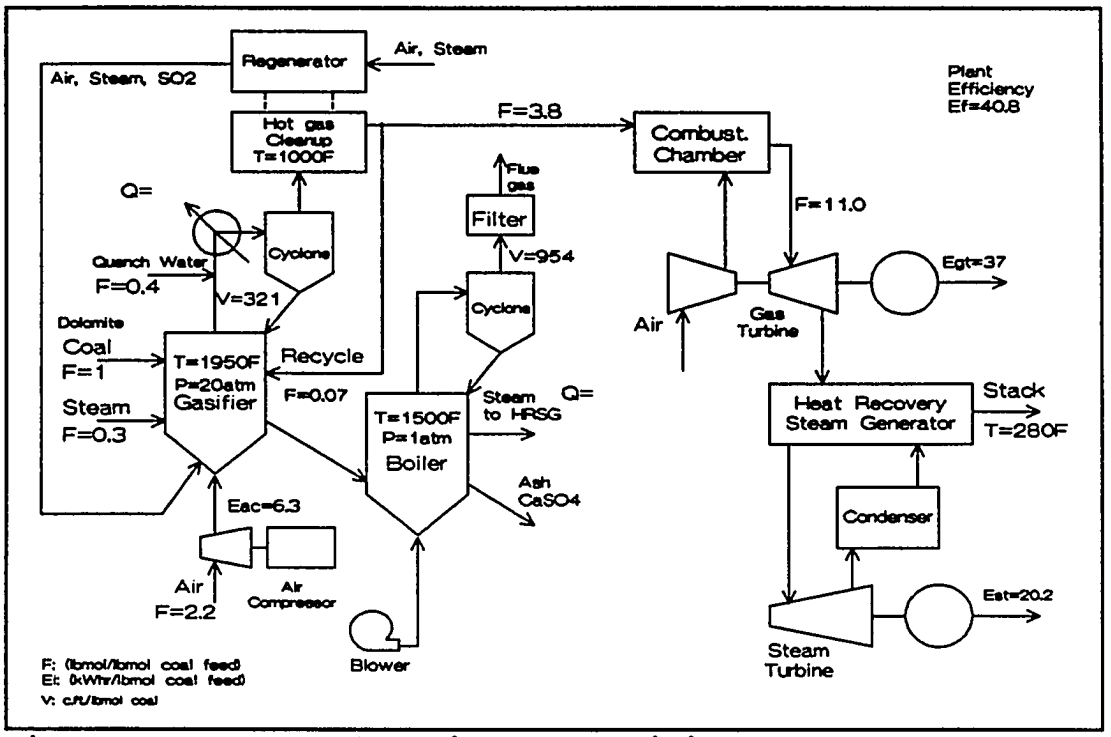


Figure 6.8 IGCC System with KRW Gasifier and Hot Gas Cleanup

It makes sense to reduce its size by using a pressurized fluid bed combustor, preferably a circulating one. If we use the pressurized fluidized bed combustor, then the flue gas can be fed to the combined cycle turbine (Figure 6.9). Having done so, it is actually preferable to reduce the conversion of the gasifier and to reduce gasifier temperature (Figure 6.10).

Table 6.1a and 6.1b gives a similar case in which the excess air in the combustor is minimized by the steam generation. The main difference between Figure 6.6, and Figures 6.9 and 6.10 is that in Figures 6.9 and 6.10, all of the coal is fed to the gasifier. There is a large amount of air that is not fed to the combustor. In Figure 6.6 all the air goes either to the gasifier or the combustor.

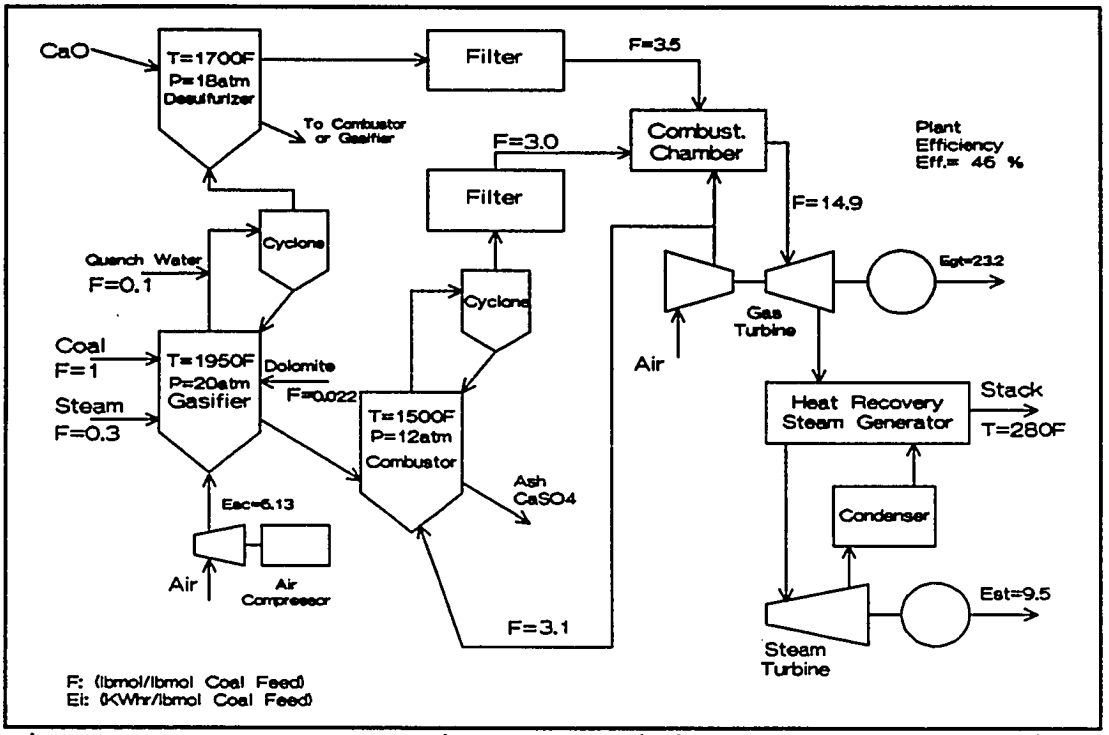


Figure 6.9 IGCC System with KRW Gasifier and CaO Desulfurizer

There is no real conceptual difference between the hybrid system and the IGCC system proposed by KRW. The actual KRW design was similar to Figure 6.8 but Figure 6.9 is a logical extension of it. We see, therefore, that IGCC systems based on fluid bed gasifiers and hybrid systems share many similarities and actually present a continuum. Let us therefore discuss some of the common properties. All of the proposed hybrid systems show two common problems.

1) The need for an efficient hot filter.

2) Use of dolomite or limestone for sulfur capture, causing a large solid waste disposal problems.

Addition of the gasifier adds two more problems.

3) The calcium sulfide in the gasifier has to be oxidized as pointed out above. It is difficult to oxidize the calcium sulfide formed in the gasifier completely.

4) Sulfur captured as calcium sulfide is less efficient than captured as sulfate. The latter is not thermodynamically constrained. It is therefore a significant advantage.

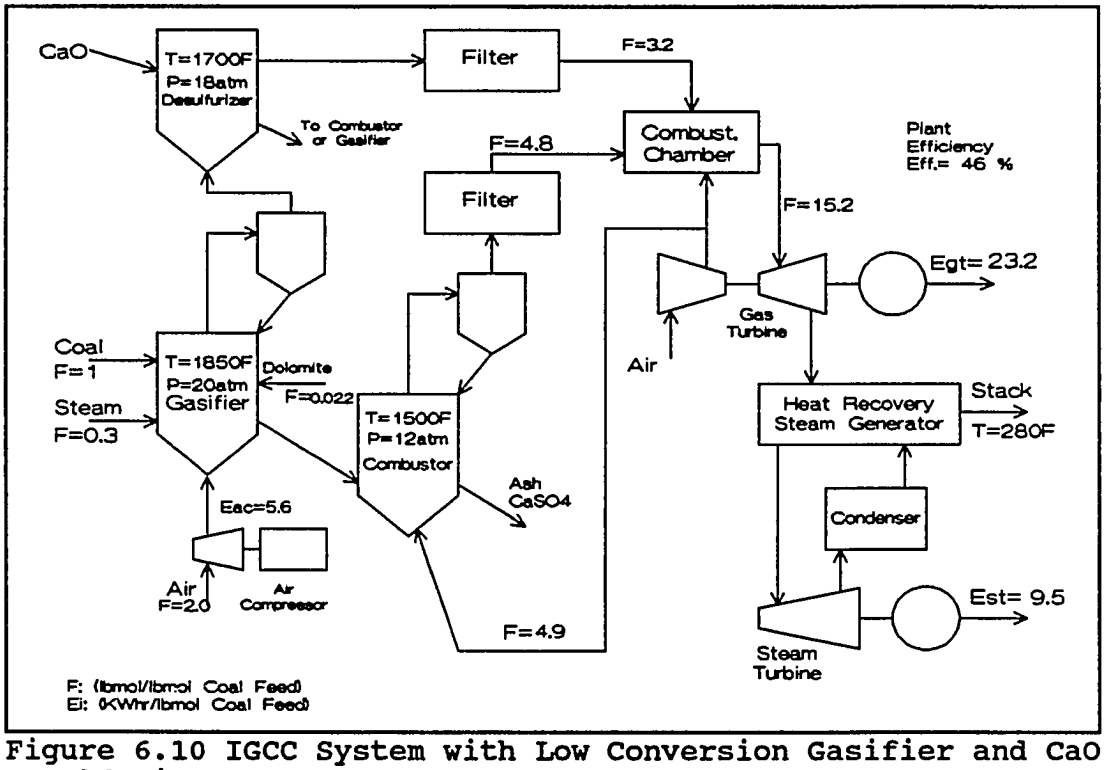


Figure 6.10 IGCC System with Low Conversion Gasifier and CaO Desulfurizer

Most probably any of the hybrid systems using a coal gasifier or carbonizer will require some form of hot-gas cleanup. In Figures 6.6, 6.7, 6.9, and 6.10 the hot-gas cleanup system proposed in Chapter IV has been used. It is

actually a second stage of sulfur capture with dolomite which is separated from the gasifier. Obviously, all the systems could use any other hot-gas cleanup system. If zinc ferrite is used,the regeneration gas is fed into the combustor.

The various systems are summarized and compared in Table 6.1a and 6.1b. As the different systems in development started independently from different assumptions about the state of available technology. It makes sense to look at the whole spectrum and ask, Where is the optimum? What are the advantages and disadvantages of each design? We also have to ask, is the technology ready for use?

We will start with the last item. Let us cite what problems have not been fully demonstrated. First, long term-use of a hot gas filter has to be demonstrated at actual conditions. In any of the systems in Figures 6.6-6.10, there is another main problem. We have no knowledge how dolomite that has been exposed to $H_2S$ and partially converted behaves in a fluid bed combustor. Does sulfide formed at the surface reduce the efficiency of sulfur capture in the combustor? We know already that it is difficult to convert the sulfide to sulfate. In that sense, this technology is not ready for demonstration until this problem is settled.

This relates to all of the hybrid systems. So let us

assume we can solve it and look at the differences between the various options. If we have a hot-gas cleanup process operating above 1450°F, then the differences in thermal efficiency between the different designs become small. If we need to cool to 1000°F, then reducing the conversion in the gasifier increases the overall thermal efficiency. So does reducing steam generation in the fluid bed boiler.

However, the latter may have disadvantages in terms of the turndown ratio. Power plants are not solely interested in achieving a high thermal efficiency at maximum power. They want to be able to maintain reasonable heat rates at lower power output. This is a crucial point in choosing between competing technologies. So is overall reliability.

As a last example, we want to propose a novel hybrid system that resulted from our system study and has superior environmental performance compared to other hybrid systems. It also has the advantage of being feasible with present technology. Its disadvantage is a lower thermal efficiency. However, the efficiency still exceeds that achieved by present coal fire power plants equipped with scrubbers.

This whole class of options, while offering a better thermal efficiency than the oxygen blown gasifier, has some common disadvantages. With presently available technology,

sulfur removal is less complete. But more important, a hot filter has, as yet, not been proven to be very efficient in removing submicron particulate.

One potential design is described in the following and is mainly intended for use with reactive coals. The reason for this will be explained later.

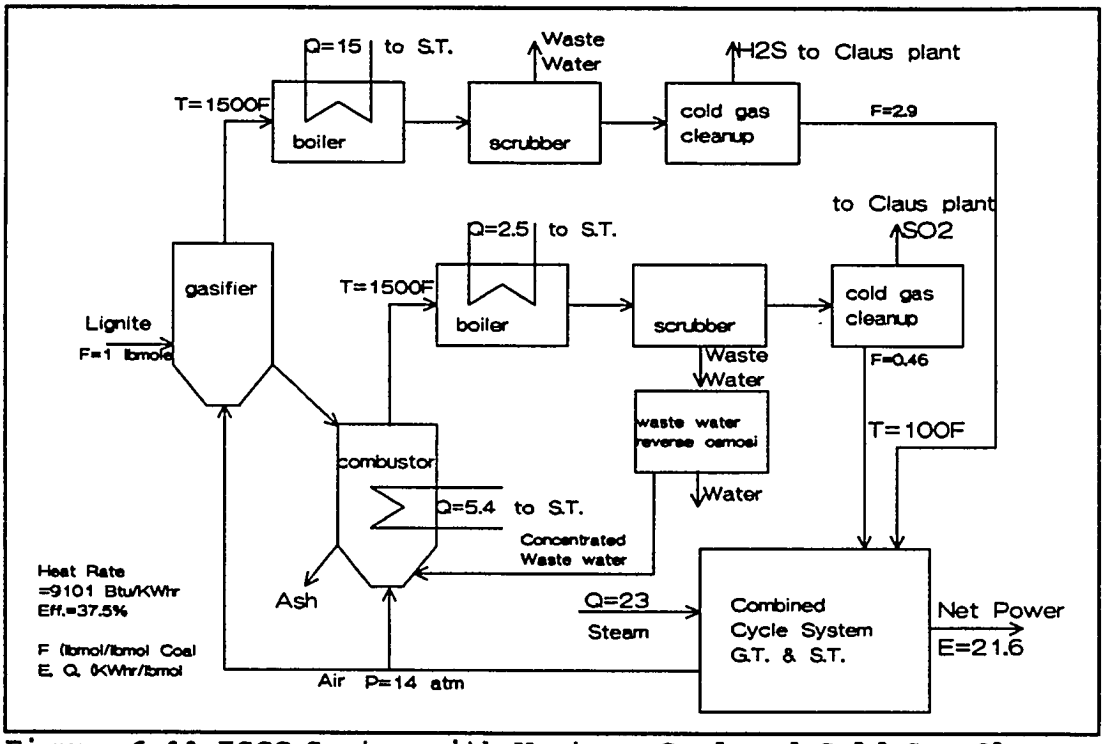


Figure 6.11 IGCC System with Western Coal and Cold Gas Cleanup

A conceptual flowsheet is given in Figure 6.11. The base of this design is a pressurized, air-blown fluidized bed gasifier operating between 85-90 percent carbon conversion. For example, for Texas lignite the gasifier operates at 1500 F. For some coals a porous inert solid added at a small

percentage (5-10 percent) will significantly decrease clinkering and ash agglomeration. It allows safer operation and scaleup. Limestone should be avoided because of the problems mentioned before.

In Figure 6.11, the low-BTU gas from the gasifier is cooled in a boiler and then washed in water to remove all particulate. $H_2S$ is then removed by conventional low temperature $H_2S$ removal processes to any desired level. The cold gas is fed to the combined cycle turbine system.

The unconverted char is fed to a small pressurized fluid bed combustor to achieve complete conversion. The flue gas of the combustor is also cooled in a waste heat boiler and washed with water. The $SO_2$ is absorbed again in a solvent process. The removed $SO_2$ is fed to a Claus plant together with the $H_2S$. This allows 99 percent sulfur removal and, if properly designed, complete removal of submicron particulate. The pressurized flue gas is then sent to the gas turbine.

Alternatively, some dolomite can be fed to a combustor to catch the sulfur. We require here less than 20 percent of the dolomite in a fluidized bed boiler or gasifier. The fluidized bed combustor can be utilized for superheating the steam. To be efficient the plant requires a reheat turbine, which means the minimum total size is 200 to 250 MW.

We give the thermal efficiency and the heat rate of the plant for one example with 90 percent carbon conversion in the gasifier in Figure 4.8 and it is close to 38 percent efficiency, based on LHV. Considering the plant is completely clean and uses available technology, this is a significant achievement.

The proposed process has another advantage. It completely eliminates the problem of volatile alkalis. There is, however, one problem still left with the above design, namely, what to do with the waste water. It can be recirculated when the total amount is small, but it has to be disposed. In our scheme this is done by concentrating it in a filter using reverse osmosis. Contrary to standard solid filters, these are able to retain submicron particles and also trace elements in the water. We are then left with the concentrated stream of waste water containing the particulate and soluble compounds.

There are two alternatives for this stream. One is to feed the water into the combustor. All particulate will agglomerate onto the ash in the flame. The other alternative is to solidify this waste stream with calcium sulfate. It should be cheaply available from power plants using dolomite to catch sulfur.

While the first option is cheaper, it requires demonstration. The second option is an available, safe backup. Such power plants would be easy and safe to operate and promise completely clean power from coal with available technology today.

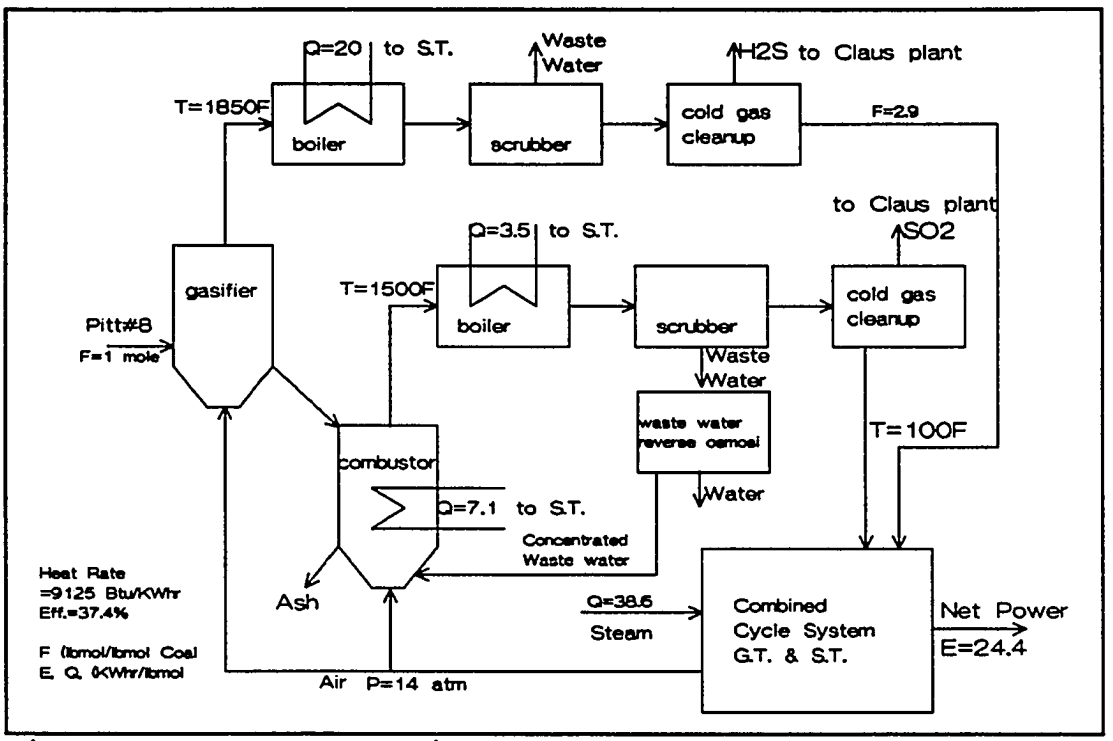


Figure 6.12 IGCC System with Eastern Coal and Cold Gas Cleanup

The same scheme can also be developed for eastern coal (see Figure 6.12). The thermal efficiency is similar. But some problems still have to be solved. We have no reliable data that a caking coal can be gasified in an air-blown gasifier without dolomite addition, though the KRW data indicates that this should be feasible. A waste heat boiler has to be added before the cyclone. Operating a cyclone at

1850°F without quench is difficult, especially without dolomite. But this system is closer to implementation than any of the other systems. It has potentially the same environmental advantages that oxygen blown gasifiers have.

The availability of a warm cleanup at 350 F would simplify the design of the above systems, similar to its impact on oxygen-blown gasifiers, and should be a research priority.

Table 1a COMPARISON OF HYBRID PROCESSES

| Process | A | B | C | D | E | F | G | H |
|---|---|---|---|---|---|---|---|---|
| Gasifier Temp. (F) | 2400 | 2400 | 1950 | 1950 | 1950 | 1950 | 1850 | 1850 |
| Gasifier Carbon Conversion (%) | 98 | 98 | 93 | 93 | 93 | 93 | 89 | 89 |
| Cleanup Temp. (F) | 77 | 400 | 1000 | 1700 | 1700 | 1700 | 1700 | 1700 |
| Boiler Steam Generat. (Btu/Btu coal feed | | 0.17 | 0.07 | 0.0 | 0.07 | 0.0 | 0.0 | 0.569 |
| Power Output (KWhr/MMBtu) | | | | | | | | |
| Gas Turbine | 68 | 77.3 | 88.3 | 106 | 101 | 103 | 105 | 45.2 |
| Steam Turbine | 39 | 51.9 | 47.9 | 44.4 | 45.4 | 43.6 | 43.2 | 81.2 |
| Plant Heat Rate (Btu/KWhr) | 11770 | 9299 | 8365 | 7437 | 7584 | 7419 | 7509 | 8224 |
| Efficiency (%) | 30 | 37 | 41 | 45.8 | 45.0 | 46.0 | 45.5 | 41.5 |

Table 6.1a

Table 1b COMPARISON OF HYBRID PROCESSES

| Process | I | J | K | L | M | N | O | |
|---|---|---|---|---|---|---|---|---|
| Gasifier Temp. (F) | 1750 | 1750 | 1500 | 1850 | 1500 | 1500 | 1500 | |
| Gasifier Carbon Conversion (%) | 61.7 | 61.7 | 89.7 | 89 | 99 | 99 | 99 | |
| Cleanup Temp. (F) | 1700 | 1700 | 100 | 100 | -- | -- | -- | |
| Boiler Steam Generat. (Btu/Btu coal feed | 0.0 | 0.26 | 0.21 | 0.25 | 0.68 | 0.68 | 0.0 | |
| Power Output (KWhr/MMBtu) | | | | | | | | |
| Gas Turbine | 102 | 82.5 | 68.3 | 68.1 | 26.8 | 44.9 | 95.6 | |
| Steam Turbine | 48.9 | 63.3 | 61.2 | 61.1 | 86.4 | 76.1 | 50 | |
| Plant Heat Rate (Btu/KWhr) | 7169 | 7534 | 9101 | 9125 | 8981 | 8126 | 6965 | |
| Efficiency (%) | 47.6 | 45.3 | 37.5 | 37.4 | 38.0 | 42.0 | 49.0 | |

Table 6.1b

## Description of Processes in Table 6.1

## (All cases use Pittsburgh #8 coal except Case K)

A) Cool water system
Oxygen blown Texaco gasifier, waste heat boiler and Selexol gas clean up system
Combined cycle turbines

B) Cool water system
Oxygen blown Texaco gasifier, water quench and Liquid cleanup process operating at 400 °F (to be developed)
Combined cycle turbines (2200 °F)

C) Modified KRW gasifier operating at 1950 F, hot gas cleanup at 1000 °F, and atmospheric fluidized bed boiler operating at 1500 °F

D) Modified KRW gasifier (1950 °F), hot gas cleanup with dolomite at 1700 °F, fuel gas quenched to 1450 °F, pressurized fluid bed combustor to treat unconverted char

E) E is similar to case D. The only difference is that a fluidized bed boiler is substituted for the combustor.

F) Case F uses the same gasifier as case D but fresh coal is fed to the combustor, such that all air reaching the turbine combustor is preheated to 1500 °F.

G) Case G is identical to case D but the gasifier is run at 1850 °F which increases the combustor load.

H) Case H uses a fluidized bed gasifier operating at 1850 °F. $H_2S$ is removed in a dolomite desulfurizer at 1700 °F and the gas is quenched to 1450 °F. Till now the case is identical to case G. However, the fresh coal is fed to a fluidized bed boiler.

I) Case I is similar to case D and G, only the gasifier operates at 1750 °F.

J) Case J is similar to case H, only the gasifier operating at 1750 °F.

K) Case K is based Texas lignite and uses a fluidized bed gasifier operating at 1500 °F. No dolomite is added to the gasifier. The gas is cooled down in a waste heat boiler to 300 °F. The gas is scrubbed with water to remove particulate. The $H_2S$ is removed in a liquid solvent process. The

unconverted ash is combusted in a pressurized fluidized bed boiler. The flue gas from the boiler is also cooled to 300 °F, the gas scrubbed and $SO_2$ removed in a liquid solvent process.

L) Case L is similar to case K only the Pitts #8 coal is substituted for the lignite. Therefore the gasifier operates at 1850 °F.

M) Case M is a pressurized fluidized bed boiler at 1500 F with a expander turbine operating at the same temperature.

N) Case N is similar to case M but the flue gas is superheated by methane to 2200 °F before expansion.

O) Case O is similar to case N but a pressurized fluidized bed combustor is substituted for the fluidized bed boiler.

# Appendix A

## CARBON CONVERSION SIMULATION

## Two Parameter Char Gasification Kinetics

For char gasification reaction with syngas, the kinetic behavior can not be described well along all reaction range using one parameter model which is first order reaction model or shrinking core model with reaction surface layer control. The parameter of first order reaction is initial reaction rate, and the parameter of shrinking core model is total conversion time of single particle. We are going to use a two parameter model to describe the both initial and final behavior of char gasification, which can be defined as:

$$x = 1 - \exp\left(\frac{-KR_o t}{1 + AKR_o t}\right) \qquad (1)$$

Where KRo is the initial reaction rate and A is a parameter to describe the final carbon conversion behaviors. These two parameters can be estimated by linear regression from plotting the following equation:

$$-\frac{1}{\ln(1 - x)} = A + \frac{1}{KR_o} * \frac{1}{t} \qquad (2)$$

Where $R_o$ is the function of temperature, pressure and gas composition in the bed. $R_o$ can be calculated by

$$R_o = \frac{r_1 p_{CO2} + r_8 p_{CO2}^2 + r_9 p_{H2O} + r_{11} p_{H2O}^2 + r_{12} p_{H2O} p_{H2} + r_4 p_{H2}^2}{1 + r_2 p_{CO2} + r_3 p_{CO} + r_{10} p_{H2O} + r_5 p_{H2}} \quad (3)$$

The rate constants used in equation(2) are given in Table A1 which have the expression of

$$r_i = k_{0i} * \exp(-\frac{E_i}{RT}) \quad (4)$$

We can integrate equation (1) with different residence time distribution function to get the average conversion.

**Integrating with CSTR Flow Pattern**

For the continue stirred tank reactor, the total output particles average conversion is calculated by the integration of

$$X_{av} = \int_0^{\infty} x \frac{1}{T_{av}} \exp(-\frac{t}{T_{av}}) dt \quad (5)$$

Substituting eq(1) to eq(5), we can get

$$X_{av} = \int_0^{\infty} (1 - \exp(\frac{-KR_o t}{1 + AKR_o t})) \frac{1}{T_{av}} \exp(-\frac{t}{T_{av}}) dt \quad (6)$$

For conveniently building into the gasifier simulation program, Let:

$$B = KR_o T_{av}, \qquad \theta = \frac{t}{T_{av}}$$

The carbon average conversion through the CSTR gasifier can be calculated by:

$$X_{av} = 1 - \int_0^{\infty} \exp(-\theta(\frac{1 + B + AB\theta}{1 + AB\theta})d\theta \tag{7}$$

This is the master curve for CSTR gasification simulation, which is the only function of A, and B. Eq(7) is plotted in Figure A1.

**Integrating with PFR Flow Pattern**

The residence time distribution function of plug flow is a delta function. The final conversion of solid particles can be calculated by:

$$X_{final} = \int_0^{\infty} x(t)\delta(t - T_{av})dt = x(T_{av}) \tag{8}$$

Substituting eq(1) to eq(8), we can get:

$$X_{av} = 1 - \exp(-\frac{B}{1 - AB}) \tag{9}$$

We plot eq(9) in Figure A1 for comparison with CSTR model.

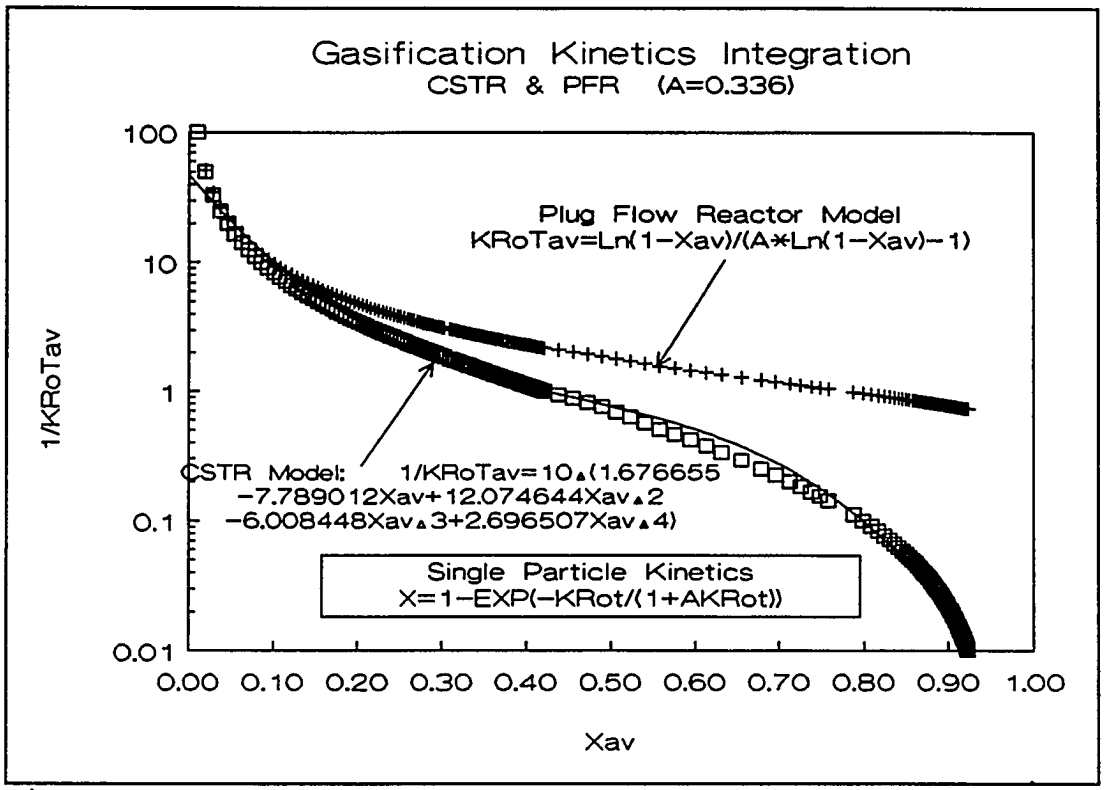


Figure A.1

Table A.1

Rate Constants for $R_o$ Calculation

$$r_i = k_{oi} * EXP(-E_i/RT)$$

| | |
|---|---|
| $K_{o1}=2.71*10^{4}$ bar$^{-1}$ min$^{-1}$ | $E_1$= 153.1 KJ mol$^{-1}$ |
| $K_{o2}=2.06*10^{-2}$ bar$^{-1}$ | $E_2$= -23.0 KJ mol$^{-1}$ |
| $K_{o3}=3.82*10^{-2}$ bar$^{-1}$ | $E_3$= -48.1 KJ mol$^{-1}$ |
| $K_{o4}=3.18*10^{7}$ bar$^{-2}$min$^{-1}$ | $E_4$= 237.4 KJ mol$^{-1}$ |
| $K_{o5}=1.53*10^{-9}$ bar$^{-1}$ | $E_5$=-209.2 KJ mol$^{-1}$ |
| $K_{o8}=1.22*10^{-2}$ bar$^{-1}$ min$^{-1}$ | $E_8$= 68.5 KJ mol$_{-1}$ |
| $K_{o9}=2.96*10_{5}$ bar$^{-1}$ min$^{-1}$ | $E_9$= 154.0 KJ mol$^{-1}$ |
| $K_{o10}=1.11*10^{1}$ bar$^{-1}$ | $E_{10}$= 29.5 KJ mol$^{-1}$ |
| $K_{o11}=4.40*10^{-3}$ bar$^{-2}$ min$^{-1}$ | $E_{11}$= 80.3 KJ mol$^{-1}$ |
| $K_{o12}=6.14*10^{-3}$ bar$^{-2}$ min$^{-1}$ | $E_{12}$= 8.4 KJ mol$^{-1}$ |

# Appendix B

## SULFUR CAPTURE SIMULATION

### Shrinking Core Model with Ash Layer Control

For predicting sulfur capture using dolomite or limestone in a gasifier, a shrinking core model with ash layer control was built into the gasifier simulation program. The sulfur capture and coal conversion can be solved simultaneously with interaction of gas and solid compositions.

Shrinking core model is an one parameter model to describe the non catalytic gas solid reaction which can be shown in Figure B1. The reaction front advances from the outer surface into the solid leaving behind a layer of completely converted and inert solid called the ash or product layer. At the same time the core of unconverted solids shrinks and finally disappears.

Consider the reaction of $C_aO$ and $H_2S$,

$$CaO + H_2S = CaS + H_2O \quad (1)$$

According to Figure B1, assuming the concentration of the reaction gas $C_{H2S}$ equals to equilibrium concentration $C_{H2S}^{e}$ at

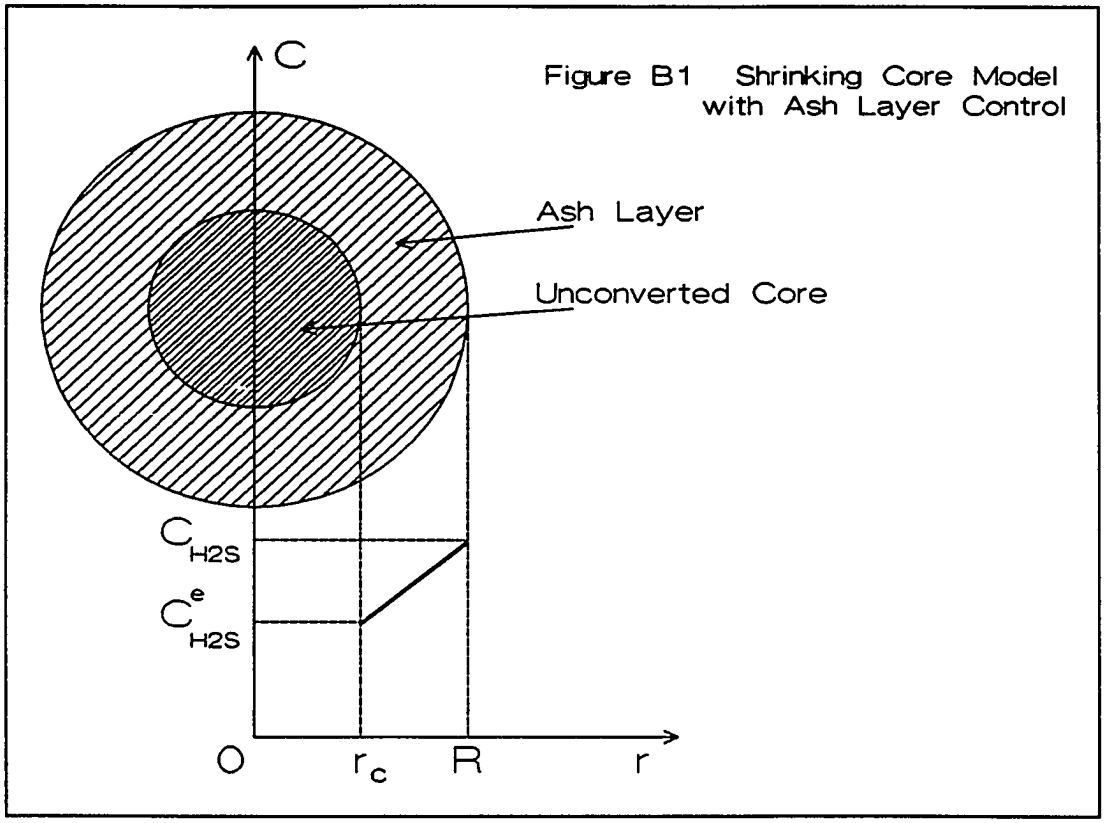


Figure B1 Shrinking Core Model with Ash Layer Control

$r = r_c$, the total reaction rate equals to the diffusion rate through the ash layer. The reaction rate of gas and solid can be written as:

$$-\frac{dn_{H2S}}{dt} = 4\pi r^2 D_{H2S}\frac{dC_{H2S}}{dr} \qquad (2)$$

where $D_{H2S}$ is the diffusion coefficient of $H_2S$ through the ash

layer. Integrating eq.(2) from $r=r_c$, $C_{H2S}=C_{H2S}^{e}$, to $r=R$, $C_{H2S}=C_{H2S}$.

which is bulk gas phase concentration.

$$-\frac{dn_{H2S}}{dt}\left(\frac{1}{r_c} - \frac{1}{R}\right) = 4\pi D_{H2S}(C_{H2S}-C^{e}_{H2S}) \tag{3}$$

From eq.(1), we have the mass conservation:

$$-dn_{CaO} = -dn_{H2S} = -\rho_p\, dV_p = -4\pi\rho_p\, r_c^2 dr_c \tag{4}$$

where $\rho_p$ is the density of the solid particle, substituting eq.(4) to eq.(3) and integrating it, The result is

$$t = \tau\left(1-3\left(\frac{r_c}{R}\right)^2 + 2\left(\frac{r_c}{R}\right)^3\right) \tag{5}$$

where $\tau$ is the time for complete conversion of the solid particle, and can be calculated by

$$\tau = \frac{\rho_p R^2}{6D_{H2S}(C_{H2S} - C^{e}_{H2S})} \tag{6}$$

The relation between the particle conversion and radius of shrinking core is

$$1 - x = \left(\frac{r_c}{R}\right)^3 \tag{7}$$

Finally, the shrinking core model can be written as a dimensionless expression which is only the function of single

particle conversion.

$$\frac{t}{\tau} = 1 - 3(1 - x)^{(2/3)} + 2(1 - x) \tag{8}$$

**Integrating with CSTR Flow Pattern**

Eq.(7) describes the reaction history of a single particle. For estimating the average conversion of total particles in the reactor Xav, we have to integrate eq.(7) with residence time distribution density function, first CSTR flow model:

$$Xav = \int_0^{\infty} x \frac{1}{Tav} \exp(-\frac{t}{Tav}) dt \tag{9}$$

where Tav is the total particles average residence time through the reactor. Substituting eq.(7) into eq.(8), get

$$Xav = \exp(-\frac{\tau}{Tav}) + [\int_0^1 2(\frac{\tau}{Tav}) x((1 - x)^{(1/3)} - 1) \exp(-\frac{\tau}{Tav})(1-3(1 - x)^{(2/3)} + 2(1 - x))\, dx] \tag{10}$$

Obviously, Xav is the function of ($\tau$/Tav) only, and $\tau$ is the total conversion time of single particle which is the function of temperature, pressure, and gas composition. $\tau$ can be calculated by

$$\tau = \frac{0.000706(15.0d_p + 710d_p^2)\sqrt{T}}{P(y_{H2S} - y^e_{H2S})} \qquad (11)$$

Tav is the average residence time of all the particles flow through the reactor which is the ratio of total bed weight to solid withdraw rate.

**Integrating with PFR Flow Pattern**

The final conversion of solid withdraw stream is

$$X_{final} = \int_0^\infty x\,\delta(t - T_{final})\,dt \qquad (12)$$

where $T_{final}$ is the total solid residence time in the reactor. Substituting eq(4) into eq.(12), we can get the explicit function of $T_{final}$ which can be written as:

$$\frac{T_{final}}{\tau} = 1 - 3(1 - X_{final}) + 2(1 - X_{final}) \qquad (13)$$

We can see both for CSTR and PFR Model The total conversion are only function of the ratio ($\tau$/Tav). $T_{final}$ in PFR model is equivalent as Tav in CSTR model. We plot two master curves both for CSTR and PFR with shrinking core ash layer control model shown in Figure B2. These two model were built

in the gasifier program to predict the sulfur capture behaviors.

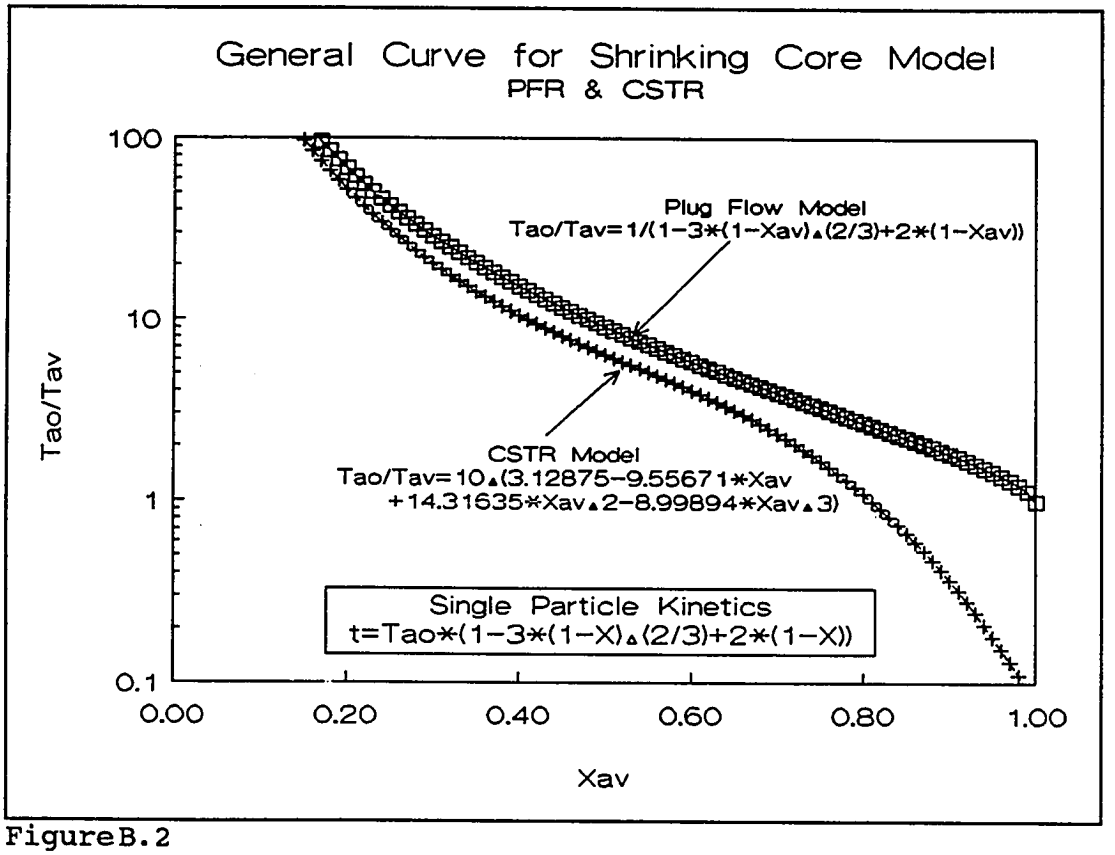


Figure B.2

# Appendix C

# Gasifier Model Description

## I. INTRODUCTION

### I.1 Program Overview

Program GASF is a steady state model to describe fluidized bed gasifier operation. The kinetics of char gasification and CaO desulfurization are built in with proper

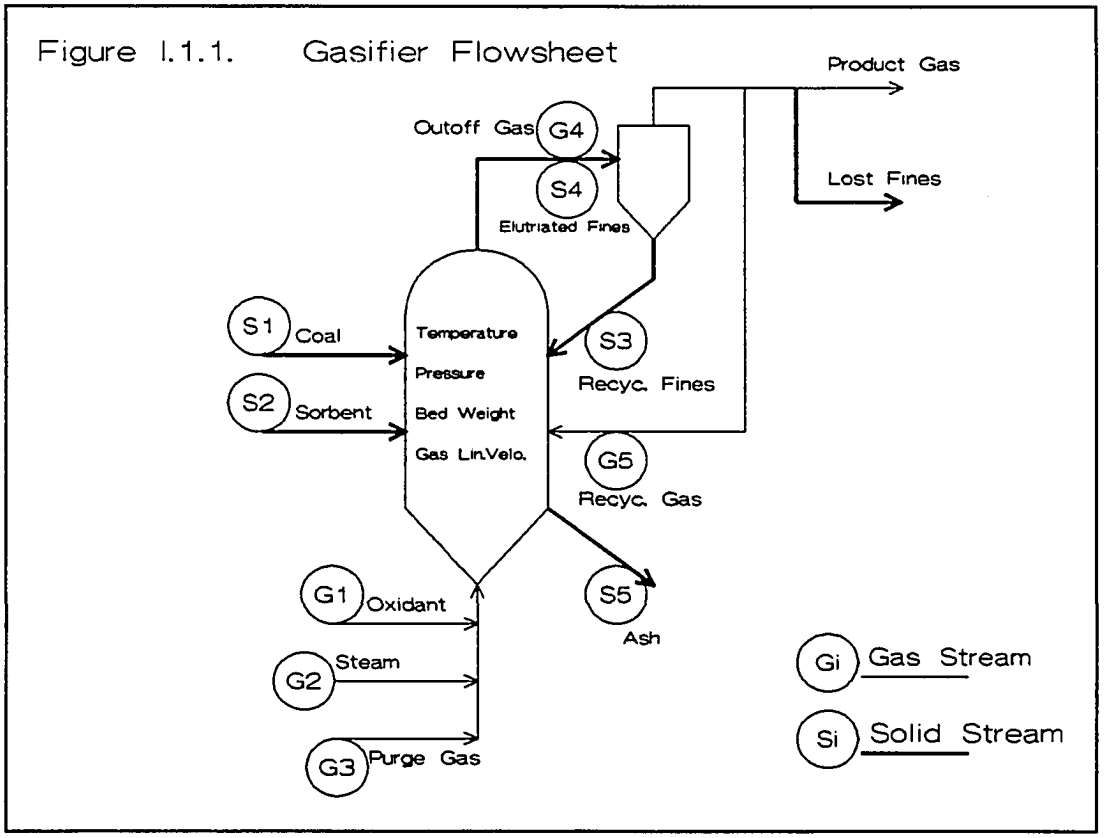


solid residence time distribution. Both kinetics and solid residence time distribution function can be defined by user.

Five solids and five gases streams with different compositions can be solved simultaneously with mass and energy balances and with two kinetics models. All these streams can be found in figure I.1.1.

The model consists of 22 equations for equal amount of state variables, in which some of them are highly nonlinear. User can specify following variables:

a) Coal flow rate, including coal properties (Stream S1);
b) Sorbent flow rate and CaCO3, MgCO3 concentrations (S2);
c) Steam flow rate (G2);
d) Purge gas flow rate and purge gas concentration (G3);
e) Elutration fines and concentration (G4);
f) Fines recycle ratio to total elutriated fines (S3);
g) Product gas recycle ratio to total out-off gas (G5);
h) All of the stream temperatures;
i) Bed temperature and pressure;
j) Bed weight, which is defined as total weight of bed material per cross section of bed;
k) Superficial velocity of production gas in bed;
l) Heat lost from the reactor surface.

There are 57 variables which can be inputted by the user through the file preparation program (FPP). These 57

variables give all necessary information required to run the main program (GASF). The results of the program include:

a) The output flowrate of the production gas (stream G4);

b) The composition of production gas (G4);

c) The oxidant required is calculate for a given bed temperature (G1);

d) Solid withdraw flowrate (S5);

e) Solid withdraw composition (S5);

f) The total carbon conversion from coal;

g) The sulfur capture & sorbent conversion;

h) Gasifier diameter for the coal flowrate.

In order to run the main program (GASF), it required the user to generate data file which obtains 57 variables using the file preparation program (FPP). The data file can be easily modified by FPP for case studies. The user is also required to give the program output file name to which the results will be printed. GASF will solve each equation in sequential fashion through a series loops algorithm. A set of non-linear equations was solved by Broyden (1972) method simultaneously, which was a tearing technique to guess a part of initial variables and to solve the rest of the equations by a special sequence. The program iterated around the tear variables, which iterative new direction were given by Jacobian matrix.

## I.2 Capabilities

The program solves the char gasification kinetics and sulfur capture kinetics with mass and energy balances together.

### I.2.1 Gasification

The single char particle reaction history can be described by

$$X = 1 - \exp\left(\frac{-KR_o t}{1 + AKR_o t}\right) \qquad \text{(I.1)}$$

Where x is single particle conversion, t is conversion progressing time (min), and K, A are the kinetic parameters. ( see appendix A ) The lumped kinetics gasification rate $R_o$ is calculated by Muhlen equation (1985):

$$R_o = \frac{r_1 p_{CO2} + r_8 p_{CO2}^2 + r_9 p_{H2O} + r_{11} p_{H2O}^2 + r_{12} p_{H2O} p_{H2} + r_4 p_{H2}^2}{1 + r_2 p_{CO2} + r_3 p_{CO} + r_{10} p_{H2O} + r_5 p_{H2}} \qquad \text{(I.2)}$$

This single particle reaction history can be integrated with CSTR or PFR or other combinations of residence time distribution function.

### I.2.2 Sulfur Capture

The sulfur compounds present in the coal are converted to hydrogen sulfide when the coal is gasified in a conventional coal gasifier. The addition of a calcium-based sorbent to the gasifier can capture and remove sulfur compounds from the fuel gas within the gasifier. Under the reducing atmosphere of the gasifier, the sorbent reacts with hydrogen sulfide to form calcium sulfide. If limestone is calcined at gasification conditions, sulfur capture occurs through the reaction of calcium oxide with hydrogen sulfide:

$$CaCO_3 \rightleftharpoons CaO + CO_2 \qquad \text{(I.3)}$$

$$CaO + H_2S \rightleftharpoons CaS + H_2O \qquad \text{(I.4)}$$

The equilibrium partial pressure for reaction (I.3) can be calculated from

$$P_{CO2}^{e} = 10^{-\frac{8308}{T} + 7.079} \qquad \text{(I.5)}$$

where $P_{CO2}^{e}$ is in atmosphere and T is in degree Kelvin. The equilibrium partial pressure of $CO_2$ in gasifiers operating at elevated pressures can exceed the equilibrium value, due to which Reaction (I.3) cannot proceed. Under these circumstances, sulfur capture takes place through the following reaction:

$$CaCO_3 + H_2S \rightleftharpoons CaS + CO_2 + H_2O \qquad (I.6)$$

The equilibrium for reaction (I.4) can be calculated by the expression

$$\frac{P^e_{H2O}}{P^e_{H2S}} = 10^{\frac{3519.2}{T} - 0.268} \qquad (I.7)$$

and the equilibrium for reaction (I.6) may be found combining equations (I.5) and (I.7) to obtain

$$\frac{P^e_{H2O} \bullet P^e_{CO2}}{P^e_{H2S} \bullet P_{total}} = 10^{\frac{-4788.8}{T} + 6.811} \qquad (I.8)$$

The kinetics of the desulfurization reactions can be expressed from the shrinking core model in the following form:

$$t = \tau \left(1-3\left(\frac{r_c}{R}\right)^2 + 2\left(\frac{r_c}{R}\right)^3\right) \qquad (I.9)$$

Where $\tau$ is the time of a single particle completely converted, which is explained in appendix B. This equation can integrated with solid residence distribution function to calculate the solid average conversion as a function of average residence time through the bed.

The driving force of sulfur capture in this kinetic model is the difference of $H_2S$ bulk concentration and equilibrium concentration in the environmental conditions of the gasifier.

The environmental condition of the gasifier depends on the feeding, pressure and temperature of the bed. The sorbent dissociation depends on the partial pressure of $CO_2$ in the bed.

# II MODEL EQUATIONS

## II.1 Basic Assumption

The model accounts for gasification kinetics and sulfur capture kinetics. These two kinetics are integrated with CSTR residence time distribution flow pattern for both gas and solid phases. The basic assumptions are described following.

### II.1.1 Coal Devolatilization

Devolatilization kinetics are instantaneous comparing to gasification kinetics.

The program calculates the devolatilization carbon conversion with consistence of stoichiometric concentration of hydrogen and oxygen in the coal. The production of devolatilization goes to the gas phase as CO, $CO_2$, $H_2$, $H_2O$ and $CH_4$.

### II.1.2 Char Combustion

Combustion kinetics are instantaneous.

Combustion products are $H_2O$, CO, and $CO_2$.

Char combusts with oxygen to yield CO and $CO_2$ at a molar ratio of unity.

II.1.3 Char Gasification

Gasification occurs uniformly through the bed as the CSTR assumption.

Species present in the gasification zone are: CO, $CO_2$, $H_2$, $H_2O$, $N_2$, $CH_4$, $H_2S$, $NH_3$, char, ash and sorbent.

The water shift reaction is at thermal equilibrium at the reactor conditions.

Gas and solid phases are well mixed.

Uniform feed particle size distribution both for coal and sorbent.

Ideal gas.

II.1.4 Sulfur Capture

The amount of sulfur released to the gas phase is proportional to the converted carbon in the coal as $H_2S$.

The algorithm for computing the sulfur capture rate depending upon whether or not the $CO_2$ partial pressure is above or below that required at equilibrium has been incorporated into the program. According the dissociation reaction of

$$CaCO_3 \rightleftharpoons CaO + CO_2 \qquad \text{(II.1)}$$

if the partial pressure of $CO_2$ is lower than the equilibrium of reaction above, assume this reaction occurs completely, there is no $CaCO_3$ existing in the solid withdraw. The sulfur capture driving force is calculated according the reaction of

$$CaO + H_2S = CaS + H_2O \qquad \text{(II.2)}$$

If the partial pressure of $CO_2$ is higher than the equilibrium of eq.(II.1), CaO disappears in solid withdraw. The sulfur capture equilibrium calculation depends on the reaction of

$$CaCO_3 + H_2S = CaS + CO_2 + H_2O \qquad \text{(II.3)}$$

In this case, the driving force for the kinetics is calculated according the equilibrium of eq.(II.3).

## II.2 Model Equations

### 1) Carbon Balance (C)

Net production gas:

$$0 = (FG4_{CO} + FG4_{CO2} + FG4_{CH4})*(1 - RGAS)$$

Lost fines:

$$+ZS4*(WS4_{char}/MW_{char} + WS4_{CaCO3}/MW_{CaCO3} + WS4_{MgCO3}/MW_{MgCO3}) *(1 - RFINES)$$

Solid withdraw:

$$+ZS5_{char}/MW_{char} + ZS5_{CaCO3}/MW_{CaCO3} + ZS5_{MgCO3}/MW_{MgCO3}$$

Coal feed:

$$-ZS1*(WCCOAL + WVCOAL)/MW_{Coal}$$

Sorbent feed:

$$-ZS2*(WS2_{CaCO3}/MW_{CaCO3} + WS2_{MgCO3}/MW_{MgCO3})$$

Purge gas:

$$-FG3*Y_{CO2}$$

### 2) Hydrogen Balance ($H_2$)

Net production gas:

$$0 = (FG4_{H2} + FG4_{H2O} + FG4_{CH4}*2 + FG4_{NH3}*1.5 + FG4_{H2S})*(1 - RGAS)$$

Lost fines:

$$+ZS4*WS4_{char}/MW_{char}*\alpha/2*(1 - RFINES)$$

Solid withdraw:

$$+ZS5_{char}/MW_{char}*\alpha/2$$

Coal feed:

$$-ZS1*((WCCOAL + WVCOAL)/MW_{Coal}*\alpha/2 + WMCOAL/MW_{H2O})$$

Purge gas:

$$-FG2$$

3) Oxygen Balance (O)

Net production gas:

$$0 = (FG4_{CO} + FG4_{CO2}*2 + FG4_{H2O})*(1 - RGAS)$$

Lost fines:

$$+ZS4*(WS4_{char}/MW_{char}*\beta + WS4_{CaCO3}/MW_{CaCO3}*3 + WS4_{MgCO3}/MW_{MgCO3}*3 + WS4_{MgO}/MW_{MgO} + WS4_{CaO}/MW_{CaO} + WS4_{CaSO4}/MW_{CaSO4}*4)*(1 - RFINES)$$

Solid withdraw:

$$+ZS5_{char}/MW_{char}*\beta + ZS5_{CaCO3}/MW_{CaCO3}*3 + ZS5_{MgCO3}/MW_{MgCO3}*3$$
$$+ZS5_{MgO}/MW_{MgO} + ZS5_{CaO}/MW_{CaO} + ZS4_{CaSO4}/MW_{CaSO4}*4$$

Coal feed:

$$-ZS1*((WCCOAL + WVCOAL)/MW_{Coal}*\beta + WMCOAL/MW_{H2O})$$

Sorbent feed:

$$-ZS2*(WS2_{CaCO3}/MW_{CaCO3} + WS2_{MgCO3}/MW_{MgCO3})*3$$

Oxidant feed:

$$-FG1*YG1_{O2}*2$$

Steam feed:

$$-FG2$$

Purge gas:

$$-FG3*(YG3_{CO2}*2 + YG3_{SO2}*2)$$

4) Nitrogen Balance ($N_2$)

Net production gas:

$$0 = (FG4_{N2} + FG4_{NH3}/2)*(1 - RGAS)$$

Lost fines:

$$+ZS4*WS4_{char}/MW_{char}*n/2*(1 - RFINES)$$

Solid withdraw:

$+ZS5_{char}/MW_{char}*n/2$

Coal feed:

$-ZS1*((WCCOAL + WVCOAL)/MW_{Coal}*n/2$

Oxidant feed:

$-FG1*YG1_{N2}$

Purge gas:

$-FG3*YG3_{N2}$

5) Sulfur Balance (S)

Net production gas:

$0 = FG4_{H2S}*(1 - RGAS)$

Lost fines:

$+ZS4*(WS4_{char}/MW_{char}*s + WS4_{CaS}/MW_{CaS} + WS4_{CaSO4}/MW_{CaSO4})$
$*(1 - RFINES)$

Solid withdraw:

$+ZS5_{char}/MW_{char}*s + ZS5_{CaS}/MW_{CaS} + ZS5_{CaSO4}/MW_{CaSO4}$

Coal feed:

$-ZS1*((WCCOAL + WVCOAL)/MW_{Coal}*s$

Purge gas:

$-FG3*YG3_{SO2}$

6) Ash Balance

Lost fines:

$0 = ZS4*WS4_{Ash}*(1 - RFINES)$

Solid withdraw:

$+ZS5_{Ash}$

Coal feed:

$-ZS1*WACOAL$

7) Calcium Balance (Ca)

Lost fines:

$$0 = ZS4*(WS4_{CaCO3}/MW_{CaCO3} + WS4_{CaO}/MW_{CaO} + WS4_{CaS}/MW_{CaS} + WS4_{CaSO4}/MW_{CaSO4})*(1 - RFINES)$$

Solid withdraw:

$$+ZS5_{CaCO3}/MW_{CaCO3} + ZS5_{CaO}/MW_{CaO} + ZS5_{CaS}/MW_{CaS} + ZS5_{CaSO4}/MW_{CaSO4}$$

Sorbent feed:

$-ZS2*WS2_{CaCO3}/MW_{CaCO3}$

8) Magnesium Balance

Lost fines:

$$0 = ZS4*(WS4_{MgCO3}/MW_{MgCO3} + WS4_{MgO}/MW_{MgO})*(1 - RFINES)$$

Solid withdraw:

$$+ZS5_{MgCO3}/MW_{MgCO3} + ZS5_{MgO}/MW_{MgO}$$

Sorbent feed:

$$-ZS2*WS2_{MgCO3}/MW_{MgCO3}$$

9) Mole Fraction Closure

$$1 = \Sigma\ YG4_i$$

10) Weight Fraction Closure

$$1 = \Sigma\ WS5_i$$

11) $CH_4$ Specified

$$0 = PROCH4*ZS1*(WCCOAL + WVCOAL)/MW_{Coal} - FG4_{CH4}*(1 - RGAS)$$

12) $NH_3$ Specified

$$0 = PRONH3*ZS1*(WCCOAL + WVCOAL)/MW_{Coal}*n - FG4_{NH3}*(1 - RGAS)$$

13) Sulfur Capture Kinetics (CaO Conversion)

$$X_{CaO}=\int_0^{\infty} x\frac{1}{Tav}\exp\left(\frac{t}{Tav}\right)dt$$

where the single particle reaction time t is a function of the CaO conversion x, which can be given by shrinking core model as following:

$$t = \tau\left(1 - 3\left(1 - x\right)^{(1/3)} + 2\left(1 - x\right)\right)$$

where $\tau$ is the single particle complete reaction time.

14) Not Used in This Version

15) Shift Equilibrium

$0 = K_p*FG4_{CO}*FG4_{H2O} - FG4_{CO2}*FG4_{H2}$

16) $CaCO_3$ Dissociation

$0 = ZS5_{CaCO3} - ZS2*W_{CaCO3}*(1 - CADISO)$

17) $MgCO_3$ Dissociation

$0 = ZS5_{MgCO3} - ZS2*W_{MgCO3}*(1 - MGDISO)$

18) Energy Balance

Output Energy (Steam #):

Off Gas (G4)

$$HO\text{-}1 = \Sigma\ FG4_i * (H_{form\ i} + \int_{298}^{Tbed} C_{pi}\ Dt)$$

Elutriated Solids (S4)

$$HO\text{-}2 = FS4 * (\Sigma\ WS4_i * (H_{form\ i} + \int_{298}^{Tbed} C_{pi}\ Dt)$$

Ash Withdraw (S5)

$$HO\text{-}3 = \Sigma\ FS5_i * (H_{form\ i} + \int_{298}^{Tash} C_{pi}\ Dt)$$

Heat Loss

$$HO\text{-}4 = HLOSS$$

Input Energy (Steam #):

Coal (S1)

$$HI\text{-}1 = ZS1 * ((1 - WMCOAL) * (H_{form\ Coal} + \int_{298}^{Tcoal} C_{p\ coal} dT) + WMCOAL * (H_{form\ H2O} + \int_{298}^{Tcoal} C_{p\ H2O} dT))$$

Sorbent (S2)

$$HI\text{-}2 = ZS2 * (\Sigma\ WS2_i * (H_{form\ i} + \int_{298}^{Tsorbent} C_{pi}\ Dt)$$

Oxidant (G1)

$$HI\text{-}3 = FG1 * (\Sigma\ YG1_i * (H_{form\ i} + \int_{298}^{Toxit.} C_{pi}\ Dt)$$

Steam (G2)

$$HI\text{-}4 = FG2*(H_{form\ H2O} + \int_{Tcond.}^{Tsteam} C_{pi}\ Dt)$$

Purge Gas (G3)

$$HI\text{-}5 = FG3*(\Sigma\ YG3_i*(H_{form\ i} + \int_{298}^{Tpurge} C_{pi}\ Dt)$$

Recycle Gas (G5)

$$HI\text{-}6 = FG4*RGAS*(\Sigma\ YG5_i*(H_{form\ i} + \int_{298}^{Trecycle} C_{pi}\ Dt)$$

Recycle Fines (S3)

$$HI\text{-}7 = FS4*RFINES*(\Sigma\ WS4_i*(H_{form\ i} + \int_{298}^{Trecycle} C_{pi}\ Dt)$$

Total Balance

$$0 = HO\text{-}1 + HO\text{-}2 + HO\text{-}3 + HO\text{-}4$$
$$-HI\text{-}1 - HI\text{-}2 - HI\text{-}3 - HI\text{-}4 - HI\text{-}5 - HI\text{-}6 - HI\text{-}7$$

19) Gasification Kinetics (Carbon Conversion)

$$X_{gasif.} = \int_0^{\infty} x \frac{1}{Tav} \exp\left(\frac{t}{Tav}\right) dt$$

where x is the single particle conversion as a function of time, which can be expressed as:

$$x = 1 - \exp\left(-\frac{KR_o}{1 + AKR_o t}\right)$$

$$X_{carb} = X_{devol} + X_{comb} + (1 - X_{devol} - X_{comb}) * X_{gasif}$$

20) Carbon Conversion Definition

$$0 = X_{gasif} * ZS1 * (WCCOAL + WVCOAL) / MW_{Coal}$$
$$- ZS1 * (WCCOAL + WVCOAL) / MW_{Coal}$$
$$+ ZS4 * WS4_{Char} / MW_{Char} * (1 - RFINES)$$
$$+ ZS5_{Char} / MW_{Char}$$

21) Linear Velocity

$$LINVE = 0.08206 * T_{bed} * \Sigma FG4_i / P_{bed} / (\pi / 4 * D_{bed}^2)$$

22) Fines Elutriation

$$0 = ZFINES - ZS4$$

Variable Definition:

F* : Molar flowrate (lbmol/hr)

Z* : Weight flowrate (lb/hr)

Y* : Mole fraction

W* : Weight fraction

T* : Temperature (°K)

P* : Pressure (atm)

*S*: Solid streams

*G*: Gas streams

$H_{form\ i}$ : Formation heat

$Cp_i$ : Heat capacity of species i

## II.2.1 Program Structure

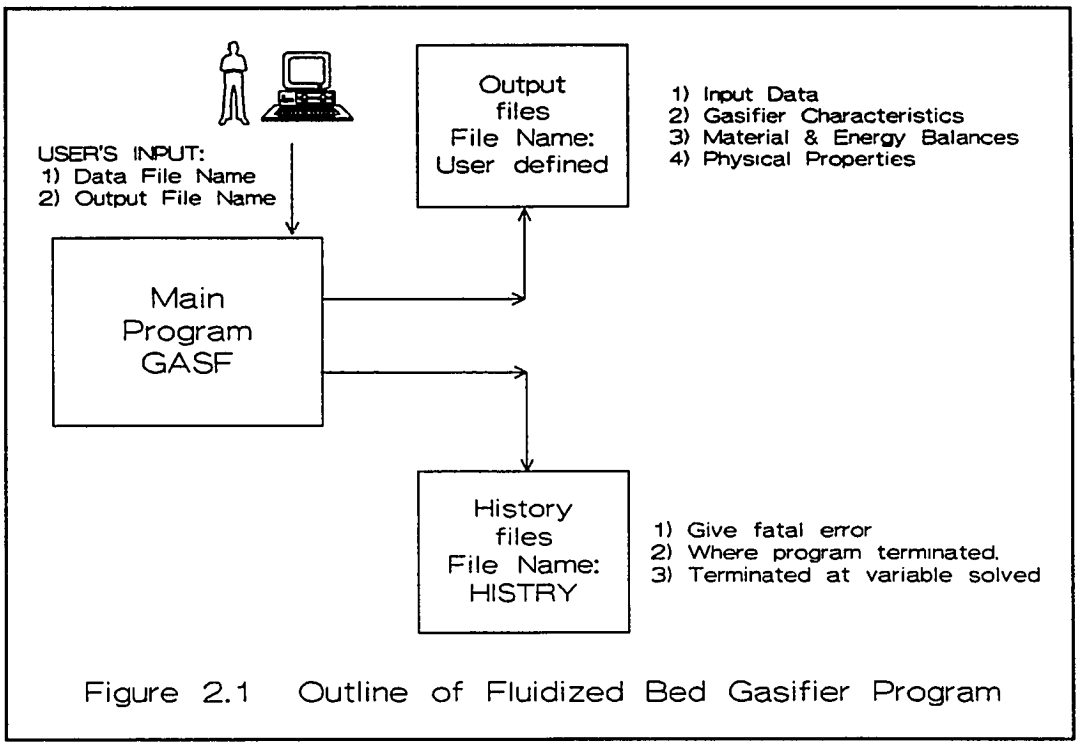


Figure 2.1 Outline of Fluidized Bed Gasifier Program

Figure 2.1 describes how the user and the program are connected. In order to run the main program (GASF), all the user has give is the input file name and output file name.

The equation solver structure is shown schematically in Figure 2.2. A brief description of each the major subroutines are given below.

### II.2.2 Program Subroutines

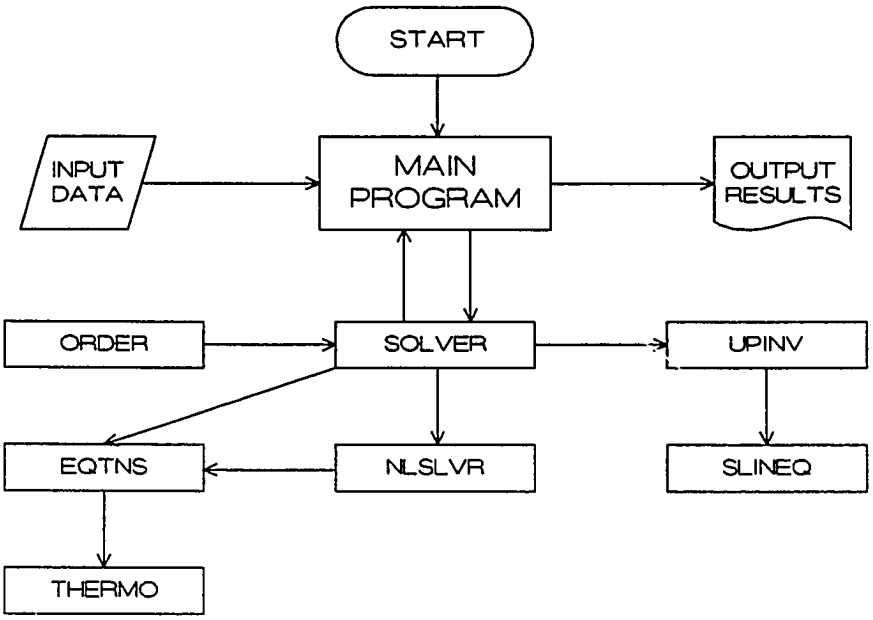


Figure 2.2 Structure of Gasifier Simulation Program

ORDER

This routine orders the equations for solutions. It selects a sequenced equation and its output variable. The routine checks for redundancy in the equations by analyzing the system's constrained Jacobian matrix. The equation sequencing is chosen so that to select a minimal tear set (tear variables and error functions).

NLSLVR

This routine solves a single non-linear equation in one variable. The method is an adaptation of the "Memory" method suggested by Shacham and Kehat (1972). This method uses a n-1 order interpolating polynomial through n previously generated

points. The method was proven superior by its authors over all other methods (Secant, Newton-Raphson, Chebyhev), and in this application has persistently converged in three or four function evaluations even for transcendental equations. This routine may be called a few thousand times during one solution.

UPINV, SLINEQ

These routine contain Broyden's Quasi-Newton method - Broyden [1965] - using the Metcalfe-Perkins (optional) stepping rule, with finite difference evaluation of the Jacobian. SLINEQ solves the generated system of linearized equations using LU factorization with refinement of the round-off errors.

EQTNS

EQTNS is a user supplied routine which contains the system's equations written as F(X)= 0. F(X) may contain algebraic or differential equations, linear or non-linear, implicit or explicit.

THERMO

A thermodynamic database developed 'in-house' and limited to components of coal gasification reactions, and methanol

synthesis. Heats of reaction are not required because SOLVER uses the elementary enthalpy references state. Reference state for thermodynamic properties is the elements in their standard states at 25 °C and 1 atm. Standard heats of formation, free energy of formation, and heat capacities are calculated from temperature dependent correlations developed by Yaws [1976].

Method of Integration (Simpson's Rule)

The program uses Simpson's rule to determine the area under the curve of different order polynomial models in each interval.

# APPENDIX D

## DISAPPEARANCE OF OXYGEN

One of the assumption in the gasifier model is that combustion of carbon and oxygen occurs instantaneously, which means that the oxygen disappears in a very shot time after being injected into the gasifier. The following calculation will suport this assumption. Consider the carbon-oxygen reaction:

$$C + 1/\phi\ O_2 = 2(1 - 1/\phi)\ CO + (2/\phi - 1)\ CO_2 \qquad \text{(D1)}$$

The specific char-gas reaction rate have been investigated by Wen and Dutta (1978), Field et al. (1967), Dobner (1976).

$$r = k_e p_{O_2}\ , \qquad k_e = \frac{1}{\frac{1}{k_d} + \frac{1}{k_s}} \qquad \text{(D2)}$$

where r is the reaction rate with the unit of $kg/m^2/sec$, $p_{02}$ is the partial pressure of oxygen surrounding the particle, $k_d$ and $k_s$ are the coefficients of gas film diffusion and surface reaction respectively. $k_d$ and $k_s$ ($kg/m^2/atm/sec$) have been given as:

$$k_d = 0.292\frac{D}{d_p T_m}\ , \qquad D = 4.26\left(\frac{T_g}{1800}\right)^{1.75}\left(\frac{1}{P}\right) \qquad \text{(D3)}$$

The parameter $\phi$ describes the product gas CO and $CO_2$ distribution. $\phi$=1, for reaction to only $CO_2$, and $\phi$=2 for

$$k_s = 87100 \exp(-\frac{17967}{T_c}) \quad \text{(D4)}$$

reaction to only CO. $\phi$ is the function of particle size and temperature.

$$\phi = \frac{2Z + 2}{Z + 2} \qquad for\ d_p \leq 0.005\ cm \quad \text{(D5)}$$

$$\phi = (2Z + 2 - \frac{Z(d_p - 0.005)}{0.095})(Z + 2) \quad \text{(D6)}$$

$$for\ 0.005\ cm < d_p \leq 0.1\ cm$$

$$\phi = 1.0 \qquad for\ d_p > 0.1\ cm \quad \text{(D7)}$$

$$Z = 2500 \exp(-\frac{6249}{T_m}) \quad \text{(D8)}$$

where $T_g$, $T_s$, and $T_m$ are the temperature of gas phase, solid phase and the average of both temperature in K.

For calculating the oxygen penetration, the constant volumetric flow rate within the combustion zone can be assumed. The differential oxygen balance can be written as:

$$\frac{v}{RT_m} dy_{O_2} = \frac{6}{d_p}(1 - \epsilon) r dx \quad \text{(D9)}$$

For oxygen conversion of 99 percent, The plots of penetration depth x versus operating temperature $T_m$ and particle diameter $d_p$ can be obtained from Eq.(9).

$$x = 9.354 \frac{v d_p}{T_m (1 - \epsilon) k_e} \qquad \text{(D10)}$$

where v (m/sec) is the superficial velocity of air leaving the jet. $d_p$ (m) is the particle diameter of the char. $T_m$ (K) is the average temperature of gas and solid. $\epsilon$ is the void fraction. $k_e$ is the intrinsic reactivity of char oxygen combustion which is defined by Eq.(2).

The effect of temperature and particle size on penetration height is shown in Figure D1.

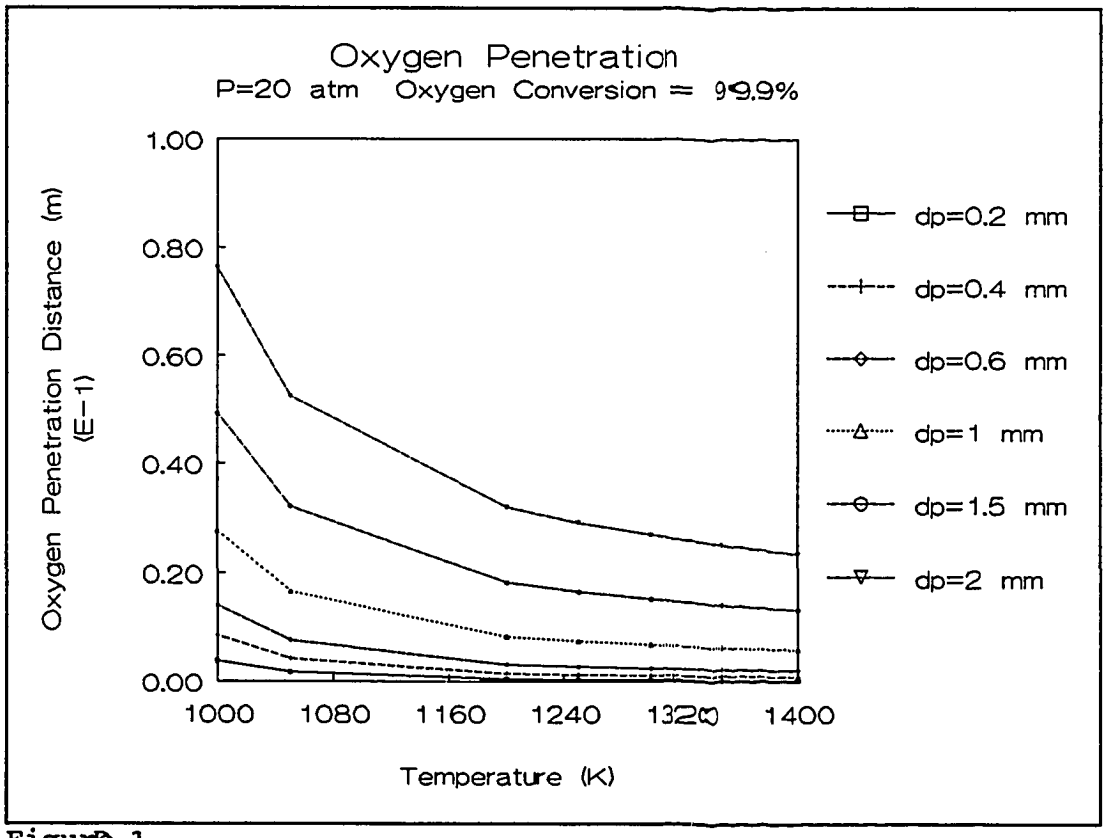


Figure D.1

## REFERENCES

Anthony, D. B. and J. B. Howard, 1976, Coal Devolatilization and Hydrogasification, AIChE Journal, Vol. 22, No. 4, p. 625-656.

Arri, L. E. and N. R. Amundson, 1978, An Analytical Study of Single Particle Char Gasification, AIChE Journal, Vol. 24, No.1, p. 72-87.

Biba,V., J. Macak, E. Klose, and J. Malecha, 1978, Mathematical Model for the Gasification of Coal under Pressure, I&EC Process Design & Development, Vol. 17, No. 1, p. 92-97.

Blake, T. R., C. Y. Wen, and C. A. Ku, 1984, AIChE Symp. Series, 234, Vol. 80, p.42.

Blake, T. R. and P. J. Chen, 1981, ASC Sym. Series, 168, p. 157.

Broyden, C. G., 1965, A Class of Mehtods for Solving Non-linear Equations, Ph. D. Thesis, Purdue University.

Broyden, C. G., 1967, Quasi-Newton Methods and their Application to Function Minimination, Math. Comp., Vol.21, p. 368-381.

Caram, H. S. and N. R. Amundson, 1979, Fluidized Bed Gasification Reactor Modeling. 1. Model Description and Numerical Results for a single Bed, I&EC Process Design & Development, Vol. 18, No. 1, p. 80-95.

Caram, H. S. and N. R. Amundson, 1979, Fluidized Bed Gasification Reactor Modeling. 2. Effect of the Residence Time Distribution and Mixing of the Particles. Staged Bed Modeling. I&EC Process Design & Development, Vol. 18, No. 1, p. 97-102.

Chen, L. H. and C. Y. Wen, 1982, Model of Solid Gas Reaction Phenomena in the Fluidized Bed Freeboard, AIChE Journal, Vol. 28, No. 6. p. 1019-1027.

Dawkins, R. P., et. al., 1985, Cost and Performance of KRW Based Gasification Combined Cycle Plants, (EPRI), 4-24

Denn, M. M. and W. Yu, 1979, Parameter Sensitivity and Kinetics-Free Modeling of Moving Bed Coal Gasifiers, Ind. Eng. Chem. Fundam., Vol 18, No.3, p. 266-268.

Dobner,S., L. Sterns, R. A. Graff, and A. Squires, 1977, Cyclic Calcination and Recarbonation of Calcined Dolomite, I&EC Process Design & Development, Vol. 16, p. 479.

Dutta S. and Y. Wen, 1977, Reactivity of Coal Char. 1. In Carbon Dioxide Atmosphere, I&EC Process Design & Development, Vol. 16, No. 1, p. 20-30.

Dutta S. and Y. Wen, 1977, Reactivity of Coal Char. 2. In Oxygen-Nitrogen Atmosphere, I&EC Process Design & Development, Vol. 16, No. 1, p. 31-36.

Ellig, D. L., C. K. Lai, D. W. Mead, J. P. Longwell, and W. A. Peters, 1985, Pyrolysis of Volatile Aromatic Hydrocarbons and n-Heptane over Calcium Oxide and Quartz, I&EC Process Design & Development, Vol. 24, p. 1080.

Finson, M. L., 1980, Coal processing for fuel cell utilization, fluidized bed coal gasification model; data analysis and predictions, Physical Science Inc. Report TR 209.

Floess, J. K., J. Plawsky, J. P. Longwell, and W. A. Peters, 1985, Effects of Calcined Dolomite on the fluidized Bed Pyrolysis of a Colorado Oil Shale and a Texas Lignite, I&EC Process Design & Development, Vol. 24, p. 730.

Govind, R., and J. Shah, 1984, Modeling and Simulation of An Entrained Flow Coal Gasifier, AIChE Journal, Vol. 30, No. 1, p. 79-92.

Goyal, A., R. F. Zabransky, and A. Rehmat, 1989, Gasification Kinetics of Wertern Kentucky Bituminous Coal Char, Ind. Eng. Chem. Res., Vol.28, No. 12, p. 1767-1785.

Haldipur, D. B., et. al. 1989, A 50-Month Gasifier Mechanistic Study and Downstream Unit Process Development Program for the Pressurized Ash-Agglomerating Fluidized Bed Gasification System, Final Report, Volume I, & II, DOE/MC/21063. NTIS/FE2106369

Katta, S. and D. L. Kealrns, 1981, Study of kinetics of Carbon Gasification Reactions, Ind. Eng. Fundam., Vol 20, No. 1, p. 6-13.

Klein, H. H., 1982, The FLAG computer program for simulation of axisymmetric fluidized bed reactors, USDOE Report DOE/METC/82-24.

Liss, B., T. R. Blake, A. M. Squires, and R. Bryson, 1984, Fluidization, Eds. D. Kunii and R. Toei, Engineering Foundation, p. 249.

Matsui, I., D. Kunii, and T. Furusawa, 1987, Study of Char Gasification by Carbon Dioxide. 1. Kinetic Study by Thermogravimetric Analysis,Ind. Eng. Chem. Res., Vol. 26, No. 1, p. 91-95.

Matsui, I., T. Kojima, D. Kunii, and T. Furusawa, 1987, Study of Char Gasification by Carbon Dioxide. 2. Continuous Gasification in Fluidized Bed, Ind. Eng. Chem. Res., Vol. 26, No. 1, p. 95-100.

Muhlen, H., K. H. Heek, H. Juntgen, 1985, Fuel, Vol. 64, p. 944-949.

Roache N. F., 1984, Reaction of $H_2S$ and Sulfur with Limestone Particles, I&EC Process Design & Development, Vol. 23, p. 742-748.

Shacham, M., and E. Kehat, 1972, An iteration method with memory for the solution of a non-linear equation, Chemical Engineering Science, Vol. 27, p. 2099-2101.

Shinnar, R., and J. C. Kuo, 1978, Gasifier study for Mobil coal to gasoline process, USDOE Report DE-2766-13UC-90D.

Shinnar, R., A. I. Avidan, Li Weng, 1986. Evaluation of Fluidized Bed Coal Gasification Present Status and Future Development Problems, Final Report, DOE/MC/21259

Simbeck, D. R. et. al., 1983, Coal Gasification System: A Duide to Status, Applications, and Economics, (EPRI), p.2-23, 2-25

Sundaresan, S. and N. R. Amundson, 1978, Studies in Char Gasification-I: A lumped Model, Chemical Engineering Science, Vol.34, No. 3, p.345-354.

Wei, J., 1979, A Stoichiometric Analysis of Coal Gasification, I&EC Process Design & Development, Vol. 18, No. 3, p. 554-557.

Wen, C. Y. and H. P. Tseng, 1979, A model for fluidized bed coal gasifier simulation, AIChE Annual Meeting, San Francisco.

Wen, C. Y. and T. Z. Chaung, 1979, Entrainment Coal Gasification Modeling, I&EC Process Design & Development, Vol. 18, No. 4, p. 684-695.

Yoon, H., J. Wei, and M. M. Denn, 1978, A Model For Moving-bed Coal Gasification Reactors, AIChE Journal, Vol. 24, No. 5, p. 79-92.

Zenz, F. A., 1983, State-of-the-Art review and report on critical aspects and scaleup considerations in the design of fluidized bed reactors, USDOE Report DOE/MC/14141-1304.